

HYDROGEOLOGIC INVESTIGATION OF THE STEVENSVILLE STUDY AREA, RAVALLI COUNTY, MONTANA: INTERPRETIVE REPORT



Kirk Waren, Todd Myse, Dean Snyder, and Ginette Abdo

Montana Bureau of Mines and Geology

Ground Water Investigation Program

Cover photo by Ginette Abdo, MBMG: irrigation in the Bitterroot Valley, Corvallis, Montana area.

**HYDROGEOLOGIC INVESTIGATION OF THE STEVENSVILLE STUDY AREA,
RAVALLI COUNTY, MONTANA: INTERPRETIVE REPORT**

September 2020

Kirk Waren, Todd Myse, Dean Snyder, and Ginette Abdo

**Montana Bureau of Mines and Geology
Ground Water Investigation Program**

Montana Bureau of Mines and Geology Open-File Report 733



TABLE OF CONTENTS

Preface.....	1
Abstract	1
Introduction.....	2
Purpose and Scope	2
Previous Investigations	2
Physiography.....	6
Climate.....	7
Geologic Setting	8
Hydrogeologic Setting	10
Water Infrastructure	10
Methods.....	12
Data Management	12
Monitoring Network	12
Groundwater	12
Surface Water.....	12
Groundwater and Surface-Water Chemistry.....	15
Irrigation Recharge to Groundwater	15
Applied Irrigation Water	15
Canal Leakage.....	17
Evapotranspiration by Phreatophytes	17
Water Well Logs.....	17
Groundwater Modeling.....	17
Results.....	17
Hydrostratigraphy and Aquifer Properties	17
Shallow Alluvial Aquifer	17
Silt and Clay Aquitard.....	18
Deep Sand and Gravel Aquifer	18
Tertiary Aquifer.....	19
Bedrock Aquifer.....	19
Groundwater	19
Potentiometric Surface.....	19
Groundwater-Level Fluctuations	19
Seasonal Groundwater Trends	19
Long-Term Groundwater-Level Trends	21
Bitterroot River Stages and Discharge.....	22
Surface-Water Conditions in the Valley Floor	25
Recharge to Groundwater from Irrigation	27

Applied Irrigation Water	27
Canal Leakage.....	27
Water Chemistry	30
General Water Chemistry	30
Water Quality Standards Exceedances.....	33
Mitchell Slough and Union Ditch.....	33
Conceptual Model.....	34
Geologic Framework	34
Groundwater Flow System	34
Hydrologic Boundaries	34
Hydraulic Properties	35
Sources and Sinks	35
Groundwater Budget.....	35
Groundwater inflow and outflow (GW_{in} and GW_{out}).....	37
Recharge from irrigated fields (IF)	37
Canal leakage (CL)	37
Riparian vegetation evapotranspiration (ET).....	38
Groundwater withdrawals (WL).....	38
Canal gains (CG).....	38
Bitterroot River gains and losses (BR_{in} and BR_{out})	38
Storage (ΔS).....	39
Groundwater Modeling.....	39
Predictive Simulations	39
Scenario 1—No Irrigation	39
Scenario 2—Near-River Irrigation Wells.....	41
Scenario 3—Irrigation Wells across the Area Provide All East Channel Irrigation Water	45
Scenario 4—Irrigation Wells across the Area Provide All East Channel Irrigation Water	49
Summary	49
Conclusions and Recommendations	51
Acknowledgments.....	52
References.....	52
Appendix A: Groundwater Monitoring Network.....	57
Appendix B: Surface Water Monitoring Network	61
Appendix C: Well Log Lithologic Categories	63
Appendix D: Surface Water and Groundwater Quality Data.....	65
Appendix E: Groundwater Model Details	69

FIGURES

Figure 1. The study area is located in the Bitterroot Valley between Stevensville and Corvallis	3
Figure 2. The study area, which encompasses 144 mi ² , is located in the central Bitterroot Valley	4
Figure 3. The physiography of the study area on the east side of the Bitterroot River	5
Figure 4. Daily average flows (1987–2015) for the Bitterroot River (Bell Crossing USGS 12350250)	7
Figure 5. Precipitation and SNOTEL records for the 30-yr period 1984 through 2013	8
Figure 6. Generalized geology in the vicinity of the study area	9
Figure 7. Major irrigation canals within or near the groundwater model area	11
Figure 8. Groundwater levels were generally monitored on a monthly basis in 60 wells	13
Figure 9. Streams and canals were gaged and pressure transducers were used at most sites	14
Figure 10. Water-quality samples were collected from wells and surface-water sites	16
Figure 11. Schematic east–west cross section at Victor Crossing	18
Figure 12. The potentiometric surface of the shallow alluvial aquifer in the valley floor	20
Figure 13. Groundwater levels typically fluctuate seasonally but differ from well to well	22
Figure 14. Long-term groundwater-level trends are typically stable in wells located in irrigated portions of the valley floor	23
Figure 15. The hydrograph of Bitterroot River flow shows a strong response to snowmelt	24
Figure 16. The discharge of the Bitterroot River during 2012 and 2013 is compared with daily average flows	25
Figure 17. Flow in Mitchell Slough during most times of the year is typically greater at Bells Crossing compared to the headgate	26
Figure 18. Specific conductivity increases at sites downstream from the Mitchell Slough Tucker Headgate	27
Figure 19. This map shows the irrigation methods for lands within and near the study area	29
Figure 20. Union Ditch flows are higher at the Double Fork Ranch when compared to Victor Crossing	30
Figure 21. Water types of selected groundwater samples are defined by predominant major ions and indicate a calcium-bicarbonate type water	31
Figure 22. Stiff diagrams display major ion chemistry of selected groundwater and surface-water samples	32
Figure 23. This 10-yr scenario eliminates all diversions, ditch leakage, and recharge from irrigated fields in the valley floor after the first irrigation season	41
Figure 24. Six high-capacity wells are placed upstream of the East Channel diversion from the Bitterroot River in cells that include river reaches	43
Figure 25. Twenty-four high-capacity wells were placed upstream of the East Channel diversion from the Bitterroot River in model cells that include river reaches	44
Figure 26. The flow out of the east branch of Mitchell Slough as changes are applied cumulatively to irrigation activities in the valley floor area	46
Figure 27. In the low K version of the model, drawdown from irrigation well pumping is greatest near well locations on the east edge of the model	47
Figure 28. In the high K version of the model, drawdown from irrigation well pumping decreases by about 75% compared to the low K version	48

Figure 29. The water sources for sprinkler-irrigated lands are incrementally converted to groundwater wells in the low (A) and high K (B) 13-mo transient models.....50

TABLES

Table 1. Groundwater recharge due to irrigation for alfalfa28

Table 2. Comparison of the conceptual model and the model budget generated from the steady-state model.....36

Table 3. Canal leakage estimated for major canals on the valley floor during the 6-mo irrigation season38

Table 4. Scenarios were simulated using low and high K versions of each model40

PREFACE

The Ground Water Investigation Program (GWIP) at the Montana Bureau of Mines and Geology (MBMG) investigates areas prioritized by the Ground-Water Assessment Steering Committee (2-15-1523 MCA) based on current and anticipated growth of industry, housing, and commercial activity, or changing irrigation practices. Additional program details are available at: <https://www.mbm.mtech.edu/research/gwip/gwip.asp>.

The final products of the Stevensville study are:

A Report that presents data, addresses questions, offers interpretations, and summarizes project results. For the Stevensville groundwater investigation the primary question is how certain lands irrigated with surface water might be converted to groundwater sources, and how conversions would affect groundwater conditions and stream flows in the central Bitterroot Valley.

This report also describes **Groundwater Models** that were developed for this study. Groundwater modelers evaluate and use the models as a starting point for testing additional scenarios and for site-specific analyses. The model files to run the models are available on the MBMG publications website at http://www.mbm.mtech.edu/mbmgcat/public/ListCitation.asp?pub_id=32329&.

MBMG's Ground Water Information Center (GWIC) online database (<http://mbm.mtech.edu/gwic/>) provides a permanent archive for the data from this study.

ABSTRACT

In recent years, flows in the Bitterroot River near Corvallis and Stevensville have shifted between an east and west channel. This results in difficult and expensive maintenance activities to sustain sufficient flow for water diverted into the East Channel for irrigation. The purpose of this investigation was to evaluate the feasibility of using groundwater to supplement or replace surface-water irrigation in the study area. We characterized the groundwater and surface-water systems in the valley floor by conducting a 13-mo field study that included monitoring groundwater levels, stream, and ditch flows. A conceptual hydrogeologic model and groundwater budget provided the basis for building three-dimensional groundwater models that

evaluate effects of major changes to irrigation practices on groundwater conditions and stream flows. The groundwater budget derived from the numerical models indicates that groundwater recharge from canal leakage and excess water applied to fields that infiltrates into the subsurface can result in up to 75% of the groundwater recharge.

Three aquifers identified in this study include a shallow alluvial aquifer composed of sands and gravels underlying the Bitterroot floodplain and low terraces. This aquifer extends, on average, to a depth of about 40 ft below ground surface. A deep sand and gravel aquifer of unknown depth is separated from the shallow alluvial aquifer by an aquitard that averages 20 ft thick. Bedrock underlies the valley floor, and there are wells completed in the bedrock along the valley margins and high terraces. The 3-layer groundwater flow models incorporated the shallow alluvial aquifer, the aquitard, and the deep sand and gravel aquifer.

Modeling results suggest that from a physical standpoint, it is feasible to use groundwater to supplement or replace surface-water irrigation. The shallow alluvial aquifers can likely produce the water needed for irrigation using sprinkler or pivot methods. The scenario that least influences the current groundwater and surface-water conditions involves converting lands that are currently irrigated with sprinkler or pivot irrigation systems to groundwater sources. This scenario generally did not affect irrigation return flows after November when compared to existing conditions.

Modeling indicated that if flood irrigation was converted to sprinkler or pivot irrigation, and all irrigated fields were supplied by groundwater, the volume of water diverted to fields would be reduced, but so would irrigation return flows to Mitchell Slough. Simulations that eliminated flood irrigation and canals result in a decline in summertime flows out of Mitchell Slough from a range of 90 to 110 cfs to 10 to 40 cfs. Groundwater levels declined 2 to 11 ft from current seasonal low water table conditions in the late spring. The groundwater levels remained at those lower levels, rather than rising each irrigation season, because all irrigation recharge was discontinued in the simulation.

Although using groundwater as a source to supplement or replace surface-water diversions is a viable option, changes in current irrigation practices can

affect groundwater recharge and subsequent irrigation return flow to Mitchell Slough and the Bitterroot River. The groundwater numerical models developed for this project can be adapted to evaluate changes in irrigation management schemes that optimize water resources.

INTRODUCTION

The Stevensville project area lies within the north-central Bitterroot Valley about 30 mi south of Missoula, in Ravalli County (fig. 1). Historically, agriculture has been the mainstay of the county's economy. In 2012, about 61,500 acres of agricultural land were irrigated in Ravalli County. Alfalfa, spring wheat, oats, and grass hay are the county's principal crops.

The Bitterroot River flows north through the valley and is used for recreation, irrigation, and fish and wildlife. The East Channel is a 6-mi-long branch of the river that diverges from the mainstem about 2.5 mi north of Woodside Crossing and returns to the mainstem about 0.25 mi south of Bell Crossing (fig. 2). The East Channel supplies water to five diversions used to irrigate nearly 4,000 acres.

Since the 1950s, the mainstem of the Bitterroot River above Stevensville has shifted channels within this braided river system, mostly abandoning the East Channel and its diversion to Mitchell Slough. Mitchell Slough is important to the irrigation infrastructure, functioning as both a source of irrigation water and a groundwater discharge area. Currently some water flows into the East Channel from the mainstem of the Bitterroot River. In low water years, irrigators have to dredge the East Channel to the mainstem to maintain an adequate water supply for irrigation. This is expensive and requires procuring multiple Federal and State permits for instream disturbances. Dredging also temporarily increases the sediment load in the Bitterroot River. Irrigators are considering alternatives to alleviate the need for extensive maintenance of the East Channel. One alternative is using shallow groundwater to supplement or replace surface-water sources for irrigation.

The study area is about 144 mi² and extends north to south from Stevensville Cutoff to Woodside Crossing near Corvallis. From west to east, the study area extends from the base of the Bitterroot Mountains to a few miles into the foothills of the Sapphire Mountains (fig. 2). Within this larger study area, we focused

on the valley floor on the east side of the Bitterroot River. The valley floor includes the Bitterroot River floodplain and low terraces (fig. 3). The numerical groundwater flow models encompass about 32 mi² and include the valley floor from north of Corvallis to west of Stevensville (fig. 3). Many study elements are restricted to this portion of the valley.

Purpose and Scope

The purpose of this investigation was to evaluate the feasibility of using groundwater to supplement or replace surface-water irrigation in the study area. To conduct this evaluation, we established the following objectives:

- Characterize the groundwater and surface-water flow system of the valley floor using information from previous studies and conducting a 13-mo field study.
- Develop a conceptual model of the hydrogeology of the valley floor based on available data.
- Develop steady-state and 10-yr transient groundwater flow models to evaluate the effects of various changes to irrigation systems on groundwater levels and surface-water flows.

Previous Investigations

Briar and Dutton (2000), Kendy and Tresch (1996), and Smith and others (2013) provide reviews and descriptions of previous work in the Stevensville study area. These sources cite a variety of geologic and hydrologic studies of the central Bitterroot Valley. The following discussion focuses on information directly relevant to this study.

Surficial geologic mapping of the Bitterroot Valley by Lonn and Sears (2001a,b,c) provides the basis for the geological information described in this Ground Water Investigation Program (GWIP) study. Lonn and Sears produced maps at the 1:100,000 and 1:48,000 scales.

McMurtrey and others (1959, 1972) investigated the geology and water resources of the Bitterroot Valley. These reports provide basic descriptions and properties of the aquifers, a potentiometric surface map, and information on stream flows and water volumes. Groundwater generally flows from the upland areas towards the Bitterroot River. In the floodplain, groundwater flows northward mostly parallel to the river.



Figure 1. The study area is located in the Bitterroot Valley between Stevensville and Corvallis.

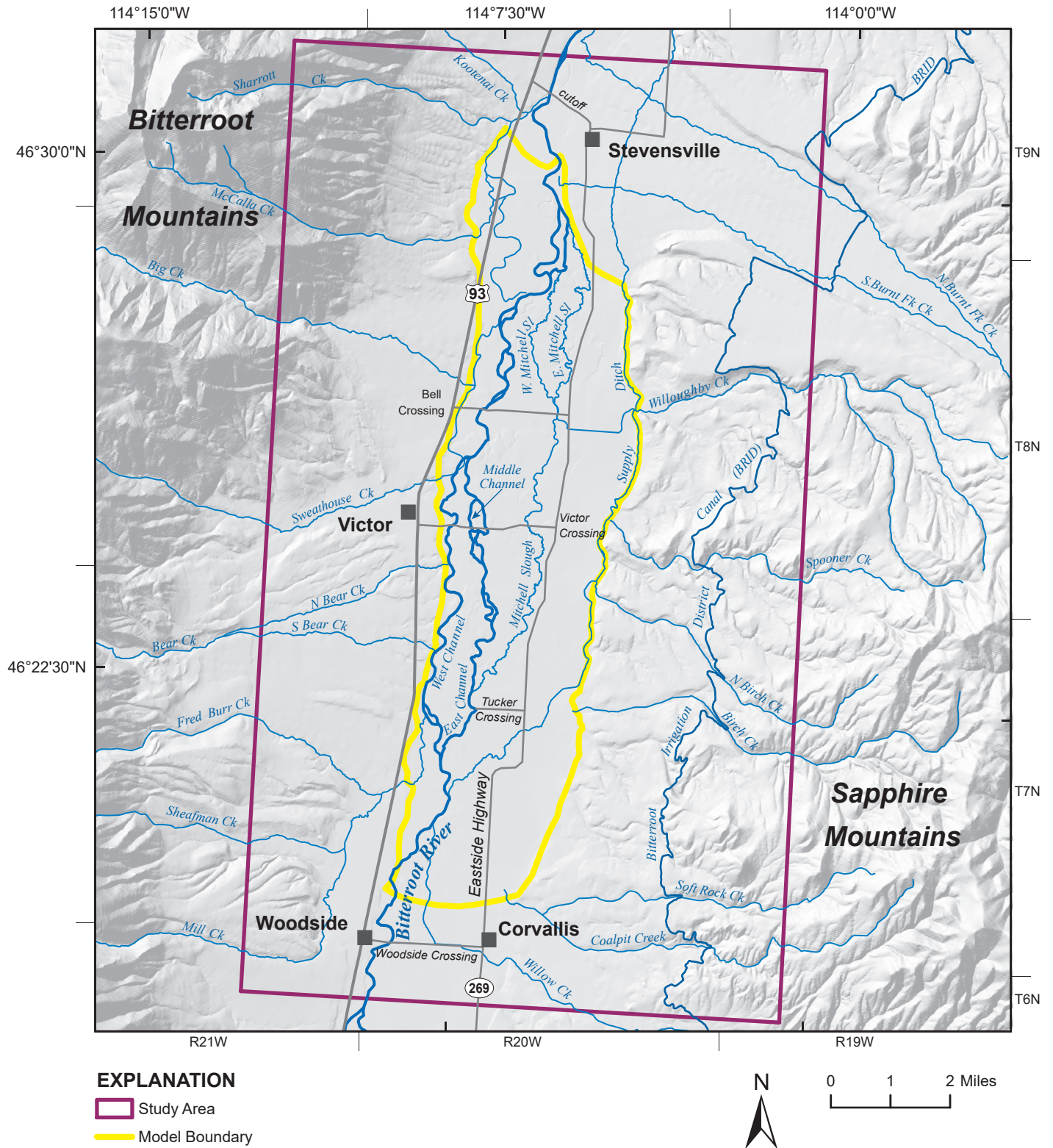


Figure 2. The study area, which encompasses 144 mi², is located in the central Bitterroot Valley near Stevensville, Victor, and Corvallis. The groundwater model area is about 32 mi².

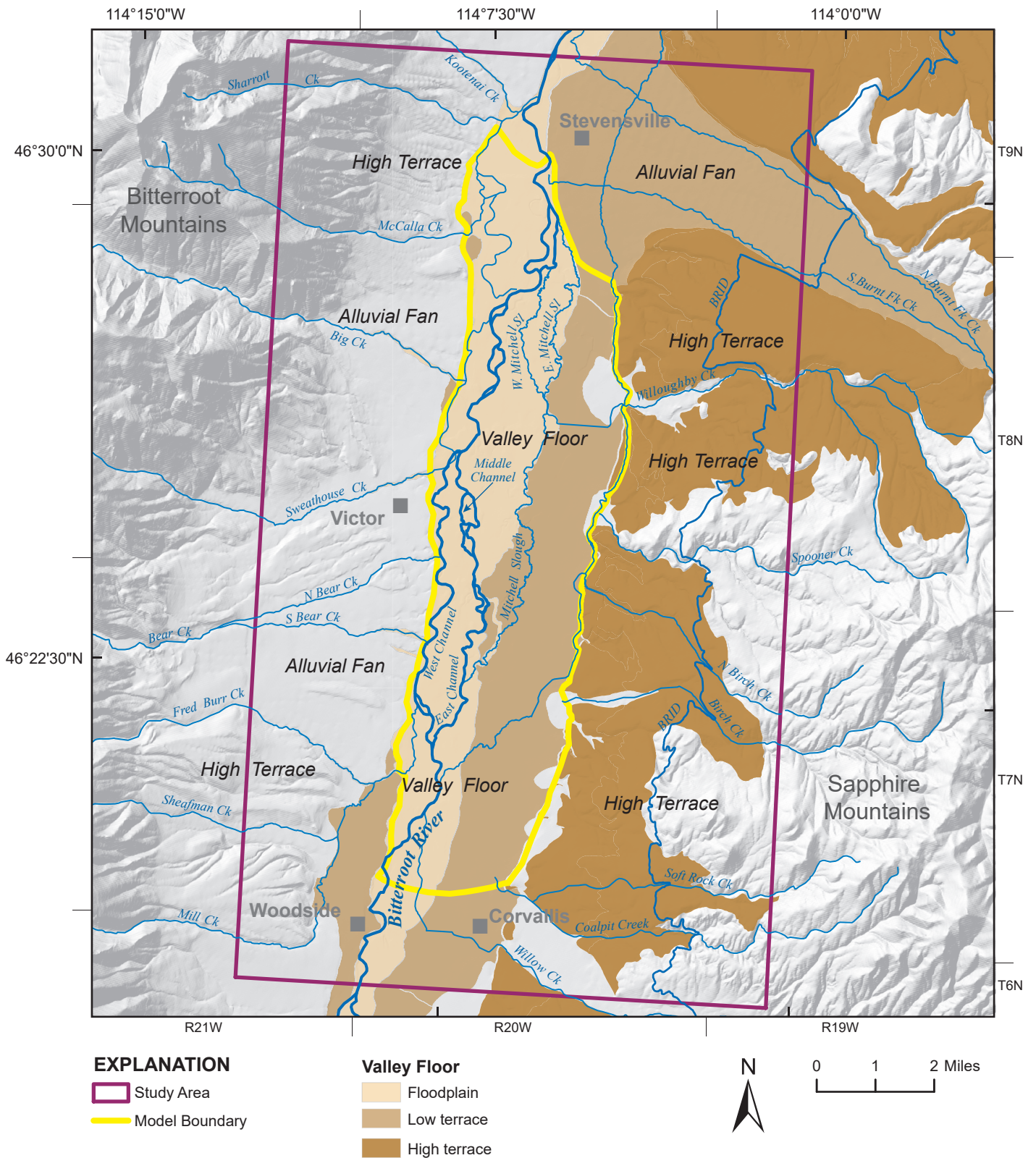


Figure 3. The physiography of the study area on the east side of the Bitterroot River includes high terraces between the mountains and the valley floor. The valley floor is relatively flat and includes the floodplain and low terraces.

Potentiometric maps developed by later investigators indicate similar flow directions (Briar and Dutton, 2000; Kendy and Tresch, 1996; LaFave, 2006a).

Seven deep boreholes drilled for uranium exploration provided information on aquifer properties, water chemistry, and assessment of geothermal gradients (Norbeck, 1980). Smith (2006a) used this information to estimate the elevation of the bedrock surface in the Bitterroot Valley.

Surficial geologic mapping by Finstick (1986) in the Victor area identified four surficial Quaternary units (high terraces, low terraces, floodplains, and moraines). Tertiary sediments surficially exposed or underlying Quaternary units on high terraces are finer grained and interbedded with sands and gravel. Finstick calculated transmissivities based on well logs and identified seasonal groundwater fluctuation patterns. Uthman (1988) conducted a similar study that extended from Hamilton to about 4 mi north of Corvallis.

The Montana Bureau of Mines and Geology (MBMG) characterized the hydrogeology of the Bitterroot Valley in the late 1990s. A series of atlases (Carstarphen and others, 2003; LaFave, 2006a,b; Smith, 2006a,b,c; Smith and others, 2013) describe the hydrogeologic framework as consisting of three main aquifers: shallow basin-fill, deep basin-fill, and bedrock. These atlases also describe aquifer properties, groundwater fluctuations, and water quality. Groundwater flow directions in the shallow and deep basin-fill aquifers described in those atlases concur with earlier work (McMurtrey and others, 1959, 1972). The characterization includes details on the extent of each aquifer and typical well depths, yields, and water quality.

Physiography

The Bitterroot Valley is an intermontane basin that trends north–south. The Bitterroot Mountains parallel the valley to the west with high glaciated peaks reaching elevations of 9,000 to 10,000 ft above mean sea level (amsl). The Sapphire Mountains east of the valley are lower in elevation, with the highest peak at about 9,000 ft amsl.

Between Corvallis and Stevensville, the valley floor is relatively flat and dips northward slightly with about 220 ft of relief. The valley floor is about 3 mi wide and includes the Bitterroot River floodplain and low terraces (fig. 3). The low terraces are subtle fea-

tures rising 4 to 5 ft above the floodplain.

High terraces, or benches, flank the valley floor. Between the Bitterroot Mountains and the valley floor, dissected high terraces and alluvial fans slope gently eastward (fig. 3). The Bitterroot Mountain front is a well-defined, linear feature. To the east, dissected high terrace remnants extend westward from the Sapphire Mountains to the valley floor. The eastern high terraces typically abut the valley floor in scarps about 50 to 150 ft high. The Sapphire Mountain front is subtler than that of the Bitterroot Mountains. McMurtrey and others (1972) provide additional details about the high terraces and tributary valleys.

About four times as many streams originate from the Bitterroot Mountains as from the Sapphire Mountains (Briar and Dutton, 2000). The Bitterroot Mountains provide greater runoff to the river than the Sapphire Mountains due to higher precipitation and closer proximity to the Bitterroot River. Within the study area, tributaries to the Bitterroot River on the west side are Mill, Sheafman, Fred Burr, Bear, Sweat-house, Big, McCalla, Sharrott, and Kootenai Creeks. On the east side of the valley, Willow, Willoughby, and North Burnt Fork Creeks flow into the Bitterroot River. Several creeks on the east side of the valley are intercepted by ditches and do not flow all the way into the Bitterroot River. Willoughby Creek flows into Mitchell Slough (fig. 3).

The Bitterroot River flows northward in a braided channel through the Bitterroot Valley. Within the central part of the study area, the Bitterroot River splits into three channels just south of Victor Crossing (fig. 2). Currently, the western channel is the mainstem of the river. Since the 1960s, the mainstem within the study area has progressively shifted from the East Channel to its current location as the West Channel. The Hamilton North 1:24,000 United States Geological Survey (USGS) topographic map (1967) shows the eastern channel (locally known as the East Channel) as the mainstem of the Bitterroot River, although much of the current westernmost channel still existed at that time. Based on the 1967 map, the East Channel appears to be disconnected from the river at its upper end near Tucker Crossing.

The East Channel is about 6 mi long. The upstream end of the East Channel diverges from a single thread river about 3 mi north of Woodside Crossing and 0.5

mi south of Tucker Crossing. The Channel returns to the mainstem Bitterroot River about 0.25 mi south of Bell Crossing. The middle channel splits from the East Channel upstream of Victor Crossing and is only about a mile long (fig. 2). All three channels are present at Victor Crossing, whereas only one channel occurs at Bell Crossing.

Melting of snowpack results in high flows in the Bitterroot River at Bell Crossing (USGS gage 12350250) in the spring and early summer (fig. 4). Peak flow generally occurs in June, typically in the range of 5,000 to 11,000 cfs, and decreases to near low flow in July (USGS, 2014). Low flow, on average, is about 400 cfs. Flow is controlled in part by releases from the upstream Painted Rocks Reservoir (fig. 1). Flow increases in the late fall and early winter due to precipitation, reduced irrigation diversions, and irrigation return flows before decreasing to baseflow through the winter until spring snowmelt. Irrigation return flow results from canal leakage and excess water applied to fields that infiltrates past the root zone and recharges groundwater. Excess irrigation water can also return directly to the river as overland flow. For purposes of this report, irrigation return flow refers to that portion that returns to the river through groundwater.

Climate

The climate of the Bitterroot Valley is typified by long winters and short, mild summers. A National Weather Service Cooperative Observer Network (COOP) weather station is located in Stevensville (fig. 1) with a period of record (POR) of 104 yr. The 30-yr average (1984–2013) annual precipitation at Stevensville COOP is 11.9 in. During the POR, 2012 and 2013 were the 36th and 6th driest years, respectively (Stevensville COOP, 2014). Annual precipitation was generally below normal from 1999 through 2013, with 2013 as the driest in 30 yr (8.3 in of rainfall; fig. 5A). Average monthly high and low temperatures (1984–2013) were 85.3°F and 16.9°F, occurring in August and December, respectively. The wettest months include May and June, with a mean precipitation of about 1.5 in, while the driest month is typically July, with about 0.7 in of rainfall.

Precipitation falls mostly as snow in high elevations. Less precipitation falls on the east side of the valley due to the rain shadow created by the Bitterroot Mountains as storms move west to east. The 30-yr average (1984–2013) snow water equivalent (SWE) at the Skalkaho Summit SNOTEL on the east side of the

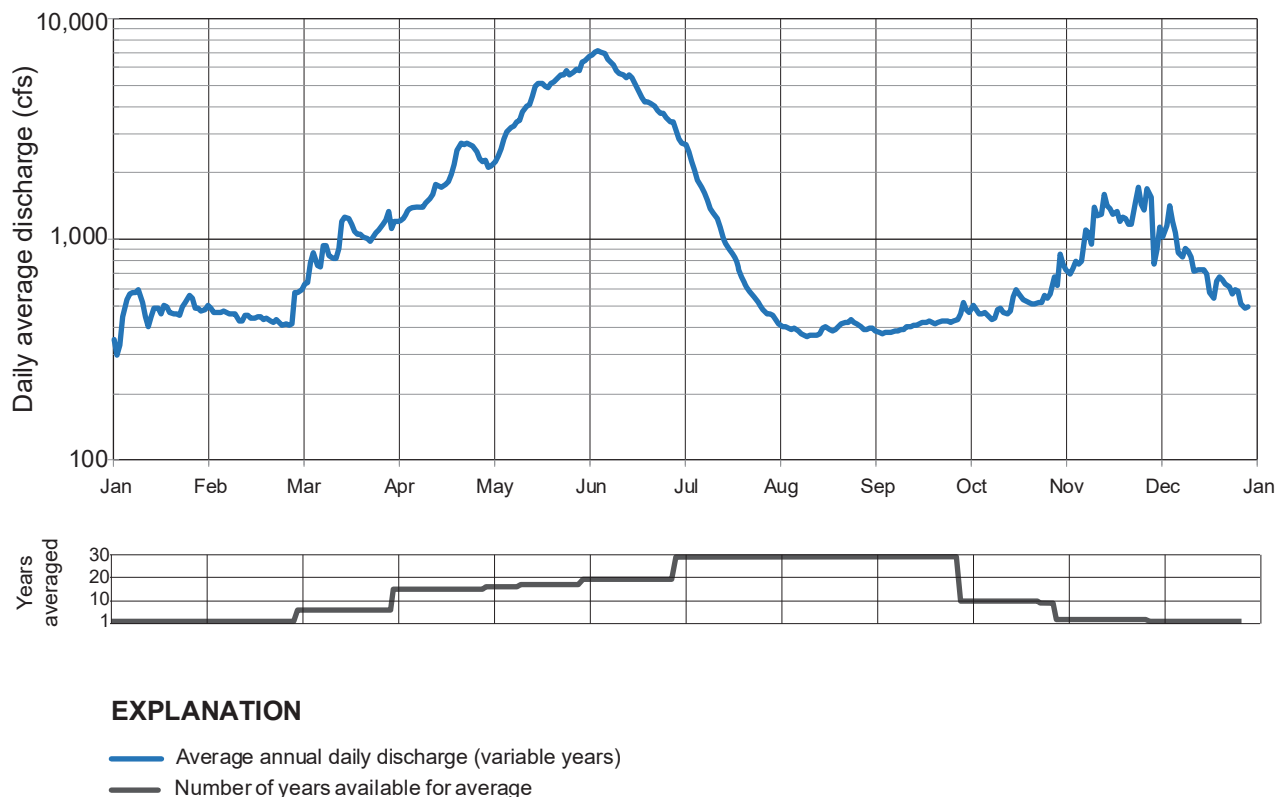


Figure 4. Daily average flows (1987–2015) for the Bitterroot River (Bell Crossing USGS 12350250) are typically highest in late May–early June and lowest in August–September and January–February. Data available to generate the hydrograph varies by month, as shown in the bottom graph.

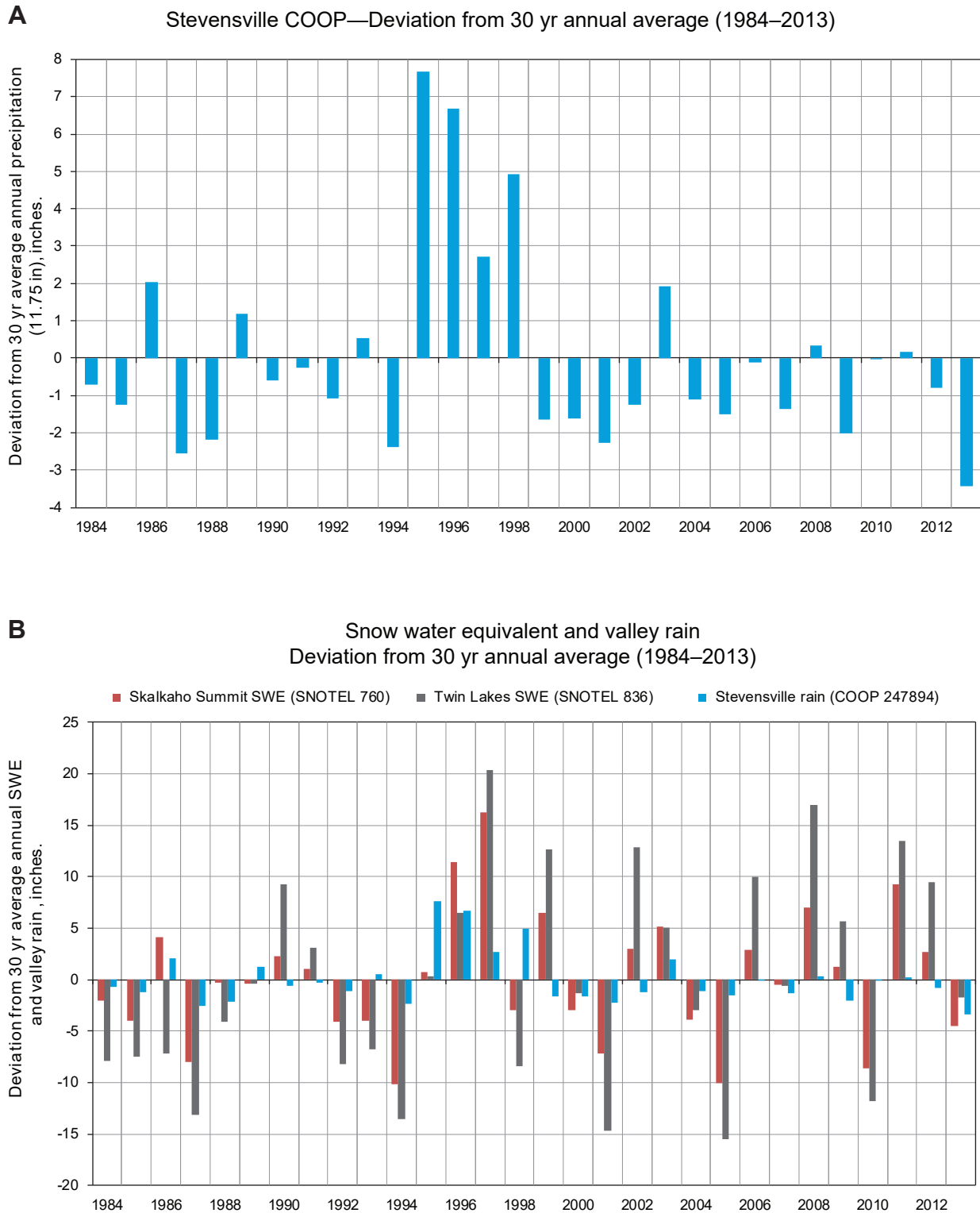


Figure 5. Precipitation and SNOTEL records for the 30-yr period 1984 through 2013 show that valley precipitation was below the 30-yr average (A) during 2011 and 2012 while SWE was above average on the east and west sides of the valley (B).

valley was 27.6 in, compared to 46.1 in at the Twin Lakes SNOTEL site to the west (NRCS, 2014; fig. 1). During 2011 and 2012, the SWE equivalent was above the 30-yr average (fig. 5B) at both SNOTEL locations while valley precipitation was near or below average. The SWE was below average during 2013.

Geologic Setting

The mountainous terrain west and east of the Bitterroot Valley is composed of granite, mylonite, and Precambrian metasedimentary rocks (Lonn and Sears, 2001a; fig. 6).

Tertiary sediments (Ts) up to 4,000 ft thick were

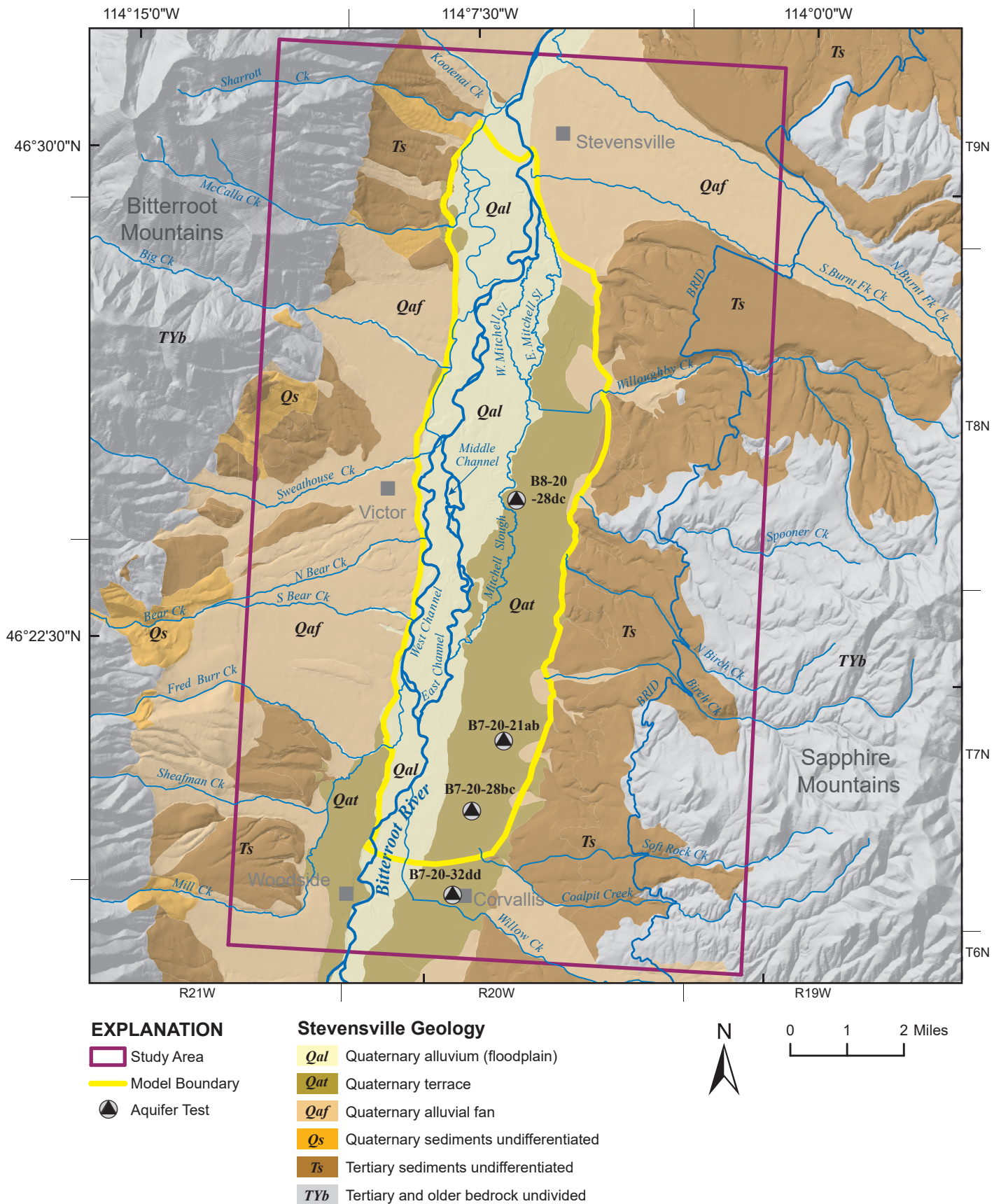


Figure 6. Generalized geology in the vicinity of the study area. Aquifer test locations from previous investigations are shown with their U.S. Geological Survey site identification numbers (McMurtrey and others, 1959, 1972).

deposited in the valley and are composed mostly of weakly lithified claystone, sandstone, and conglomerate (Smith and others, 2013). These sediments form the bulk of the high terraces west and east of the valley floor.

Surficial deposits composed of Quaternary sediments overlie Tertiary basin-fill in much of the valley. The valley floor is composed of Quaternary alluvium (Qal) in the floodplain and Quaternary alluvial terraces (Qat) on the low terraces (fig. 6). These surficial deposits are associated with the Bitterroot River and are about 50 ft thick (Smith, 2006b). These sediments include extensive deposits of sand and gravel, and cobbles with minor zones of silty and clayey sediments filling in abandoned or low-energy channel environments. This study focuses on the Quaternary alluvium and alluvial terraces and the uppermost part of the underlying Tertiary sediments.

Glacial outwash, till, debris flows, and alluvial fans overlie the Tertiary sediments at many locations on the high terraces west of the valley floor. East of the valley floor, alluvial outwash fans are mapped near Burnt Fork Creek and near Willoughby Creek (fig. 6). Quaternary sediments on the high terraces form a thin cover that, in some areas, ranges up to 50 ft thick.

Hydrogeologic Setting

This description of the hydrogeologic setting is based on previous, regional-scale investigations that include the study area. Groundwater elevations are highest in fractured bedrock aquifers in the mountainous areas and lowest in the downstream portions of the valley floor. Groundwater moves from the Bitterroot and Sapphire Mountains toward the Bitterroot River. Groundwater in bedrock aquifers discharges to springs, streams, and to adjacent basin-fill and shallow unconfined aquifers.

The potentiometric surface in the high terraces slopes toward the valley floor. Local irregularities in the surface occur at larger tributary valleys and ridges extending outward from the mountain fronts. Groundwater is relatively shallow and unconfined in the floodplain and low terraces. The water table gradient within the valley floor is relatively low, with flow to the north, similar to the land surface topography. In general, the water table gradient beneath the low terraces is also low but flow is toward the floodplain.

Smith and others (2013) generally describe shallow basin-fill aquifers in the Bitterroot Valley at depths within 75–80 ft of the land surface. Composed of coarse-grained recent alluvial deposits or Tertiary age sand and gravel, most shallow basin-fill aquifers are unconfined. Low-permeability silt and clay deposits present near land surface and within deeper basin-fill aquifers are described by LaFave and others (2013) as partially confining or leaky confining units. Deeper basin-fill aquifers are at depths greater than 75–80 ft below land surface and consist of coarse-grained alluvial deposits and Tertiary sedimentary bedrock formations.

Seasonal discharge patterns in the Bitterroot River and irrigation activities affect groundwater levels. These groundwater-level changes drive groundwater movement in shallow aquifers. Groundwater fluctuations in wells are discussed by McMurtrey and others (1959, 1972), Finstick (1986), Uthman (1988), and LaFave (2006a). Other physical processes and events, such as evapotranspiration, recharge, pumping, and barometric pressure changes also affect water levels.

Water Infrastructure

About 25,000 irrigated acres are within the study area (MT-DOR, 2012). About 62% of this acreage is flood irrigated, 34% sprinkler irrigated, and 4% pivot irrigated. Irrigation water is conveyed through a canal and ditch system (fig. 7).

The Bitterroot Irrigation District (BRID) Canal, constructed in the early 1900s, is the largest single canal and irrigation project in the valley, conveying about 260 cfs through the study area. Located on the eastern high terraces, the canal is about 70 mi long and provides water to about 17,000 irrigated acres, mostly on the eastern high terraces (fig. 1). Lake Como reservoir, just north of Darby, supplies source water for the BRID. Lake Como is in the Rock Creek drainage, about 5 mi upstream of Rock Creek's confluence with the Bitterroot River.

In the valley floor, the Corvallis Canal and the Supply Ditch are the principal canals that divert water from the Bitterroot's mainstem. The Corvallis Canal diverts water just north of Hamilton, about 3 mi south of the study area. The Supply Ditch diverts water within the study area. Major diversions from the Bitterroot River's East Channel include Mitchell Slough and Victor, Spooner, and Gerlinger Ditches (fig. 7).

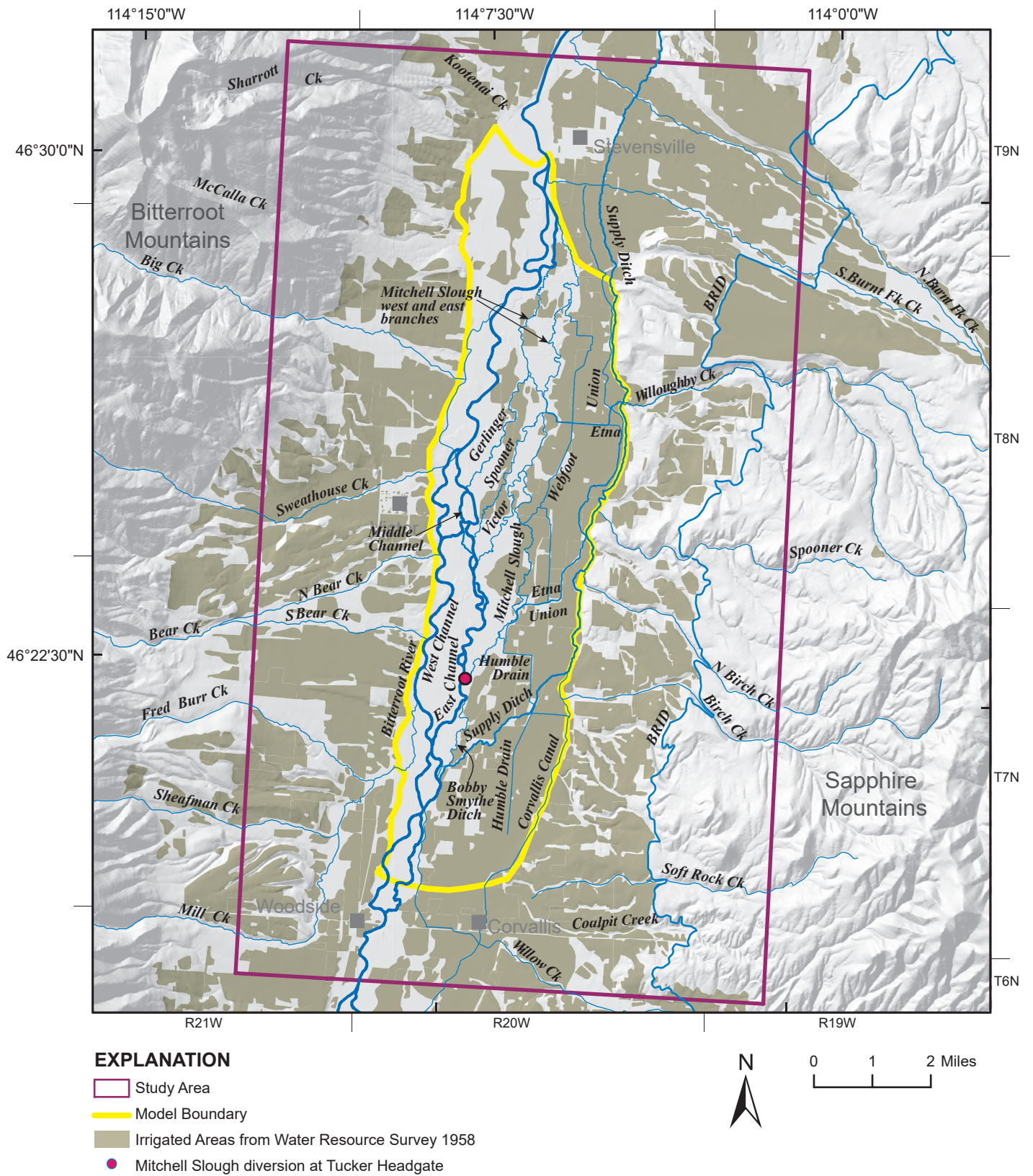


Figure 7. Major irrigation canals within or near the groundwater model area. The irrigated lands coverage in this map is from the Ravalli Co. Water Resource Survey (MT-DNRC, 2007).

Water from the East Channel is diverted into Mitchell Slough at Tucker Headgate (fig. 7). Flow at this headgate varies from about 40 to 100 cfs in late spring and summer and less than about 25 cfs most of the winter and early spring. North of Bell Crossing, Mitchell Slough bifurcates into east and west branches that rejoin into one branch about 3 mi downstream (figs. 2, 7). The Union, Etna, and Webfoot Ditches are diverted from Mitchell Slough.

Irrigated lands displayed on the map (fig. 7) are from the Montana State Engineer's Office Ravalli County Water Resources Survey (1958). This coverage shows the extent of irrigation in the 1950s. The current status of irrigated lands is addressed later in this report.

Some irrigation needs are met with groundwater. The Montana DNRC water rights database (MT-DNRC, 2016) contains records of 18 irrigation wells within the model area. These sites have reported places-of-use that are typically less than 100 acres.

Groundwater supplies most domestic water use within the model area. MBMG's Ground Water Information Center (GWIC) database (GWIC, 2014) contains 772 well records within this area, 556 of which are listed as domestic wells. Other reported well uses include stock water, monitoring, public water supply, fire protection, geotechnical, geothermal, irrigation, unknown, and other.

The term "drain" or "drain ditch" used in this report refers to small ditches constructed to drain excess irrigation water and to portions of low-lying canals that gain groundwater. In some cases, the groundwater is irrigation return flow.

METHODS

We designed a monitoring network to evaluate groundwater and surface-water dynamics for this study. This information supported development of a conceptual hydrogeologic model and a groundwater budget for the model area. These supported construction and calibration of the steady-state and transient flow models. Surface-water data collection focused on the Bitterroot River, canals, ditches, and streams on the floodplain, and ditches and streams on the low terrace east of the river.

Data Management

Data collected during this study are archived in the MBMG's GWIC database, accessible at: <http://mbmoggwic.mtech.edu/>. Data related to this project are available here: <https://mbmoggwic.mtech.edu/sqlserver/v11/menus/menuProject.asp?mygroup=GWIP&myroot=BWIPST&ord=1&>

Monitoring Network

Groundwater and surface-water data collected for this project are compiled in appendices A and B. GWIC contains additional information about each monitoring location. GWIC identification numbers for wells (e.g., well 266089) and surface water (e.g., site 242228) are used in this report. A licensed, professional surveyor measured latitude, longitude, and elevation at all wells and staff gages using a survey grade GPS in December 2012.

Groundwater

We established a monitoring network of 60 wells to obtain water-level and water-chemistry information (fig. 8; table A-1). Eleven of these are long-term monitoring wells that are a part of Montana's state-wide monitoring network. Most wells in the network are domestic or stock wells, and some are not currently in use. These wells were selected based on hydrogeologic setting, geographic location, historical record, and well-owner permission. Water levels were measured monthly except during the irrigation season when selected wells were measured every other week. Eighteen wells were equipped with pressure transducers with data loggers (referred to as pressure transducers throughout the rest of the report) programmed to record water levels hourly. The monitoring network includes five piezometers installed for this project; these provide groundwater levels adjacent to Gerlinger Ditch in the shallow alluvial aquifer.

Surface Water

To evaluate surface-water conditions in the study area, we measured surface-water stage and discharge at 36 locations (11 natural channels and 25 canal locations; fig. 9; appendix B). At 22 of these sites, pressure transducers installed in stilling wells recorded stage hourly. We measured surface-water flows monthly, except during the irrigation season, when some of the sites were measured every other week. Data were also

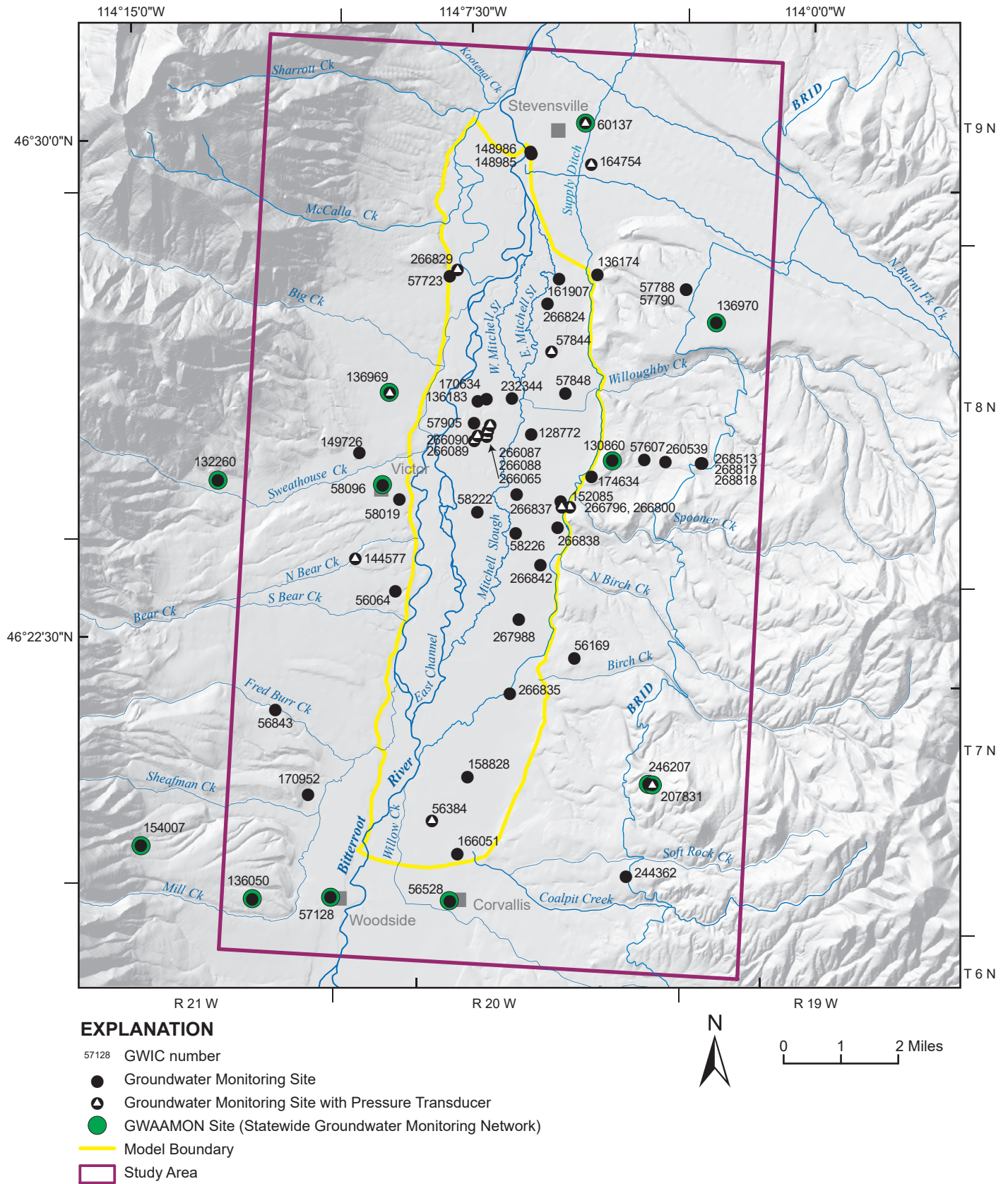


Figure 8. Groundwater levels were generally monitored on a monthly basis in 60 wells; selected wells were equipped with pressure transducers to record more frequent measurements.

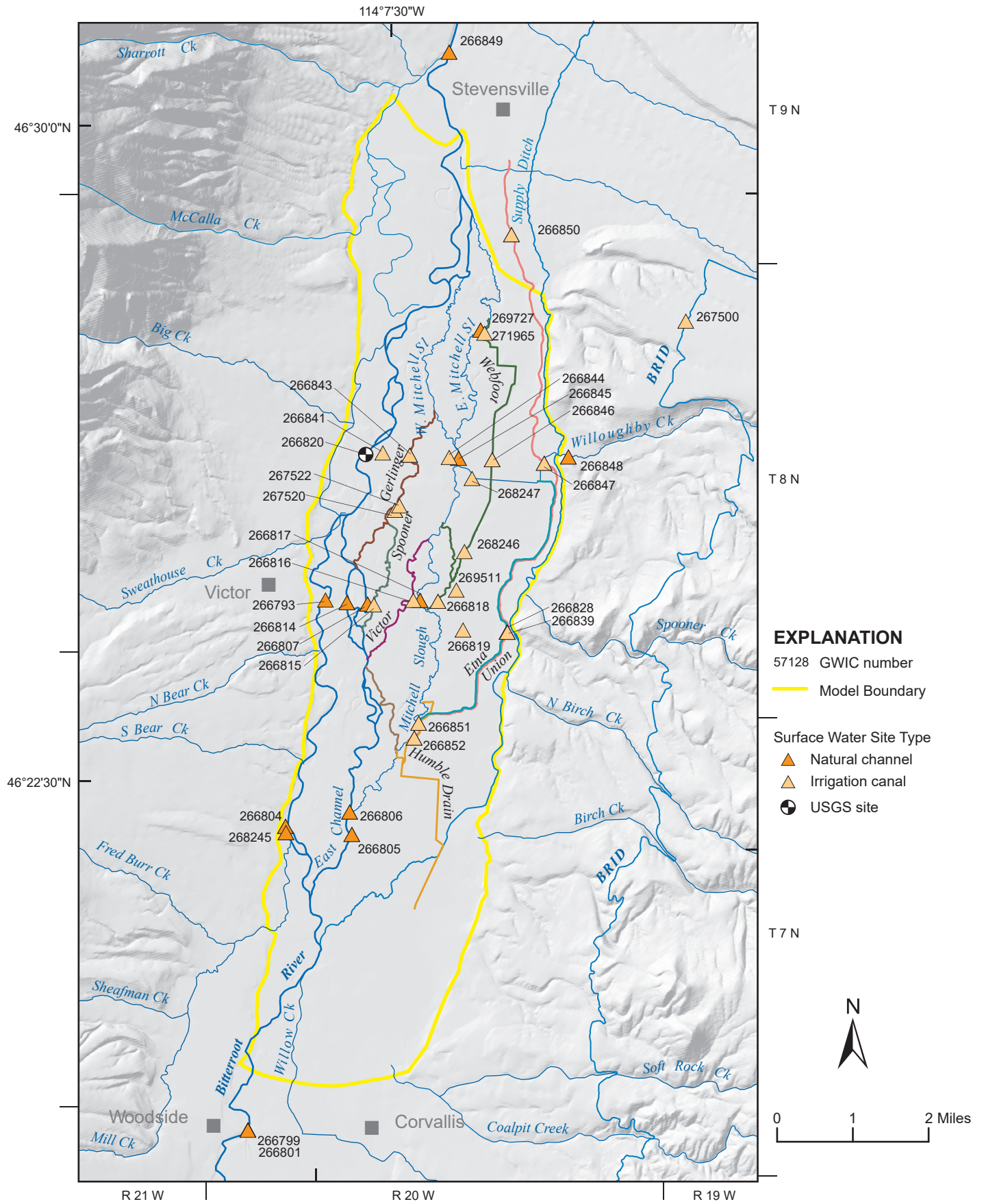


Figure 9. Streams and canals were gaged and pressure transducers were used at most sites to record stage between gaging events.

obtained from a USGS gaging station on the Bitterroot River (USGS 12350250; site 266820). Though this station normally does not operate in the winter, it was operational through the 2012/2013 winter.

Routine measurements at surface-water sites included discharge, stage, specific conductance (SC), and temperature. We developed rating curves to estimate flows for stages recorded between streamflow measurements. At some sites, growth of aquatic vegetation in the summer disrupted the stage–discharge relationship, and a separate rating curve was developed for these conditions. Flows estimated with the summertime rating curves are identified as “calculated flow with vegetation.” Flows estimated during the rest of the year are designated as “non-vegetation” flows.

Groundwater and Surface-Water Chemistry

We sampled water from 32 wells and 14 surface-water sites (fig. 10), primarily during August 2012. Samples were analyzed for major ions, trace metals, and stable isotopes of oxygen and hydrogen (^{18}O and ^2H). Water-quality parameters, including SC, pH, and temperature were measured in the field during sample collection and in the laboratory. SC, expressed in units of micro-Siemens per centimeter ($\mu\text{S}/\text{cm}$), is a measure of water’s ability to conduct an electric current.

Prior to sampling, wells were purged of at least three bore volumes and until water-quality parameters stabilized. Additional samples for only isotopic analyses, and measurements of specific conductance and temperature, were collected at most surface-water sites. Samples for isotopic analysis involved collecting unfiltered and unpreserved water in 20-ml HDPE bottles. Specific conductance and temperature were measured in the field with a YSI handheld probe calibrated using a NIST certified standard ($1,413 \mu\text{S}/\text{cm}$).

The MBMG Analytical Lab analyzed major and trace elements and measured basic parameters. Isotope samples were analyzed by Isotech Labs and the University of Waterloo Isotope Lab. Isotopic values measured in samples were compared to a standard (VSMOW) and the ratio is reported by the lab as $\delta^{18}\text{O}$ and δD . All samples were collected and handled according to MBMG standard operating procedures.

Irrigation Recharge to Groundwater

Irrigation practices typically cause a seasonal rise in groundwater levels and result in irrigation return

flows to drain ditches and streams. Estimates for components of irrigation recharge, including applied irrigation water and loss through canals, were developed for the groundwater budget.

Applied Irrigation Water

The general equation to calculate recharge from applied irrigation is based on the water applied to the crops, precipitation, and the consumptive water use by crops [i.e., evapotranspiration (ET)], expressed as:

$$\text{Groundwater Recharge} = (\text{Applied Irrigation Water} + \text{Precipitation}) - \text{ET}.$$

We estimated the amount of applied irrigation water based on the crop and the irrigation method (i.e., flood, sprinkler, pivot). We simplified the estimate by using alfalfa, which is the largest single-crop acreage reported for the area; 3,198 of 6,274 total acres are planted in alfalfa.

Irrigated acreage and the type of irrigation were determined using the Final Land Unit (FLU) Classification database (NRIS, 2010). We checked these data with field observations and by overlaying the dataset with 2006, 2009, 2011, and 2013 National Agriculture Imagery Program (NAIP, 2011) imagery. The FLU dataset was updated with this information to reflect current irrigation methods and areas.

The amount of water applied to irrigated areas varies based on the efficiency of the irrigation method. Estimates of irrigation efficiency are 80, 70, and 45 percent for pivot, sprinkler irrigation, and flood irrigation, respectively [Natural Resource Conservation Service (NRCS), written commun., 2011]. We used the Net Irrigation Requirement (NIR) of alfalfa to estimate the water applied to an alfalfa crop. NIR values were obtained from the Ravalli County Irrigation Water Requirements Crop Data Summary (NRCS, written commun., 2012). For example, we assumed that if the NIR for alfalfa is 5 in for the month of April, a sprinkler that is 70% efficient delivered 7.14 in ($5 \text{ in}/0.70$).

We used a monthly time step for estimating recharge from applied irrigation water, based on monthly precipitation amounts reported by the Stevensville COOP. The consumptive water use (ET) of alfalfa was calculated using the Blaney–Criddle method (NRCS, written commun., 2012).

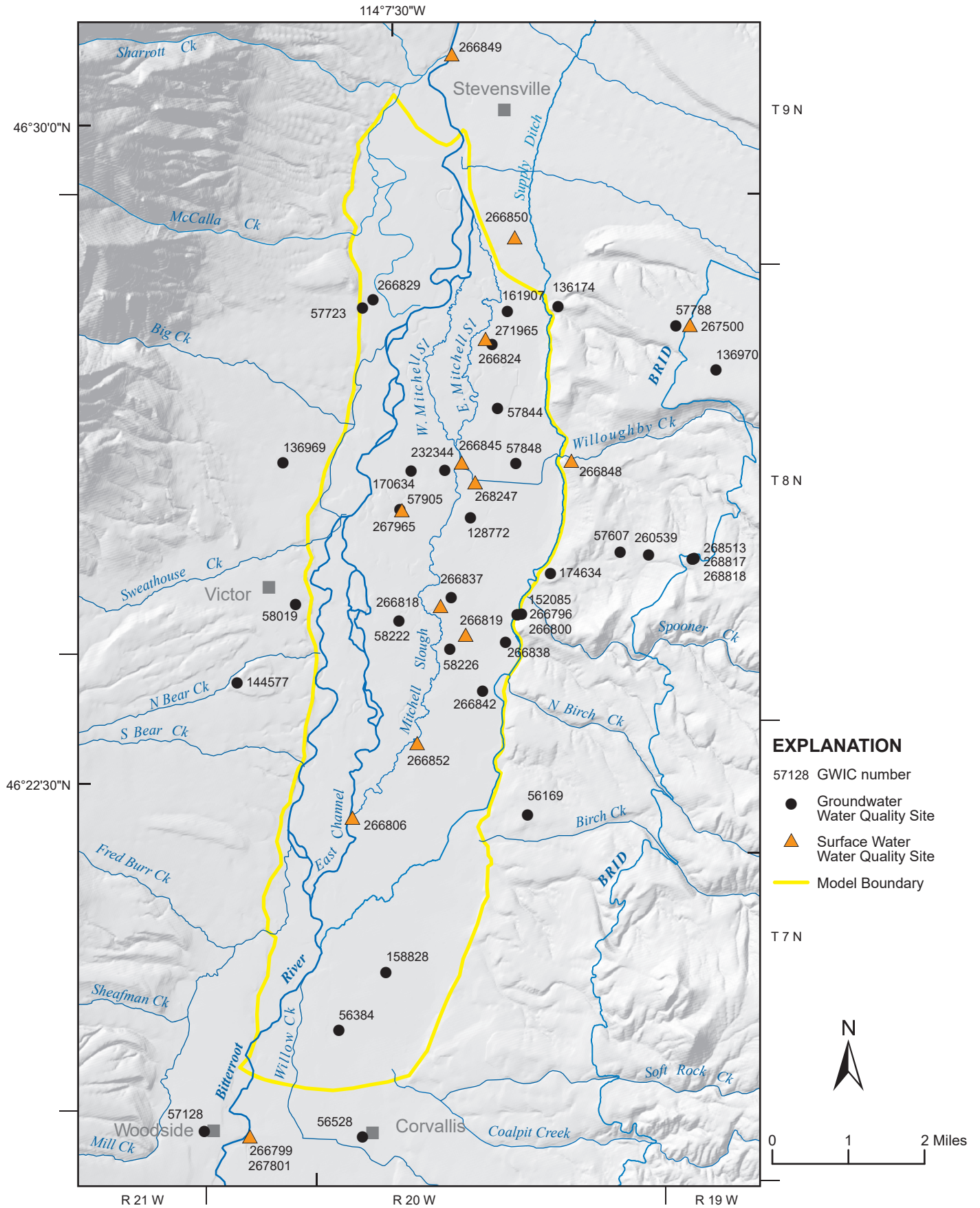


Figure 10. Water-quality samples were collected from wells and surface-water sites throughout the study area.

Canal Leakage

We examined leakage rates along a 2.2-mi section of Union Ditch from its headgate (near site 266852) to Victor (about 0.35 mi south of Victor Crossing, site 266839; fig. 9). No diversions were found in this reach. The inflow–outflow method was used to determine canal seepage (Sonnichsen, 1993). Stage was recorded hourly with pressure transducers at the headgate and at the downstream end near Victor. Rating curves were developed by correlating manual flow measurements to stage. Stages recorded with transducers were then used to calculate hourly ditch flow. The rate of loss (or gain) is expressed as the total loss (or gain) divided by the distance between two stations (cfs/mi).

We also considered leakage rates for a second, longer reach of Union Ditch from its headgate (near site 266852) to a site just south of Stevensville (site 266850), a reach of about 8 mi. On this reach, we measured flows and estimated withdrawals for irrigation and calculated an estimate of leakage. The estimates of irrigation withdrawals relied on irrigated acres and the efficiency of the irrigation method.

Groundwater is generally mineralized and carries more total dissolved solids (TDS) than water diverted from the Bitterroot River. Specific conductance can be used to estimate the TDS in a water sample (Hem, 1992). Here, we use SC to assess groundwater discharge along various reaches of canals, comparing SC measurements along surface-water reaches. Increases in SC suggest areas with more groundwater discharge.

Evapotranspiration by Phreatophytes

Cottonwood and willow acreage were identified by satellite imagery using the LANDFIRE database (USGS, 2010). An average evapotranspiration rate of 22 in/yr was applied to riparian areas, based on work by Hackett and others (1960) and Lautz (2008). This is a reasonable rate for large phreatophytes such as cottonwoods and willows in Montana and Wyoming. Evapotranspiration from phreatophytes was considered in the overall groundwater budget and groundwater models.

Water Well Logs

We used information from water well logs to evaluate subsurface conditions and generate estimates of aquifer properties. Drawdown is the difference

between the reported static and pumping water levels. The reported well yield is divided by the drawdown to generate a specific capacity value (gpm/ft). Driscoll (1986) provides the method used to estimate transmissivity from specific capacity. We estimated hydraulic conductivity (K) at each well by dividing the transmissivity by the saturated aquifer thickness. This analysis included records from 40 wells completed in the shallow aquifer and 17 wells completed in the deep aquifer (appendix A; table A-2).

Logs for water wells located in the study area were obtained from the GWIC database and well locations were verified using cadastral data or other means. This resulted in 271 well logs with accurate locations to evaluate subsurface hydrogeologic conditions. As described in appendix E, groundwater modeling software was used to interpret these logs and develop the geologic framework for the models. The drillers' descriptions of geologic materials were categorized into 18 lithologic units (appendix C).

Groundwater Modeling

We developed numerical groundwater models to simulate major changes in irrigation activities and assess subsequent effects on groundwater levels and surface-water flows. The conceptual model, presented later in the report, describes the hydrology and hydrogeology of the simulated area and provides the framework for developing the numerical model. Details on the model construction and calibration are provided in appendix E.

RESULTS

This section describes the hydrogeology of the Stevensville area based on the analysis and interpretation of data collected during this study and from previous investigations. Much of this information supported development of the conceptual model, presented below.

Hydrostratigraphy and Aquifer Properties

The hydrostratigraphy includes three aquifers and one aquitard. Figure 11 shows the general hydrostratigraphy of the study area.

Shallow Alluvial Aquifer

The shallow alluvial aquifer consists of the floodplain and low terrace deposits composed of Quaternary fine to medium sand and fine- to coarse-grained

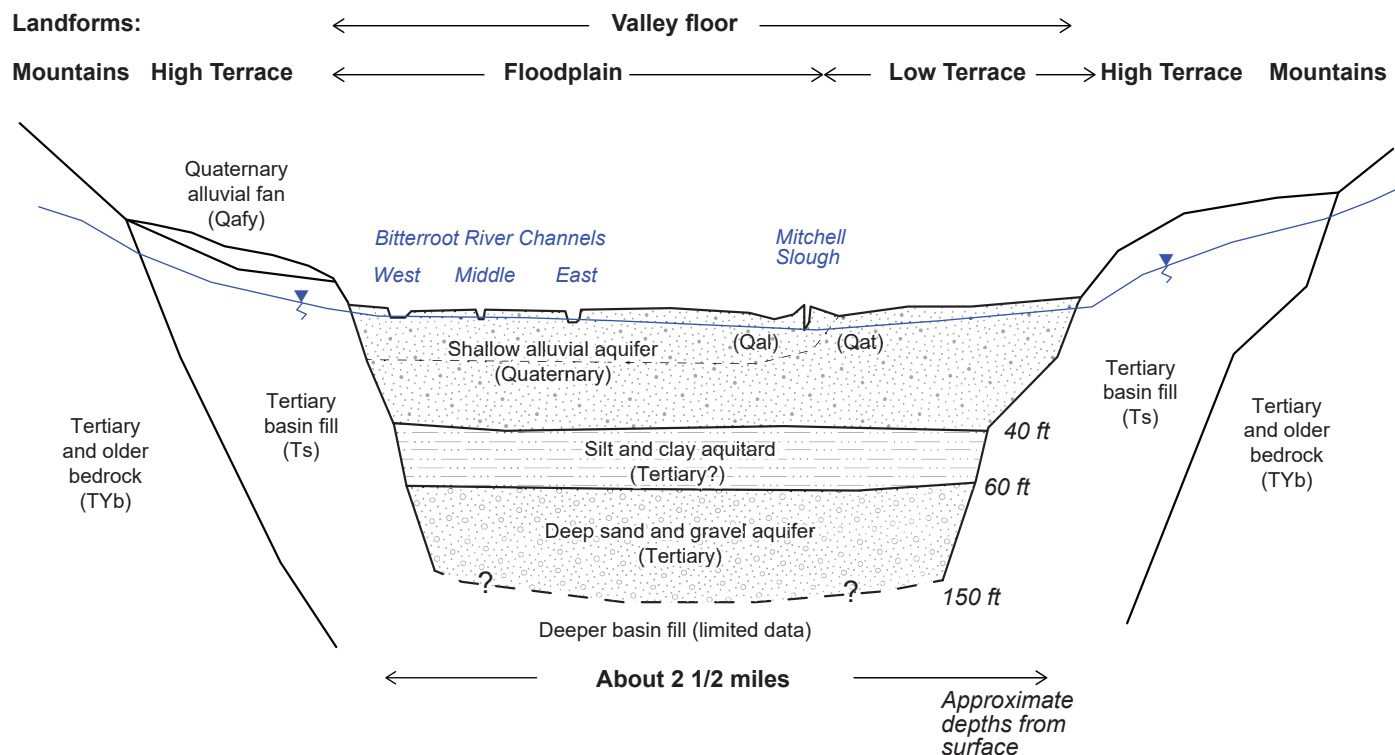


Figure 11. Schematic east–west cross section at Victor Crossing (not to scale) shows the shallow alluvial aquifer (Qal and Qat), the silt and clay aquitard, and the deep sand and gravel aquifer. Refer to figure 6 for geologic unit descriptions.

gravels (Qal and Qat; fig. 11). The bottom of the aquifer can extend to 90 ft below ground surface (bgs), but the average depth is about 40 ft (fig. 11). Well logs report an average static depth to water of 10 ft, with an average well yield of 54 gpm. Estimates of transmissivity and hydraulic conductivity, based on specific capacity tests, range from 100 to about 4,000 ft²/d, and 4 to 215 ft/d, respectively.

Uthman (1988), relying on literature values, estimated hydraulic conductivity of the valley floor sediments at 130 ft/d. Finstick (1986) estimated a transmissivity of 320 ft²/d for the alluvial sediments based on specific capacity. Assuming an aquifer thickness of 40 ft, this results in a hydraulic conductivity of about 8 ft/d.

Several aquifer tests are reported from the valley floor area. McMurtrey and others (1959, 1972) provide estimates for transmissivity from four tests conducted on the low terrace between Corvallis and Stevensville (fig. 6). These test sites were shallow pits or wells less than 15 ft deep completed in the alluvium. They report a range in transmissivity from 17,000 to 31,000 ft²/d. Assuming an aquifer thickness of 40 ft, hydraulic conductivity ranges from 425 to 775 ft/d.

Silt and Clay Aquitard

Well records document a layer of predominantly fine-grained sediment underlying the shallow aquifer. This unit consists primarily of sand, silt, and clay, based on lithologic descriptions from records of 17 deep wells (appendix A; table A-2). The thickness of the unit varies from about 2 to 30 ft, averaging about 20 ft (fig. 11).

Seasonal groundwater-level responses in the shallow alluvial aquifer and the deep sand and gravel aquifer are similar; however, wells completed in the deep sand and gravel aquifer (wells 57905 and 136183) produce a potentiometric surface that is about 0.7 ft above wells in the shallow alluvial aquifer, indicating the silt and clay act as an aquitard, confining the deep sand and gravel aquifer.

Deep Sand and Gravel Aquifer

The deep sand and gravel aquifer underlies the aquitard, and consists of Tertiary alluvium (fig. 11). The depths of wells completed in this aquifer range from 58 to 163 ft (appendix A; table A-2). Well logs report sand and gravel at these depths, with an average depth to static water level of 17 ft and yield of 58 gpm. Transmissivity, estimated from specific capacity tests, ranges from 53 to 2,299 ft²/d. Based on the esti-

mated aquifer thickness at each well (total well depth subtracted from the top of the formation), hydraulic conductivity ranges from 4 to 287 ft/d.

Tertiary Aquifer

The Tertiary aquifer includes the basin-fill that underlies the high terraces and bounds the Quaternary and Tertiary alluvial deposits (fig. 11). This aquifer consists of low-permeability silt and clay with sand and gravel intervals (Smith, 2013). McMurtrey and others (1972) estimated the transmissivity of the eastside Tertiary aquifer based on aquifer tests in five wells. They report a range of 2,400 to 18,000 gpd/ft (320–2,400 ft²/d). Assuming an aquifer thickness equal to the reported depths of these five wells, the hydraulic conductivity varies from 5 to 120 ft/d. However, the two higher values were associated with wells less than 30 ft deep. The three deeper wells, with depths from 47 to 160 ft, produced hydraulic conductivity values from 5 to 10 ft/d.

Uthman (1988) discussed the results of McMurtrey and others (1972), concluding that a transmissivity of about 7,500 gpd/ft (1,000 ft²/d) was reasonable for clay-rich water-bearing zones, such as these Tertiary deposits. This results in hydraulic conductivities of 5 to 10 ft/d, based on aquifer thicknesses of 100 to 200 ft.

Bedrock Aquifer

The bedrock aquifer is surficially exposed near the project boundary to the east and west of the Bitterroot River (fig. 6). Based on well logs, three of the four bedrock wells in our monitoring network are completed in granite (wells 154007, 246207, and 260539). The fourth well (207831) is located less than 100 ft from well 246207 and therefore is also most likely completed in granite. Water yields reported on well logs for these wells ranged from 6 to 15 gpm. The bedrock aquifer was not extensively characterized during this study, nor is it included in the groundwater model domain. While it is important locally to homes and ranches that rely on it for water supply, the bedrock is generally a low-yield aquifer and not a significant source of groundwater compared to the aquifers described above.

Groundwater

Potentiometric Surface

Water levels measured in wells completed in the shallow alluvial aquifer and the stage at selected

stream sites during March 2013 were used to develop the potentiometric surface map (fig. 12). Groundwater elevation data from this study was limited on the high terraces, and we relied on the shallow basin-fill groundwater contours generated by LaFave (2006a) to guide development of the 2013 potentiometric surface map.

Groundwater flows perpendicular to potentiometric contours, and this map shows that groundwater flows from the high terraces in the Tertiary aquifer towards Quaternary alluvium underlying the valley floor. The groundwater gradient in the Tertiary aquifer ranges from 100 to 300 ft/mi (0.019 to 0.057). Beneath the eastern low terraces of the valley floor, leakage from several canals influences groundwater flow. Within the valley floor area, groundwater in the shallow alluvial aquifer flows northward with a gradient of about 15 ft/mi (0.003). The potentiometric surface for the valley is similar to that mapped by McMurtrey and others (1972) 40 yr earlier.

Groundwater-Level Fluctuations

Recharge to aquifers occurs through precipitation, snowmelt, irrigation return flows, and losing streams. Groundwater discharges to streams, springs, and wells. The timing and magnitude of seasonal groundwater trends provide information on the sources of aquifer recharge. Long-term records that extend over several years or decades may show the influence of stresses on the hydrogeologic system, such as drought, wet periods, or changes in groundwater pumping.

The hydraulic conductivity of aquifer sediments and whether an aquifer is under confined or unconfined conditions affect the response of groundwater levels to changes in recharge or pumping. Because hydraulic conductivity and the extent of confined conditions can vary locally, water-level response is not always predictable and is often specific to an individual well. Wells used in this study to illustrate seasonal and long-term groundwater response are shown in figure 8.

Seasonal Groundwater Trends

Seasonal changes in groundwater levels reflect factors such as the well location (floodplain, low or high terrace, and bedrock) and the influence of surface water, irrigation, and precipitation.

Groundwater levels in aquifers beneath the floodplain generally reflect Bitterroot River stage and the

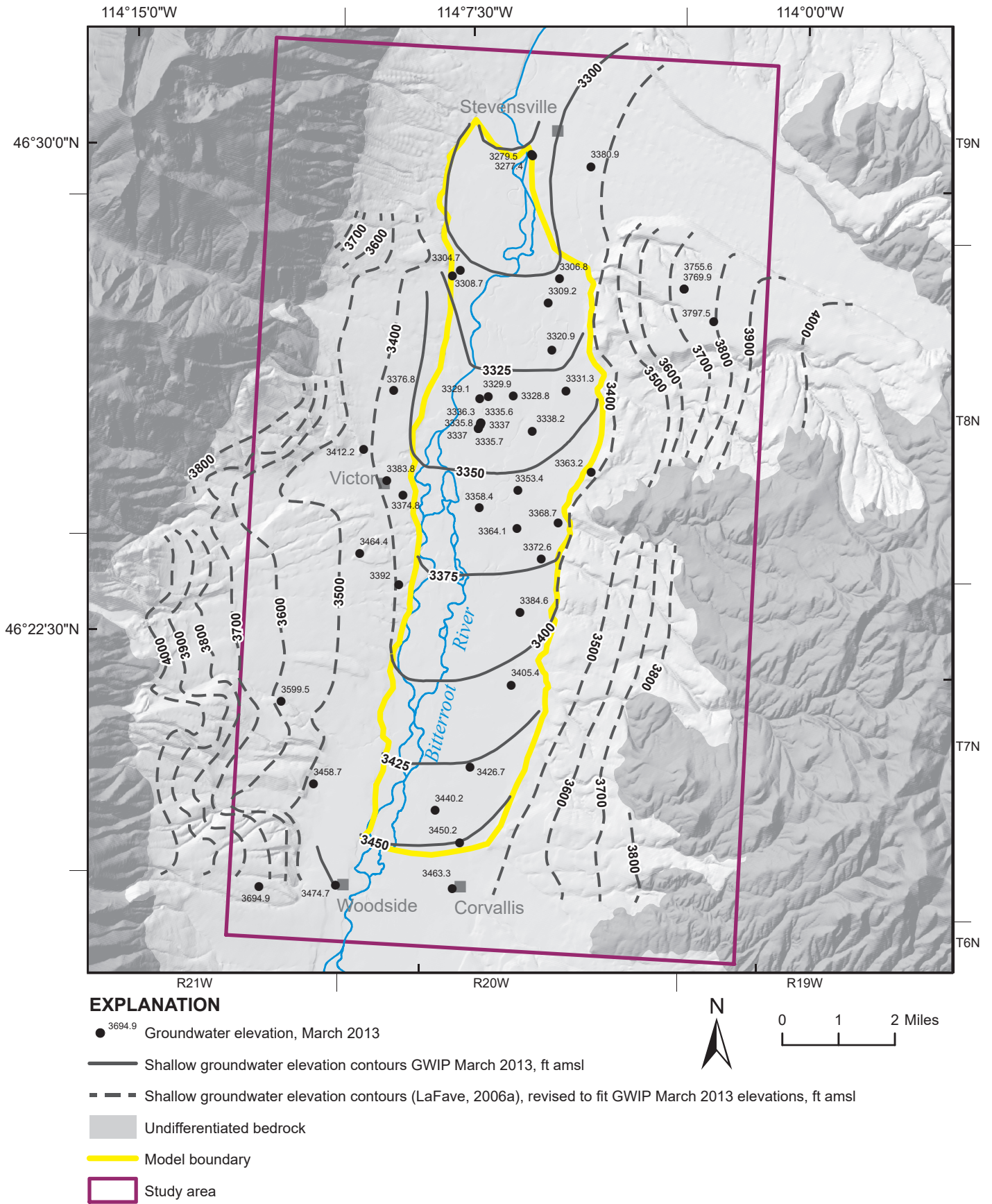


Figure 12. The potentiometric surface of the shallow alluvial aquifer in the valley floor is based on the measurements made during March 2013 and listed in appendix A. The dashed contours shown in the high terrace areas are based on the potentiometric contours from LaFave (2006a), modified in some areas with recent data.

influence of nearby ditches and irrigation activities. Groundwater levels monitored in the floodplain were from wells completed in the shallow alluvial aquifer or the underlying deep sand and gravel aquifer.

The hydrograph for well 266089 illustrates the relationship between groundwater and the nearby Gerlinger Ditch, which is diverted from the Bitterroot River (fig. 13A). The 21-ft-deep well is 27.5 ft from the ditch staff gage (site 267520). The Bitterroot River stage record is from the nearest gaging site (site 266820), about 0.85 mi downstream. Stage fluctuations are similar in the ditch, the Bitterroot River, and groundwater during high flows (May–June), the ditch responding mostly to headgate management and irrigation return flows. Groundwater elevation exceeds the ditch stage most of the year, indicating groundwater discharge to the ditch. The Gehrlinger Ditch, which flows all year, acts as a groundwater drain during the non-irrigation season.

Wells monitored in the low terrace areas are completed in the shallow alluvial and the deep sand and gravel aquifers. Groundwater levels in wells monitored on the low terrace typically reach a minimum level at the end of winter or early spring and rise rapidly in May or June at the onset of irrigation and peak runoff. Water levels remain elevated during the summer as a result of irrigation recharge, typically decline rapidly in the early fall, and taper off in the winter (fig. 13B). Groundwater levels monitored in the low terrace fluctuate about 6 ft seasonally.

Wells monitored in the high terrace areas are completed in either bedrock or the Tertiary aquifer, at depths ranging from 80 to 550 ft. Generally, the largest seasonal groundwater fluctuations observed during this study occur in the Tertiary aquifer, along the high terrace. Representative hydrographs show three seasonal groundwater responses: (1) little seasonal change, (2) response to irrigation activities, and (3) a delayed response to irrigation. Relatively deeper wells (180–340 ft) completed in bedrock and in Tertiary sediments on the high terrace tend to show little seasonal groundwater-level response (fig. 13C). Shallow wells (87–162 ft) on the high terrace completed in the Tertiary aquifer, downgradient of the BRID, typically show response to irrigation recharge (fig. 13D). A wintertime peak in groundwater elevation occurs in some deep wells in the Tertiary aquifer (fig. 13E), and is likely related to a delayed response to irrigation recharge.

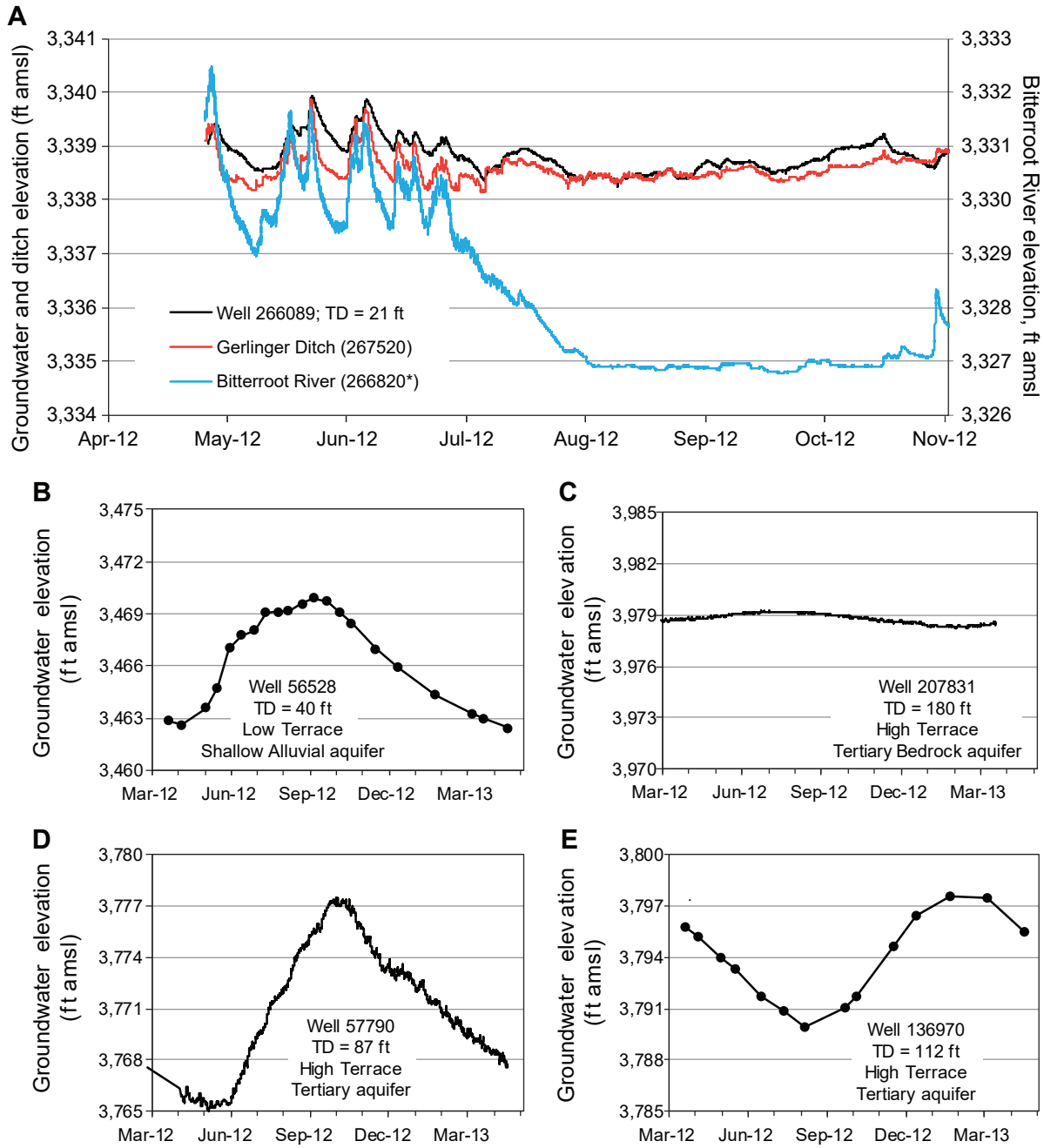
Long-Term Groundwater-Level Trends

Eleven statewide groundwater monitoring network (GWAAMON) wells provide long-term groundwater-level data. We apply Smith's (2006c) classification system for long-term water-level trends in Bitterroot Valley aquifers to understand these records. Water-level responses fit into five categories: irrigation, irrigation and runoff, runoff, stream recharge, and usage.

Well 56528, located in Corvallis on the low terrace, provides the only long-term record from within the valley floor. Monitoring extends from 1972 to present day, with a break in the record from 1983 to 1993. Water levels fluctuate seasonally between about 6 and 16 ft (fig. 14A). The seasonal pattern is similar to groundwater fluctuations observed in the valley floor area (fig. 13B), with greater than average amplitude. This record indicates groundwater levels are stable over the period of record, and the seasonal variations are driven principally by irrigation recharge. This record demonstrates that groundwater levels at all times of year are artificially high due to recharge from irrigation; this response is common in irrigated valleys.

The record from well 136969 extends from 1957 to present day (fig. 14B). This well is located on the eastern toe of the western high terraces, about 2 mi directly north of Victor and about ½ mi west of the floodplain (fig. 8). Annual highs are within 5 ft throughout the period of record. A step change in water level in 2001 is attributed to climatic influence, as the 1 ft drop in water level occurs during a below normal precipitation period (fig. 5). This record reflects generally stable annual levels, with water-level rise each summer and decline in the fall/winter in the irrigated, central portion of the study area. Other wells with similar records are completed at lower elevations on high terraces or alluvial fans, including wells 57128, 136050, 132260, 58096, and 60137. Water levels in these wells are generally stable over the period of record, with seasonal fluctuations on the order of 5 to 15 ft.

Water levels in wells completed in the marginally productive Tertiary and bedrock aquifers of the high terraces, especially at higher elevations, show more variable conditions. Water levels in well 130860, completed in the Tertiary aquifer, were stable until 2007 (fig. 14C), when they appear to be affected by increased summertime pumping. Water levels are drawn



*The data is derived from US Geological Survey site 12350250 (Bitterroot River at Bell Crossing).

Figure 13. Groundwater levels typically fluctuate seasonally but differ from well to well as demonstrated by these hydrographs.

down about 40 to 100 ft and recover substantially, but not completely, during winter. Other wells in the Tertiary aquifer show similar large fluctuations, including wells 134503 and 136970.

Two wells completed in the Tertiary bedrock aquifer on the eastern high terrace also reflect effects of pumping from low-productivity aquifers. Wells 207831 and 246207 (figs. 14D and 14E, respectively), are located about 4 mi northeast of Corvallis. Well 207831 is a 180-ft-deep domestic well with water-level declines

through 2006 due to pumping. This well was replaced by well 246207, drilled about 380 ft from well 207831 to a depth of 440 ft. Water levels in well 207831 recovered as the water levels declined in the new pumping well.

Bitterroot River Stages and Discharge

Discharge peaks in the Bitterroot River during 2012 and 2013 correspond to spring snowmelt from the Sapphire and Bitterroot ranges and fall precipitation events (fig. 15). Because the Bitterroot Range is

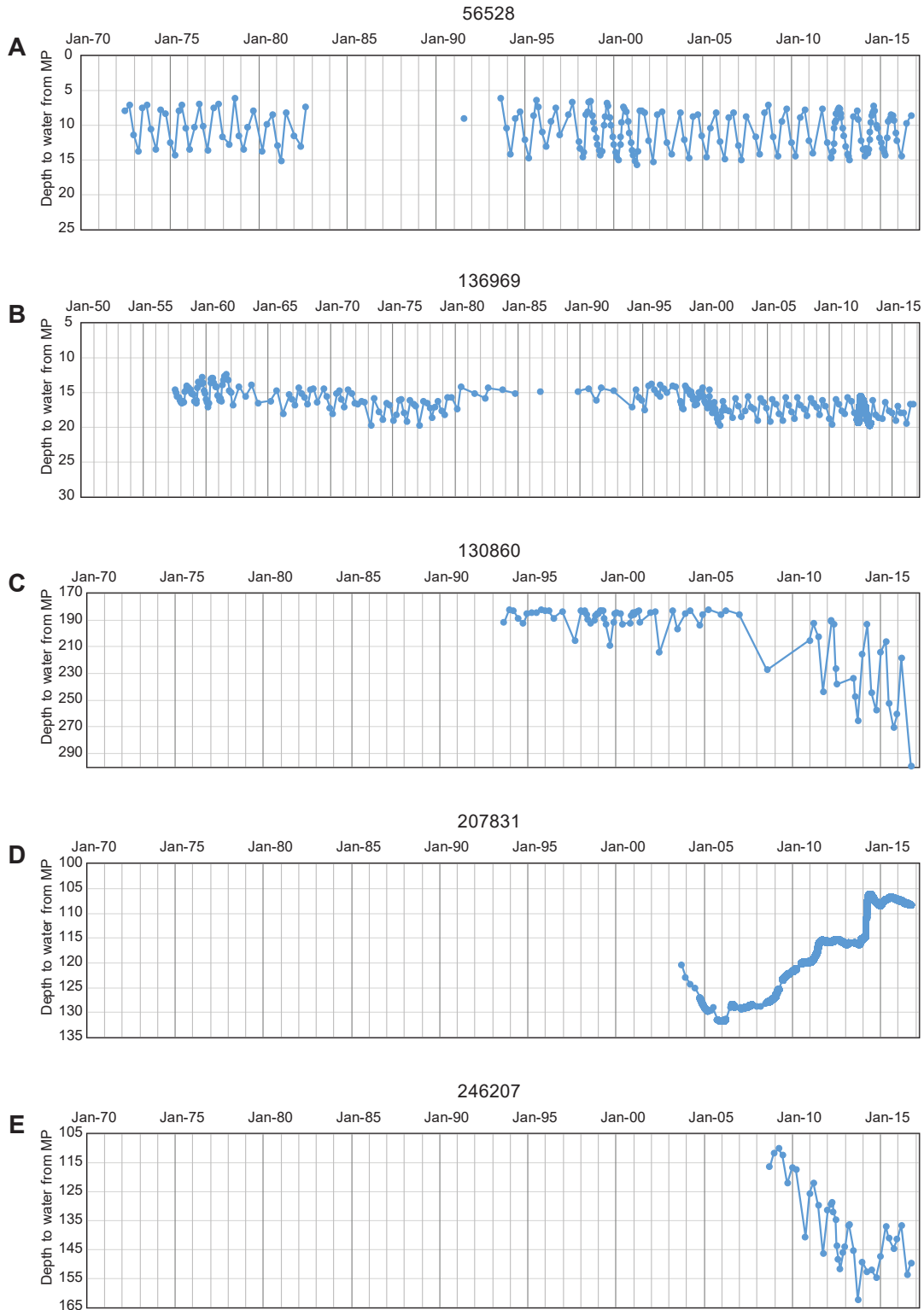


Figure 14. Long-term groundwater-level trends are typically stable in wells located in irrigated portions of the valley floor, as displayed in graphs A and B. Water levels in well 130860 (C) are likely affected by nearby seasonal pumping, which appears to have increased after 2006. The water levels shown in graphs D and E are from wells that are several hundred yards apart. Well 207831 (D) was replaced by the use of well 246207 (E) around 2008.

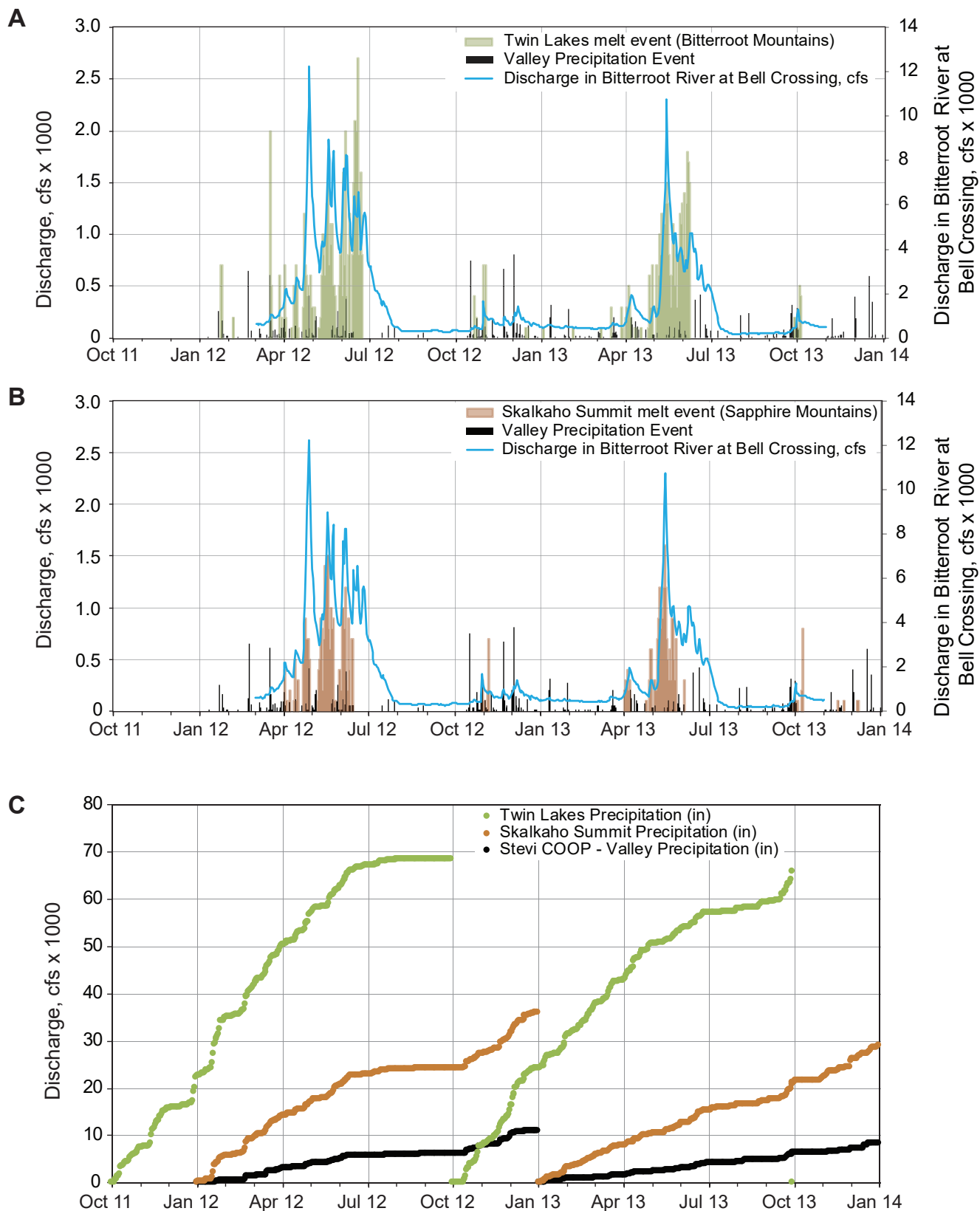


Figure 15. The hydrograph of Bitterroot River flow shows a strong response to snowmelt (NRCS, 2014). Precipitation data from Stevensville COOP (2014).

at a higher elevation, snow lingers in the mountains and contributes to summer discharge peaks, typically in mid to late June (fig. 15A). Discharge is also controlled by releases from Painted Rocks Reservoir into the West Fork of the Bitterroot River and summer irrigation withdrawals that reduce the flows in the river and its tributaries. Discharge increases following the irrigation season, in October through December.

During this study, peak flow at Bell Crossing (USGS gage 12350250) occurred earlier, and at a greater magnitude, than average conditions. Discharge reached about 13,000 cfs in April 2012 and 12,000 cfs in May 2013, compared to the 20-yr average of about 7,200 cfs in early June (fig. 16). Low flows occur in August through October, decreasing to 300 cfs and to about 200 cfs in 2012 and 2013, respectively. The Bitterroot River commissioner maintains river discharge above 200 cfs by augmenting flow with water from Painted Rocks Reservoir. Low flows in 2012 and 2013 were below average low-flow conditions.

The timing of fall discharge peaks reflect weather patterns. In 2012, this peak occurred in late October at about 1,800 cfs. In 2013, the peak occurred earlier, in late September, at a flow of about 1,400 cfs, as a result of a large, 7.2-in precipitation event (Twin Lake SNOTEL Site NRCS, 2014). On average, the fall discharge peak occurs in mid- to late November. Typically, the USGS discontinues stream gaging at Bell Crossing in October; however, this project funded the USGS operation of the station through the winter of 2012. Fall discharge peaks are affected by early season snowmelt/precipitation events, reduced irrigation diversions, and irrigation return flows.

Surface-Water Conditions in the Valley Floor

Management of surface water in the floodplain and low terraces influences groundwater levels beneath the valley floor. Irrigation canals divert surface water from about mid-April to mid- to late October and contribute to groundwater recharge where the canals lose water to the aquifer. Canals located within the floodplain and some portions of the low terraces either gain or lose

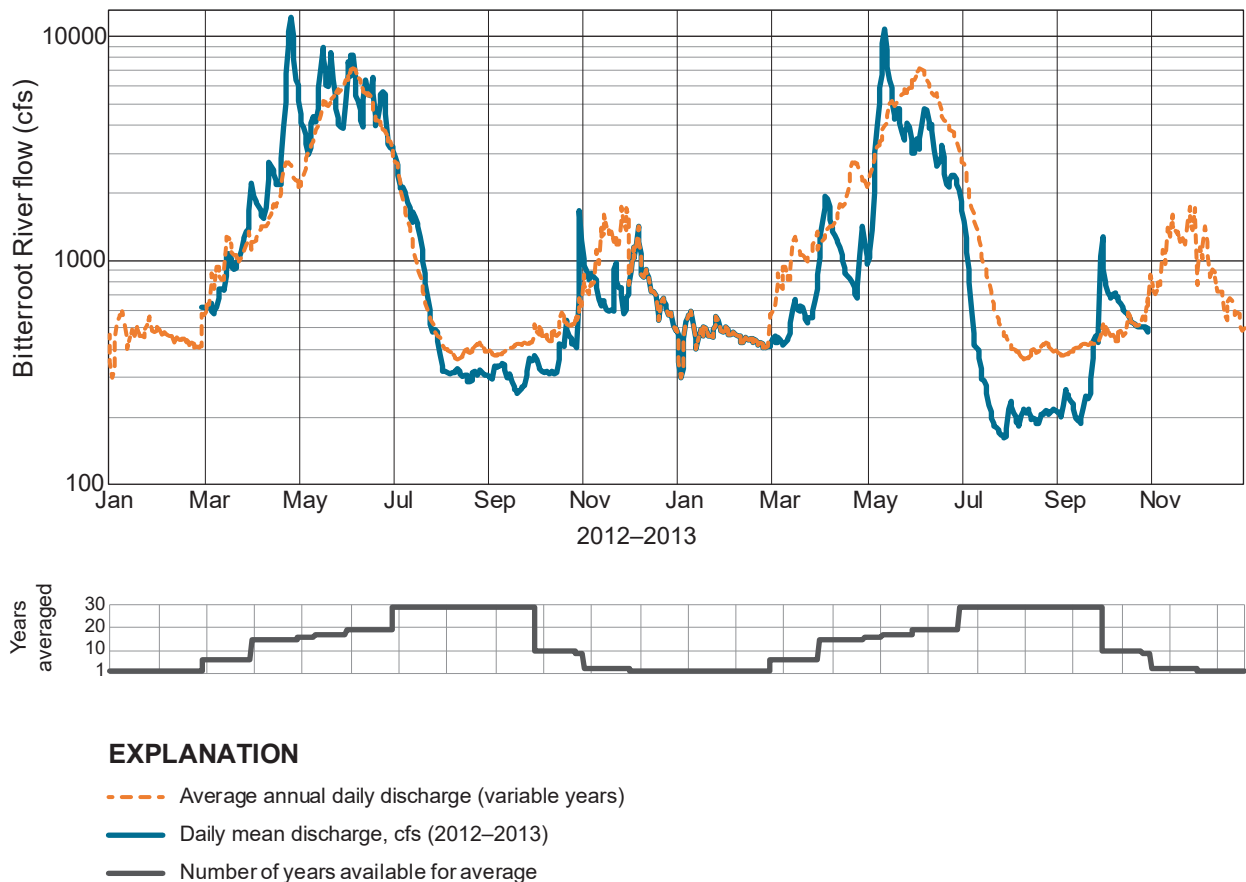


Figure 16. The discharge of the Bitterroot River during 2012 and 2013 is compared with daily average flows (1997–2015). Data from 2012–2013 show that peak flows occurred earlier than the daily average flows.

water depending on the head in the canal relative to the water table. Typically, canals and ditches located on higher ground toward the east edge of the low terrace lose water to the underlying aquifer.

Mitchell Slough flows year-round. A headgate controls the amount of water delivered from the East Channel during irrigation season. Water leaking beneath the headgate continues to flow in Mitchell Slough while the headgate is closed. Mitchell Slough also gains water from other ditches and groundwater.

In 2012, from April to late July, flow at the headgate ranged from 20 to 105 cfs, averaging 54 cfs (fig.

17). During the rest of the irrigation season, flow was less variable, ranging from 36 to 53 cfs and averaging 43 cfs. The headgate was closed on October 31; after the closure, flow averaged 8 cfs.

During 2013, peak flow at the headgate was about 80 cfs—approximately 25 cfs lower than peak flow during the 2012 irrigation season. On July 1, 2013, discharge sharply increased when local irrigators dredged the East Channel to improve its connection to the Bitterroot River.

The flow increase in the Slough from the headgate to Bell Crossing indicates that the slough gains water

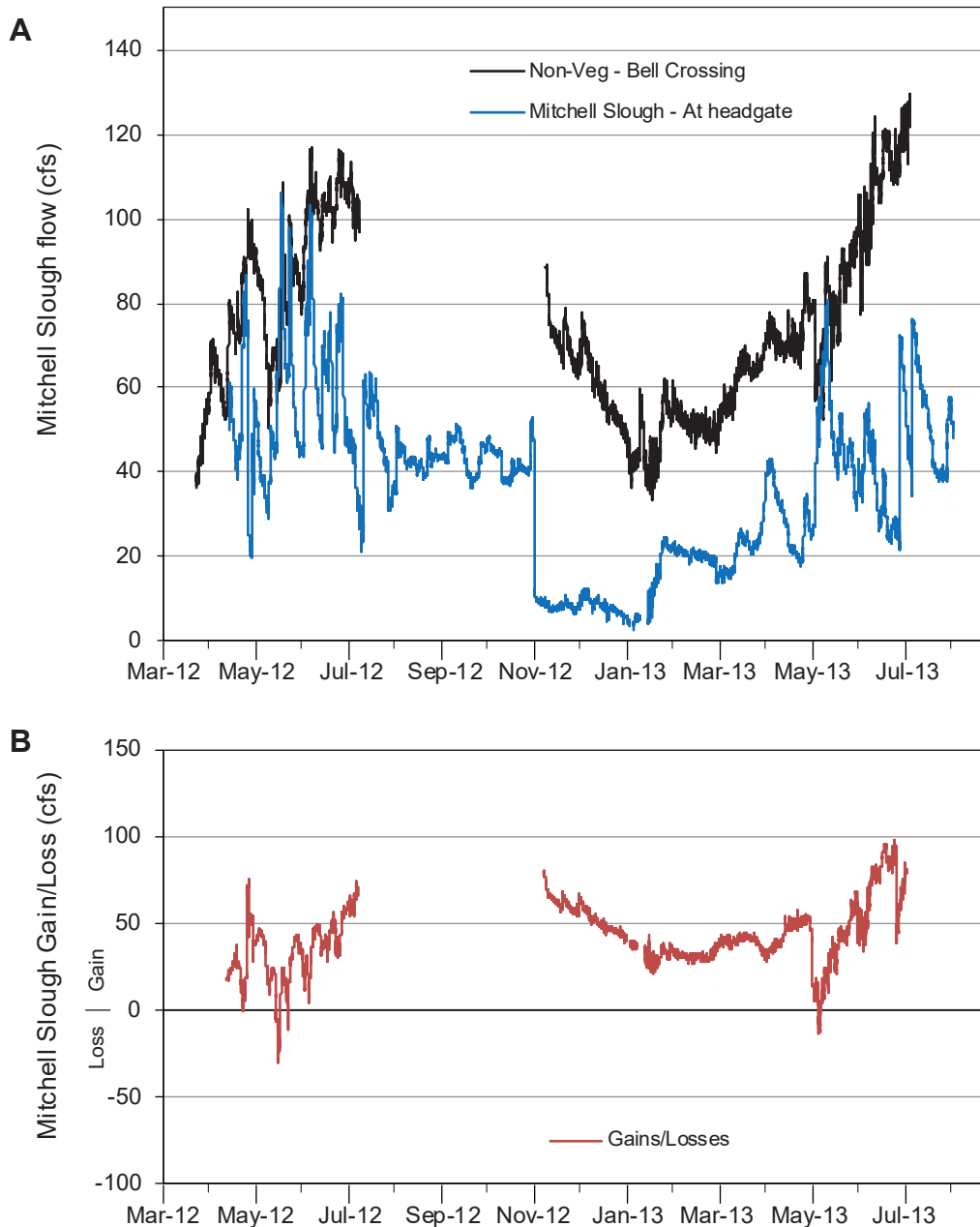


Figure 17. Flow in Mitchell Slough during most times of the year is typically greater at Bells Crossing compared to the headgate (A). Therefore, the Slough gains flow in this reach during most times of the year (B). Vegetation growing in the canal causes deviations from the stage–discharge relationship; therefore, these data are not presented for the summer months at Bell Crossing.

from both groundwater and surface water from ditches (fig. 17B). The gain in discharge between the headgate and Bell Crossing ranges from 0 to 100 cfs, and increases as irrigation season progresses. The correlation between these gains and the irrigation season suggest the gain is primarily irrigation return flow. Specific conductance measured along the slough provides strong evidence for groundwater contributions (fig. 18). These results are discussed in the Water Chemistry section.

Recharge to Groundwater from Irrigation

Groundwater recharge from irrigation is a combination of excess water applied to fields that is not consumed by the crops and loss of water from canal leakage.

Applied Irrigation Water

We estimated monthly recharge from excess applied irrigation water for alfalfa by considering the irrigation method and the acres irrigated by each method (table 1). Negative recharge values result from potential ET exceeding precipitation and indicate that no recharge occurred that month. The distribution and method of irrigation are shown in figure 19. Within the model area, 3,378 acres are flood irrigated and 4,198 acres are irrigated by sprinkler and pivot. Estimates

of irrigation recharge are 18.6 in per year from flood, about 6.3 in from sprinkler, and 4.0 in from pivot irrigation. The bulk of this recharge occurs in June, July, and the first half of August.

Canal Leakage

We examined leakage rates along a 2.2-mi section of Union Ditch from the Double Fork headgate (site 266852) to about 0.35 mi south of Victor Crossing (site 266839; fig. 9). Union and Etna Ditches, located on the low terrace, are diverted from Mitchell Slough. Union Ditch flows northward to Stevensville (fig. 7). Etna Ditch runs parallel to Union Ditch, and its headgate is located near the Union Ditch headgate. The amount of ditch flow is determined by the stage of Mitchell Slough as well as release of water through their respective headgates. In 2012, Union Ditch’s discharge averaged 29 cfs (ranging between 7 and 48 cfs; fig. 20) and Etna Ditch’s discharge averaged 19 cfs (ranging between 6 and 51 cfs).

No known diversions exist in the 2.2-mi reach of Union Ditch. Leakage from the ditch over the entire reach averaged 7.6 cfs (3.5 cfs/mi), with a range of 1 to 19 cfs. Leakage was greater from mid-May to early August, averaging 5.2 cfs/mi. Leakage decreased through the rest of the irrigation season to about 2.0

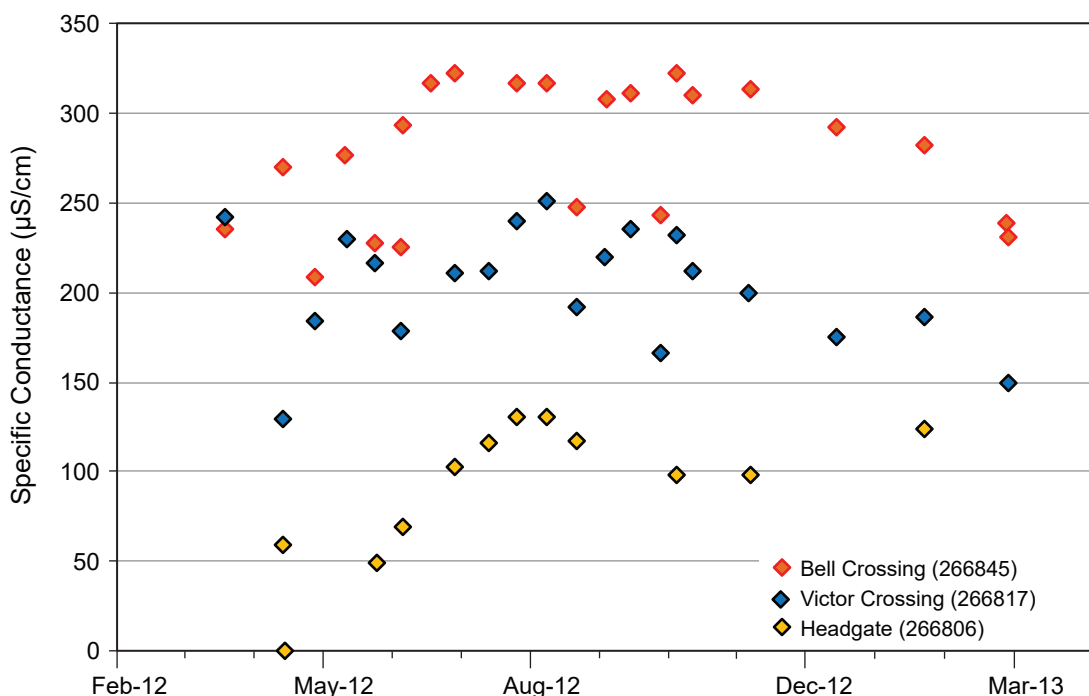


Figure 18. Specific conductivity increases at sites downstream from the Mitchell Slough Tucker Headgate, suggesting gains from higher SC groundwater. Locations on Mitchell Slough are shown in figure 9.

Table 1. Groundwater recharge due to irrigation for alfalfa.

	Percent Efficient	Net Irrigation Requirement (in)	NIR*/ Efficiency	Precip** (in)	Total Applied	ET (in)	Recharge (in)
April (starting at the 10th of April)							
Flood	45%	0	0	0.75	0.75	1.23	-0.48
Sprinkler	70%	0	0	0.75	0.75	1.23	-0.48
Pivot	80%	0	0	0.75	0.75	1.23	-0.48
May							
Flood	45%	0.81	1.80	0.73	2.53	3.89	-1.36
Sprinkler	70%	0.88	1.26	0.73	1.99	3.89	-1.90
Pivot	80%	1.09	1.36	0.73	2.09	3.89	-1.80
June							
Flood	45%	4.93	10.96	1.18	12.14	5.77	6.37
Sprinkler	70%	4.98	7.11	1.18	8.29	5.77	2.52
Pivot	80%	5.14	6.43	1.18	7.61	5.77	1.84
July							
Flood	45%	6.66	14.80	0.72	15.52	7.19	8.33
Sprinkler	70%	6.70	9.57	0.72	10.29	7.19	3.10
Pivot	80%	6.80	8.50	0.72	9.22	7.19	2.03
August							
Flood	45%	4.21	9.36	0.59	9.95	6.05	3.90
Sprinkler	70%	4.27	6.10	0.59	6.69	6.05	0.64
Pivot	80%	4.47	5.59	0.59	6.18	6.05	0.13
September							
Flood	45%	0	0	0	0	2.37	-2.37
Sprinkler	70%	0	0	0	0	2.37	-2.37
Pivot	80%	0	0	0	0	2.37	-2.37
Season (sum of positive values, above 6 mo)							
Flood	45%	16.61	36.92	3.97	40.89	26.50	18.6
Sprinkler	70%	16.83	24.04	3.97	28.01	26.50	6.3
Pivot	80%	17.5	21.88	3.97	25.85	26.50	4.0

*NIR, Net Irrigation Requirement

**Precipitation

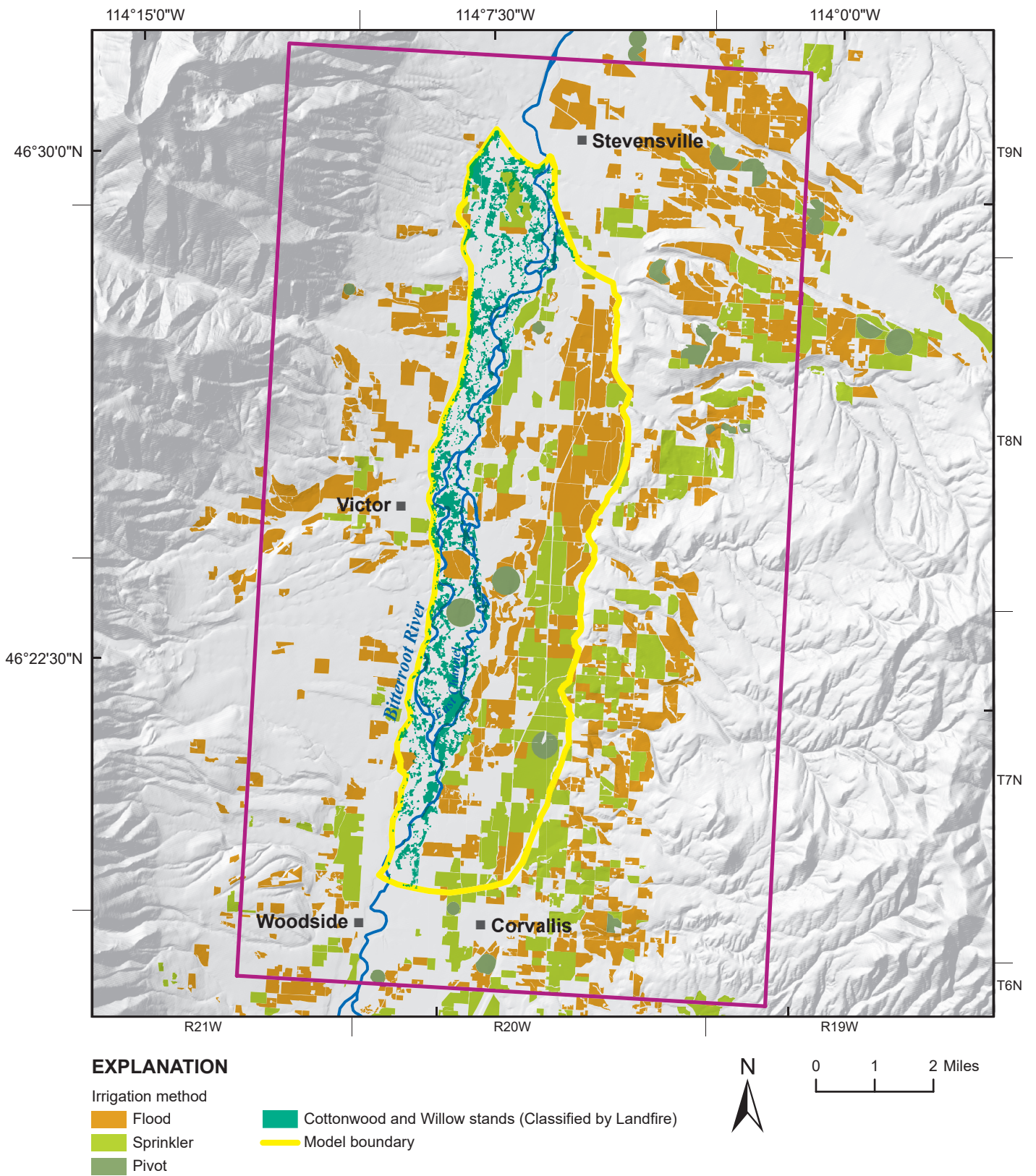


Figure 19. This map shows the irrigation methods for lands within and near the study area, and the mapped cottonwood and willow groves in the floodplain.

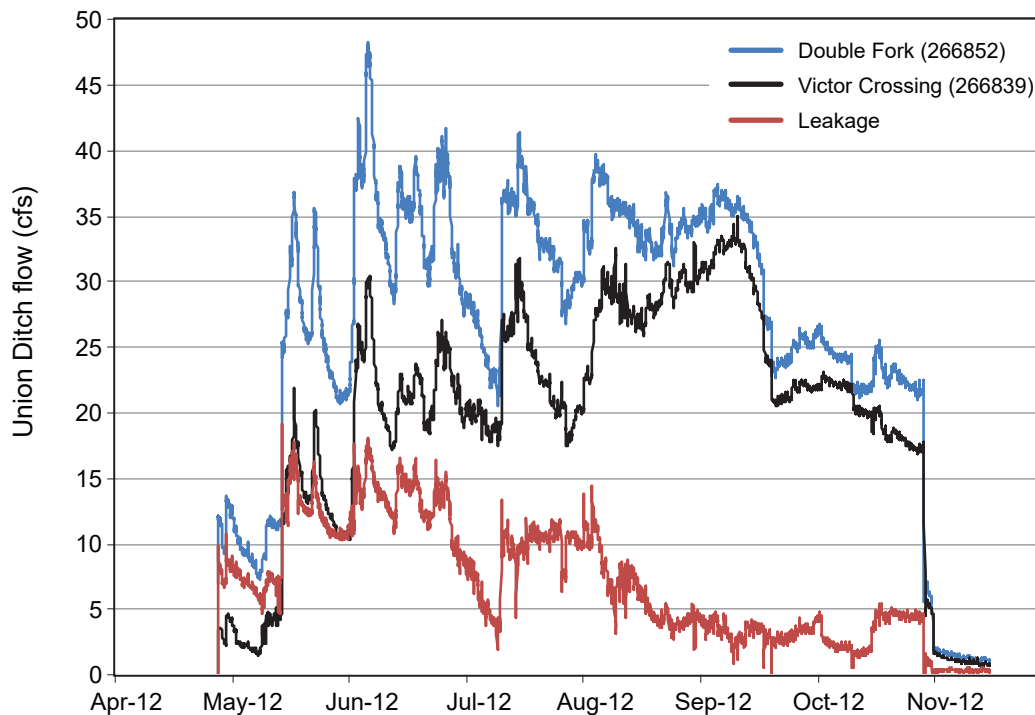


Figure 20. Union Ditch flows are higher at the Double Fork Ranch when compared to Victor Crossing. There are no known diversions between these gaging sites, so canal leakage is determined by the difference in the estimated flows.

cfs/mi (fig. 20). Less ditch loss may be due to increased vegetation within the ditch and/or sedimentation that restricted flow. Specific conductance measured in Union Ditch at the headgate and near Victor was steady, varying only by 10 $\mu\text{s}/\text{cm}$. This indicates that groundwater is not entering the ditch, supporting the interpretation that the ditch loses water along this reach.

Another estimate of leakage from Union Ditch was made along the 7.6-mi reach extending from the headgate (site 266852) to the north near Stevensville (site 266850). Flow diverted from the Union Ditch headgate averaged around 35 cfs. Flow was about 8 cfs near Stevensville. The crops irrigated with ditch water require about 12 cfs based on an estimated 1,200 acres (MT-DNRC, 2016) of irrigated alfalfa. Therefore, about 15 cfs is unaccounted for, resulting in an estimated average loss of 2 cfs per mile.

Water Chemistry

Water chemistry varies throughout the natural environment and can provide information about the source and movement of groundwater and surface water through a hydrologic system. We characterized water chemistry based on major cations and anions and measurements of SC.

General Water Chemistry

Water analyses from Bitterroot River samples indicate the river has a calcium-bicarbonate type water, with increasing TDS in a downstream direction. The TDS in the Bitterroot River during August 2012 increased downstream from 50.8 mg/L at Woodside Crossing (site 266799) to 89.8 mg/L at Stevensville cutoff (site 266849).

Groundwater samples from all wells in the valley floor have calcium-bicarbonate type water (fig. 21). Because the Bitterroot River is the source of most of the irrigation water on the valley floor and irrigation water provides groundwater recharge, shallow groundwater is, not surprisingly, the same type of water. Groundwater samples from wells outside of the valley floor have variable water types due to higher sodium and magnesium concentrations.

Stiff diagrams (fig. 22; Stiff, 1951) provide a graphical representation of the major ion chemistry of water samples in millequivalents per liter (meq/L). The increasing TDS in the Bitterroot River samples, indicated by the wider symbol, results from higher concentrations in the downstream sample (TDS increases from 51 mg/L at Woodside Crossing (site 266799) to 90 mg/L at Stevensville (site 266849);

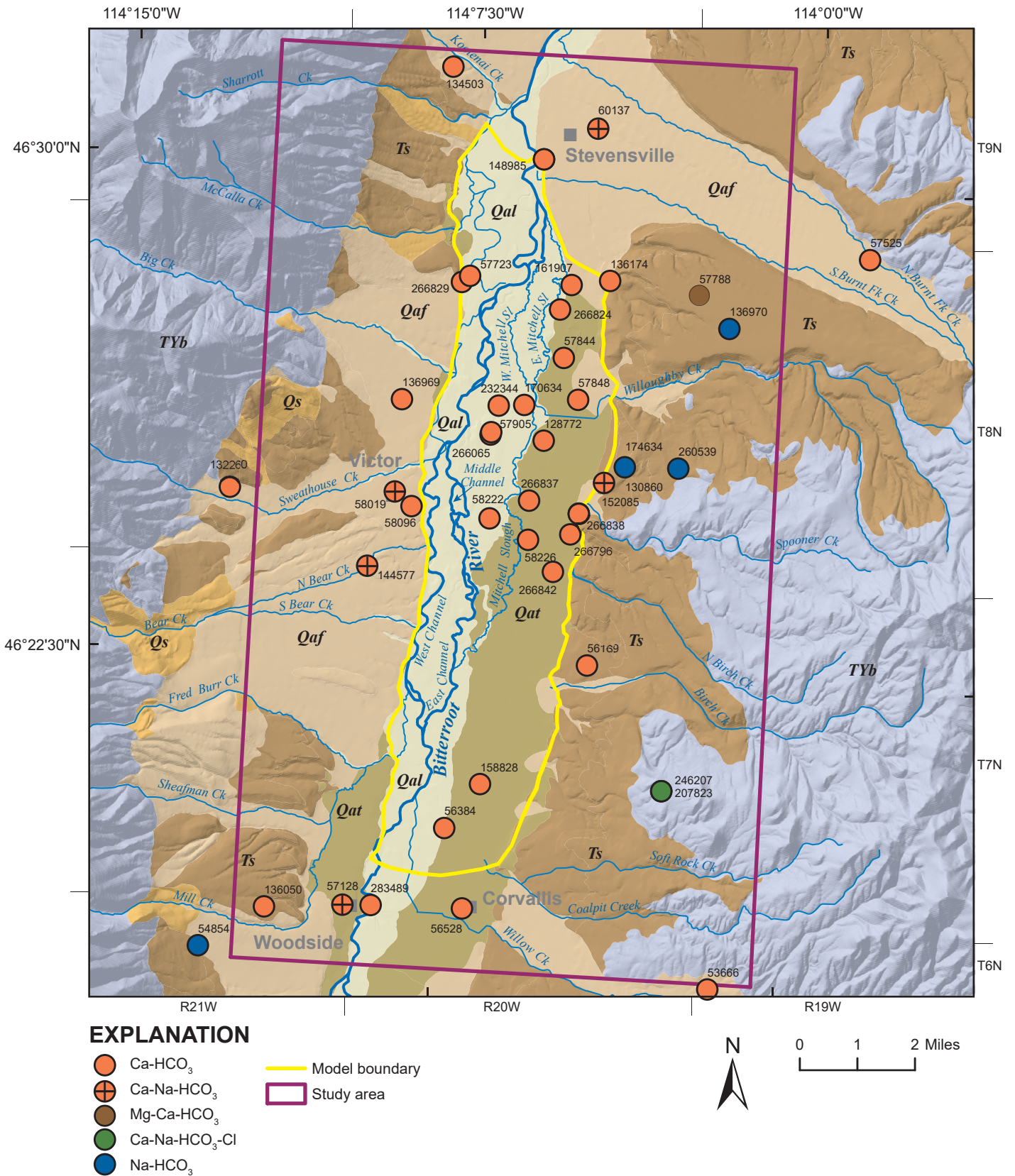


Figure 21. Water types of selected groundwater samples are defined by predominant major ions and indicate a calcium-bicarbonate type water.

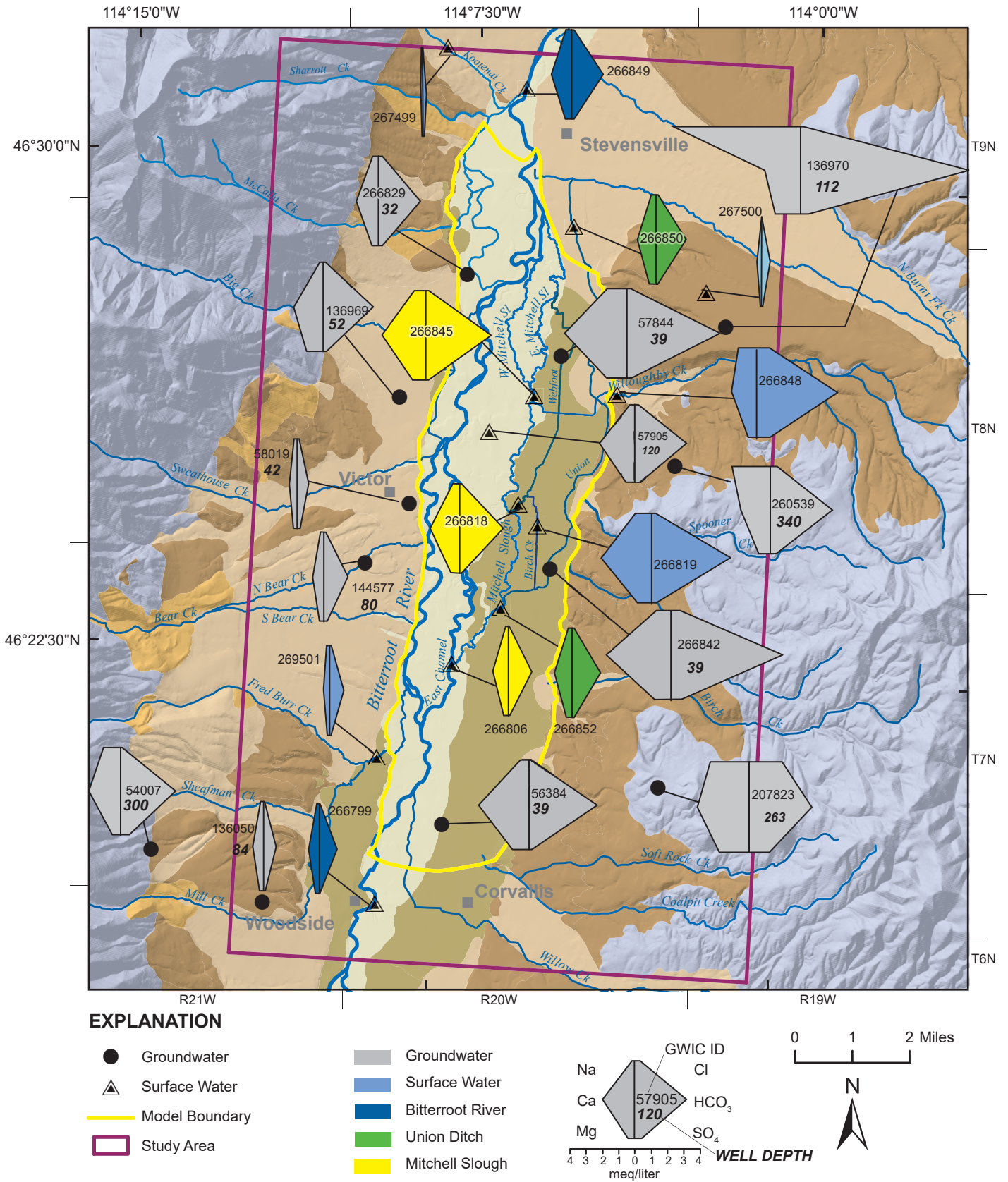


Figure 22. Stiff diagrams display the major ion chemistry of selected groundwater and surface-water samples. Wider Stiff diagrams show that groundwater on the east side of the valley has higher TDS than west side groundwater.

appendix D). Groundwater and surface-water samples east of the Bitterroot River are generally higher in TDS than river water. The increasing TDS of Bitterroot River water downstream suggests contributions of higher TDS groundwater and surface water.

Groundwater along the valley margins contains more chloride and sodium, reflecting the chemistry of the bedrock and Tertiary sediments. Sodium, chloride, and high TDS are common constituents in highly evolved groundwater with long residence times, such as that found in east side water. Sodium concentrations increase in groundwater because sodium is relatively non-reactive and because it exchanges with calcium (cation exchange). Chloride concentrations increase by dissolution and accumulation of a relatively non-reactive ion (Hem, 1992).

Water in west side tributaries is low in TDS relative to the river. These streams flow from a vast area of less reactive granite and bedrock. Consequently, the groundwater from wells west of the river, which receive irrigation recharge from western tributaries, is low in TDS compared to wells east of the river. The increasing TDS in the Bitterroot River demonstrates that the gains in high-TDS groundwater and surface water overwhelm the influence of the low-TDS surface-water additions from the western tributaries.

Water Quality Standards Exceedances

Water quality in the study area is generally good, with some exceptions. All groundwater and surface-water samples were within the recommended limits for irrigation water (USDA, 2011). The EPA's secondary maximum contaminant level (SMCL) for TDS in drinking water is 500 mg/L. The TDS from 32 wells and surface-water sites ranged from 35 to 480 mg/L with an average of 213 mg/L.

Some groundwater samples analyzed indicated exceedances of Montana's maximum contaminant level (MCL) or EPA's SMCL level for drinking water (MDEQ, 2010). Groundwater from three wells in the floodplain (wells 266824, 266065, 232344) exceeded the SMCL for iron of 0.3 mg/L, with concentrations ranging from 0.7 to 2.3 mg/L. Groundwater from well 266065 also exceeded the 0.05 mg/L SMCL for manganese with a concentration of 0.75 mg/L. This well, drilled to monitor groundwater levels near a ditch, is shallow, with a depth of 24 ft. The MCL for arsenic,

10 µg/L (MDEQ, 2010), was exceeded in a 440-ft-deep well completed in the bedrock aquifer (246207) with a concentration of 16.5 µg/L. The uranium MCL of 30 µg/L was exceeded at two wells completed in the Tertiary aquifer: well 57788, 108 ft deep, with a concentration of 39.0 µg/L, and well 136970, a 112-ft-deep well with 30.4 µg/L uranium. Uranium and arsenic are common in granitic plutons, and the source of these constituents in groundwater is likely naturally occurring from aquifer sediment or bedrock.

Mitchell Slough and Union Ditch

Specific conductance and TDS measured along Mitchell Slough provides evidence for groundwater discharge to the slough. The average SC of 100 µS/cm at the Mitchell Slough headgate increases to about 200 µS/cm at Victor Crossing, eventually increasing to 320 µS/cm at Bell Crossing (fig. 18). Groundwater discharge is further supported by the dampening in the seasonal variability in SC as water moves downstream. Since groundwater does not have a strong seasonal variation in SC, the dampening of SC in Mitchell Slough indicates a higher percentage of groundwater present. The SC of groundwater in the valley floor averages about 290 µS/cm. On the high terrace the SC averages about 500 µS/cm. An influx of higher SC groundwater from the valley floor and the high terraces causes the increase in SC in the slough at the downstream measuring locations.

TDS of the water in Mitchell Slough also provides evidence for the discharge of groundwater to the slough. The Stiff diagram for the slough at Tucker Headgate (site 266806) is similar to that of the Bitterroot River at Woodside (site 266799), with just slightly higher concentrations of all major ions. Although the water type stays the same, Stiff diagrams at Victor Crossing (site 266818) and at Bell Crossing (site 266845) show that TDS increases downstream, supporting the conclusion that higher TDS groundwater discharges to the slough. Conversely, the TDS in Union Ditch at the headgate (site 266852) and at Stevensville (a distance of about 7.6 mi; site 266850; fig. 22) is similar, indicating the lack of groundwater discharge to the ditch. Flow measurements along this reach indicates the ditch loses surface water to groundwater (fig. 20).

CONCEPTUAL MODEL

A conceptual model is an interpretation of the characteristics and dynamics of the physical groundwater flow system. It is based on the analysis of all available hydrogeologic data for the study area. The conceptual model includes the system's geologic framework, aquifer properties, groundwater flow direction, locations and rates of recharge and discharge, and the locations and hydraulic characteristics of natural boundaries (Anderson and others, 2015). This conceptual model describes conditions for the groundwater model area on the valley floor.

Geologic Framework

The water table within the valley floor is close to the land surface and generally unconfined in the shallow alluvial aquifer. These deposits extend to an average depth of about 40 ft bgs, and consist of braided stream-channel floodplain deposits. Cobbles are exposed in the streambed, but riverbank deposits exposed by erosion have a sand-sized matrix. Silt and clay are less common in near-surface outcrops except within soils.

Fine-grained sediments, dominantly silt and clay, underlie the Quaternary alluvium and form the silt and clay aquitard. This low-permeability layer confines the underlying sand and gravel. It is variable in thickness, ranging from about 2 to 30 ft in the study area. The deep sand and gravel aquifer underlies the silt and clay aquitard (fig. 11). Although interpreted on a regional basis as a thick aquifer consisting of multiple permeable zones that are separated by low-permeability material, well logs are limited to depths of about 150 ft in the valley floor area and the thickness of the deep aquifer is not known.

Groundwater Flow System

The configuration of the water table mimics the topography. Groundwater flows from high elevations toward the Bitterroot River valley floor. Gradients are relatively steep in the less transmissive bedrock and high terrace sediments. Gradients are flatter in the valley floor, where coarse, braided stream deposits form a transmissive aquifer. Groundwater in the valley floor is generally within 20 ft of ground surface and flows to the north, where it discharges to ditches and streams.

Groundwater flow in the valley floor sediments is controlled by the system's geometry, the position

of the Bitterroot River, and the presence of irrigation canals and drain ditches. Locally, the configuration of the water table is disrupted by the river or low-lying ditches that capture groundwater. The potentiometric surfaces of McMurtrey and others (1972) and for this study are based primarily on later-winter data (March). The effects of spring and summer high flows and irrigation activities are minimal at this time of year. Thus, in late winter the study area approaches a more natural condition that might exist if there were no irrigation in the area. However, water levels in many wells are still declining when the next irrigation season ensues, indicating that groundwater does not return to pre-development conditions.

Irrigation canals operate about 6 mo of the year, from about mid-April to mid- to late October. Within the groundwater model area, these canals are located on the floodplain and low terraces. Canals lose or gain water to/from the underlying aquifer, depending on their position and relation to the water table. Flows and water quality in the canals helped identify losing and/or gaining conditions

Groundwater and surface-water exchange is affected seasonally by events such as spring runoff and irrigation practices. Spring runoff causes seasonal high flows in the Bitterroot River, which commonly peak around the first week in June. Those peak flows affect water levels in floodplain wells and in shallow water features adjacent to the river. Water levels in the wells tend to rise and fall along with the river stages. These responses illustrate that groundwater and surface water are hydraulically well connected in the valley.

Excess irrigation water applied to fields recharges the shallow aquifer through irrigation return flow. Our estimates indicate that most of this irrigation recharge occurs in June, July, and the first half of August.

Hydrologic Boundaries

The Bitterroot River is at or near the western edge of the groundwater model area, except at the north end within a few miles south of Stevensville. Our area of interest lies east of the Bitterroot River, and the river forms a hydrologic boundary generally near the west edge of the model. The western edge of the valley floor forms a hydrologic boundary west of the river. This is treated as a no-flow boundary in the numerical model. Any water entering the area from the western high terraces probably flows northward or discharges

to the Bitterroot River and is assumed to have no effect on the model area. The Bitterroot River stage is important, because it controls the interaction of water between the river and groundwater east of the river. High stage during spring runoff likely causes bank storage, affecting groundwater conditions near the river.

In the numerical model, the eastern boundary of the conceptual model is treated as a groundwater flux boundary and represents groundwater contributions from the eastern high terraces. The north and south model boundaries are considered permeable and extend to similar aquifer materials in each direction.

The canals, including canals at higher elevations on the terraces and low-lying features such as Mitchell Slough, vary, with some gaining flow from groundwater discharge and others losing water to recharge groundwater. For example, the flow data and water quality of Supply and Union Ditches suggest that these features do not gain substantial amounts of groundwater during the summer. Thus, they are principally canals that leak and are a source of seasonal groundwater recharge.

Mitchell Slough, on the other hand, is characterized by gains from groundwater sources. These sources include direct discharges from the shallow aquifer and other drains fed by groundwater that flow into Mitchell Slough. Some canals appear to both lose and gain water to the shallow groundwater system, with this relationship changing seasonally along certain reaches.

Hydraulic Properties

The hydraulic properties of the valley floor sediments vary spatially across the area of interest. The values determined from pumping shallow wells or pits vary considerably and may be biased high because such wells and pits are preferentially located in coarse alluvium, such as cobble beds left in abandoned stream channels. The estimated hydraulic conductivity of the shallow alluvial aquifer ranges from 400 to 800 ft/d. We used a hydraulic conductivity of 200 ft/d as an initial condition in the numerical model. This is within the same order of magnitude as the aquifer tests. This value is also in the low to mid-range for clean sand and gravel found in the literature (USBR, 1977; Freeze and Cherry, 1979; Fetter, 1980; Heath, 1983). The shallow alluvial aquifer is treated as an unconfined aquifer.

Calibration of the numerical model, discussed in the appendix, demonstrated that a hydraulic conductivity of 200 ft/d provided a good match between simulated and observed conditions. However, a hydraulic conductivity of 2,000 ft/d yielded improved calibration. This suggests that the conductivity of the aquifer material ranges between these values, which fall within the range for clean sand and gravel (USBR, 1977; Freeze and Cherry, 1979; Fetter, 1980; Heath, 1983).

A silt and clay aquitard underlies the shallow alluvial aquifer. We assumed a hydraulic conductivity of 1 ft/d for this unit, which is within the literature ranges for silt, sandy silt, and clayey sand (Fetter, 1980).

We estimated a hydraulic conductivity of 4 to 287 ft/d with a geometric mean of 43 ft/d for the deep sand and gravel aquifer. Assuming that the deep aquifer is more compacted than the shallow system, we selected 50 ft/d as a reasonable hydraulic conductivity for the aquifer. The deep sand and gravel aquifer is considered confined.

Sources and Sinks

Sources of recharge to groundwater in the valley floor area include canal leakage, infiltration of excess irrigation water, and stream losses. Intra-aquifer flow also transmits groundwater into the area from the high terraces and the upgradient Bitterroot Valley. Groundwater recharge from non-irrigated lands was considered negligible based on the assumption that evapotranspiration exceeds precipitation during the summer months and recharge during the winter months is negligible.

Sinks, or locations of groundwater discharge, include discharge to streams, canals, and the Bitterroot River. Additional sinks include evapotranspiration by phreatophytes, well pumping, and groundwater flow out of the study area to the downgradient portions of the Bitterroot Valley. These sources and sinks interact with the shallow groundwater in the valley floor area.

Groundwater Budget

We developed a monthly groundwater budget to better understand the groundwater system and the magnitude of sinks and sources in the model area. That budget was developed from previously available information and data collected during this study. The groundwater budget (table 2) includes the irrigated

acres and ditches of the valley floor east of the Bitterroot River. We considered areas west of the Bitterroot River, which extend the shallow alluvial aquifer to its physical limit, as providing groundwater storage and interaction with the Bitterroot River.

The general form of the groundwater budget equation is:

Water in = water out ± changes in groundwater storage.

The water budget equation includes the following components:

$$GW_{in} + IF + CL + BR_{in} = GW_{out} + ET_p + WL + CG + BR_{out} + \Delta S,$$

where GW_{in} is groundwater inflow (acre-ft/yr); IF is recharge from irrigated fields (acre-ft/yr); CL is canal leakage (acre-ft/yr); BR_{in} is Bitterroot River losses to the aquifer; GW_{out} is groundwater outflow (acre-ft/yr); ET_p is evapotranspiration by phreatophytes (acre-ft/yr); WL is withdrawals from wells (acre-ft/yr); CG is canal gains (acre-ft/yr); BR_{out} is Bitterroot River gains from the aquifer; and ΔS is changes in storage (acre-ft/yr).

Groundwater inflow and outflow (GW_{in} and GW_{out})

Groundwater fluxes through the shallow alluvial aquifer from the Bitterroot Valley upgradient (GW_{in}) and downgradient (GW_{out}) were calculated using Darcy's Law where $Q = -KiA$, where Q is the volumetric flow (ft³/d), K is the hydraulic conductivity (ft/d), i is the groundwater gradient (dimensionless) and A is the area (ft²) through which flow occurs (Freeze and Cherry, 1979). The average valley width was estimated at 14,000 ft, the saturated thickness at 44 ft, the gradient at -0.003, the hydraulic conductivity at 200 ft/d, and both GW_{in} and GW_{out} at about 369,600 ft³/d (4 cfs) or 3,100 acre-ft/yr.

Replacing hydraulic conductivity with the upper range value of 2,000 ft/d increases the volumetric flow rate by 10 times, to about 31,000 acre-ft/yr. The valley geometry at each end of the model is irregular, and the hydraulic gradients may vary over time. The purpose of this calculation is to estimate the magnitude of the flow; the numerical model generates flow rates and serves to refine this estimate, accounting for both the irregular aquifer geometry and temporal variability in the gradient. Thus, the same value is applied to the north and south boundaries in this budget.

Groundwater inflow also included contributions from the eastern high terraces. Groundwater flux from the Tertiary aquifer underlying the eastern high terraces (GW_{in}) was derived from calculations by Stewart (1998), who estimated 88,000 ft³/d over a 10,000 ft transect between the high terraces and the valley floor in the Eightmile Creek vicinity, east of Florence. This equates to a little more than 1 cfs over nearly 2 mi of transect. We compared this to another estimate, for a mile (5,280 ft) width of the high terrace, a hydraulic conductivity range of 5 to 10 ft/d for the Tertiary aquifer sediments, a saturated aquifer thickness of 200 ft, and a gradient of -100 ft over ¾ mi, or 3,960 ft distance. This produced an estimate of 1.5 to 3 cfs/mi. While this flow may contribute groundwater to the eastern edge of the valley floor aquifers, a portion of the groundwater likely discharges to springs, seeps, and streams outside of the numerical model boundary. Therefore, a conservatively low value of about 0.5 cfs/mi based on Stewart's estimate (1998) was used, resulting in a flow rate of 43,200 ft³/d per mile of groundwater inflow along the eastern edge of the valley floor. The eastern edge of the model adjacent to the high terraces is about 10.3 mi long, so the total estimated inflow is about (10.3 mi x 43,200 acre-ft/mi) 3,700 acre-ft/yr. Thus, assuming a low-K value, GW_{in} from the Bitterroot Valley and eastern high terraces combined is estimated at 6,800 acre-ft/yr.

Recharge from irrigated fields (IF)

Estimated recharge from irrigated fields is reported in table 1. A recharge rate of 1.6 ft/yr was applied for flood-irrigated fields. The sprinkler and pivot areas were combined, because pivot irrigation is a small percentage of the irrigated acreage, for a recharge rate of about 0.5 ft/yr. The model domain includes 7,576 irrigated acres, with 4,198 acres of sprinkler/pivot irrigation and 3,378 acres of flood irrigation. Applying these recharge rates to these acres resulted in an estimated 7,167 acre-ft/yr of IF.

Canal leakage (CL)

Canal leakage was estimated by applying leakage rates to principal canals on the low terrace. Leakage from irrigation canals was significant in other similar studies (Waren and others, 2012; Bobst and others, 2014; Abdo and others, 2013; Sutherland and others, 2014). G. Abdo (oral commun., 2012) summarized canal seepage loss for numerous Montana canals. These losses ranged from 0.05 to 2.2 cfs per mile, with a median value of 1.15 cfs per mile.

Estimates of canal leakage on the valley floor were based on available data (table 3). A value of 2 cfs was applied to Union Ditch based on field measurements and an estimate of the leakage between the headgate and Union Ditch at Stevensville. We estimated 1.5 cfs per mile of seepage from Supply Ditch and Corvallis Canal. This was an intermediate value considering the estimate of 2 cfs per mile along Union Ditch and the median value reported by Abdo for large Montana canals of 1.15 cfs per mile. Etna and Webfoot Ditches were assigned seepage values of one-half of the Union Ditch estimate based on flow measurements in the ditches.

Canals on the floodplain, such as the Strange, Spooner, and Gerlinger Ditches, likely contribute recharge to the groundwater system. Based on ditch measurements, these ditches generally flow less, and a value of 1 cfs/mi was applied to these features.

Each canal leakage rate was multiplied by the length of the canal over the 6-mo irrigation season for a total leakage amount of 20,500 acre-ft/yr.

Riparian vegetation evapotranspiration (ET)

Cottonwood and willow-inhabited lands extend throughout a corridor along the Bitterroot River (fig. 19). An average evapotranspiration rate of 22 in/yr (Hackett and others, 1960; Lautz, 2008) was multiplied by the 1,865 acres of riparian vegetation in the model area, resulting in an estimated evapotranspiration of 3,420 acre-ft per year.

Groundwater withdrawals (WL)

Groundwater withdrawals by wells (WL) was estimated from the work of Bobst and others (2014), who

quantified the consumptive use for domestic wells in the North Hills Groundwater Investigation area near Helena, Montana at 0.5 acre/ft per year.

Records for 772 wells within the model area indicate that there are 556 domestic wells. Other well uses include monitoring, unused, public water supply, fire protection, and irrigation wells. Because some wells use virtually no water, while irrigation wells probably use vastly more, the 0.5 acre/ft per household use was applied to all 772 wells. Although this estimate was obtained by simplifying estimates of water use, especially for non-domestic wells, the total estimated water withdrawals of 390 acre-ft/yr was deemed adequate because it is a small portion of the overall budget (table 2).

Canal gains (CG)

Groundwater discharge to canals and drains (CG), including discharge to Mitchell Slough, was derived by balancing the groundwater out volumes with the groundwater in volumes. Mitchell Slough may lose some water to groundwater upstream of Victor Crossing, but downstream of the Webfoot Ditch diversion (fig. 7) the Slough follows the east edge of the floodplain and is a topographically low feature. Here the Mitchell Slough acts as a drain, gaining flow from the groundwater system and irrigation return flows. The groundwater discharge to all canals and drains is 21,200 acre-ft/yr.

Bitterroot River gains and losses (BR_{in} and BR_{out})

Flux from the Bitterroot River to groundwater was estimated at 4,100 acre-ft/yr using a preliminary steady-state groundwater flow model that included

Table 3. Canal leakage estimated for major canals on the valley floor during the 6-mo irrigation season.

Canal	Seepage rate (cfs)	Canal Length (mi)	Total Seepage (acre-ft/yr)
Corvallis Ditch	1.5	3.6	1,960
Union Ditch	2	7.6	5,510
Etna Ditch	1	5	1,811
Supply Ditch	1.5	11.2	6,090
Webfoot	1	4.9	1,770
Gerlinger	1	3.2	1,160
Strange	1	2.78	1,010
Spooner	1	3.3	1,200
Total ditch seepage			20,511

most of the higher-volume elements of the groundwater budget (BR_{in}). Groundwater discharge to the Bitterroot River based on the preliminary model was 10,400 acre-ft/yr (BR_{out}). Seasonal bank storage, a process expected to occur during spring runoff, was not included in this budget. The volume of water that enters and exits the shallow aquifer through this mechanism occurs at nearly the same time as large changes in river stage.

Storage (ΔS)

Groundwater levels are typically similar at the end of each irrigation season, as demonstrated by long-term hydrographs (fig. 14). We therefore assumed no change in storage ($\Delta S = 0$).

GROUNDWATER MODELING

Groundwater models were developed to assess effects related to changes in irrigation practices on the groundwater system and stream flows. The model area extends across the valley floor (fig. 2). Mitchell Slough is the principal drain for applied irrigation water in the irrigated portion of the model domain. The flow in Mitchell Slough is of special interest, because it carries most of the irrigation return flows out of the study area. Therefore, the simulated flow in Mitchell Slough is an important measure of change in irrigation return flow in model simulations.

Model development required substantial simplifications and assumptions. This model is not intended to exactly match reality, but to simply capture, or mathematically render, key elements driving the hydrogeologic system. For example, a particular diversion might be simulated with a seasonal average diversion rate, even though in reality the diversion rate varies daily. Likewise, estimates of irrigation recharge could be adjusted throughout a transient simulation based on climatic conditions, such as drought. A simplification made during this modeling effort was to rely on seasonal estimates of irrigation recharge for a single crop, alfalfa, for several irrigation methods. Details on model construction and calibration are provided in appendix E.

Predictive Simulations

The steady-state models are useful for evaluating the overall, long-term effects of changes to average groundwater conditions. Transient models provide information about time-dependent questions, for exam-

ple, the timing and magnitude of changes in groundwater levels and flow in streams and ditches. The transient model has two time lengths: a 13-mo version and a 10-yr version. The 13-mo version simulates the period April 2012 through April 2013. The 10-yr version models the period April 2012 through late March 2022. In the 10-yr baseline model, each irrigation season is simulated with our estimates of 2012 groundwater recharge from leaking irrigation canals and excess irrigation water applied to fields. The 2012 Bitterroot River stages and irrigation diversions were similarly repeated in each year of the transient simulation. All of the predictive simulations were run twice, utilizing the low K (layer 1: 200 ft/d) and high K (layer 1: 2,000 ft/d) versions of the models.

The scenarios evaluated the potential effects on groundwater and surface water from changing irrigation practices (table 4). These included:

Scenario 1—No irrigation—eliminates all irrigation activities in the valley floor.

Scenario 2—Surface water diverted from the East Channel for irrigation at Tucker Headgate is replaced by groundwater supplied by pumping wells adjacent to the river.

Scenario 3—All water diverted from the East Channel is replaced by 51 wells strategically placed throughout the model area to supply water to irrigated fields.

Scenario 4—East Channel irrigation water that supplies sprinkler-irrigated fields is replaced in three increments by wells located throughout the irrigated land. Each of the three increments were based on acreage serviced by particular canals.

Scenario 1—No Irrigation

The steady-state and 10-yr transient models were used to evaluate groundwater and surface-water systems response if all irrigation in the valley floor area was eliminated. While this scenario is unlikely, it provides an estimate close to pre-development conditions, before irrigation. However, irrigation drain ditches remain active in the model and accumulate flow in places, differing from pre-development conditions.

The transient model included simulation of the initial irrigation season, from April 2012 through March 31, 2013, with all irrigation activities included. After

Table 4. Scenarios were simulated using low and high K versions of each model.

Scenario	Model	Simulation Design	Results
Calibrated models	Steady-state	Simulating current conditions	Reasonable calibration for steady-state and transient simulations
	13-mo Transient		
	10-yr Transient	Simulating conditions (April 2012–March 2022) based on 2012 groundwater recharge estimates.	
Scenario 1: No irrigation	Steady-state	All irrigation diversions, ditch leakage, and irrigated fields removed.	Groundwater levels in the valley floor decline to about the Bitterroot River elevation. Mitchell Slough summer flow diminishes from about 110 cfs to 10–40 cfs.
	10-yr Transient	All irrigation diversions, canals, and irrigated fields removed after 1 yr of normal operation.	
Scenario 2: Near-river high-rate irrigation wells	10-yr Transient	Groundwater, pumped from high-rate wells near the Bitterroot River, supplies water into Mitchell Slough at the Tucker Headgate.	The models suggest that the scheme is feasible but would require high-capacity, near-river wells.
Scenario 3: Individual irrigation wells providing all East Channel irrigation water	13-mo Transient	51 individual irrigation wells provide irrigation water normally supplied by surface water from the East Channel —All diversions and recharge from irrigation features are removed from the model.	The model suggests that such a scenario is feasible. Mitchell Slough flows would decrease to about same range as scenario 1.
Scenario 4: Individual irrigation wells incrementally providing East Channel sprinkler-irrigated fields water	10-yr Transient	Groundwater from 27 individual irrigation wells incrementally replace water normally supplied to sprinkler-irrigated fields from the East Channel. Increments include fields serviced by (1) Webfoot Ditch, (2) Gehrlinger Ditch and Mitchell Slough, and (3) Union, Etna, Victor and Spooner Ditches.	Because the irrigation ditches and flood irrigation continue operating in this scenario, the changes to the system are subtle.

the model time of March 2013, all diversions and the ditch leakage were set to zero. The east side flux boundary remained intact, so these runs simulate the Bitterroot River Irrigation District canal and associated irrigated lands.

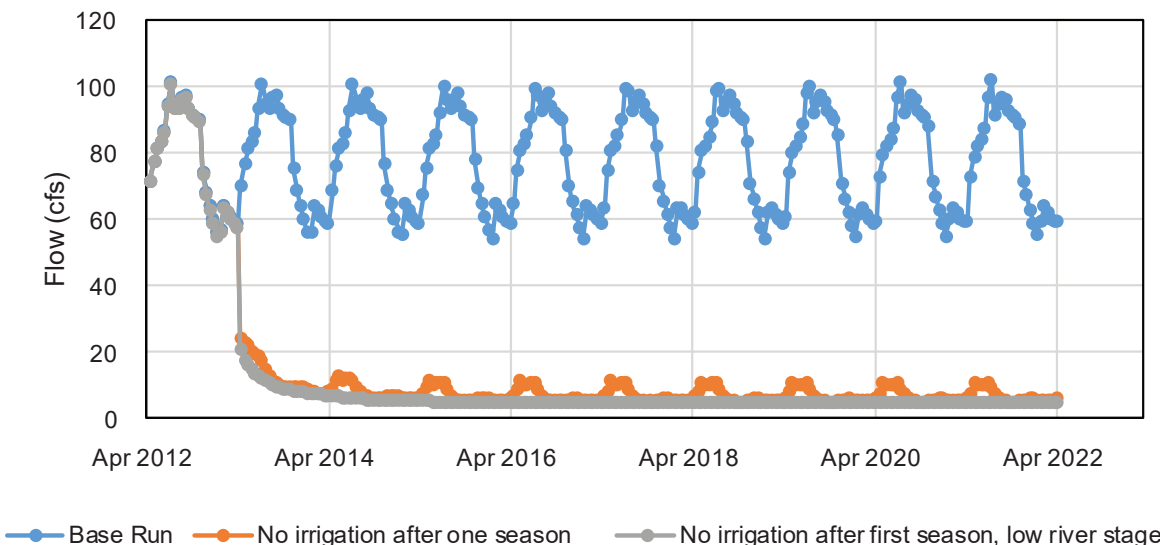
Results suggest that groundwater levels would decline to about the level of the Bitterroot River. Groundwater levels in wells near the river change little. In wells on the low terrace, static water levels declined 2 to 11 ft compared to current observed seasonal lows. Water levels remained constant rather

than rising each irrigation season. The simulation suggests that without irrigation, summertime flows out of Mitchell Slough drop from 90 to 110 cfs to about 10 to 40 cfs (fig. 23). The annual rise in the hydrographs with no irrigation (fig. 23B) indicates that high stage in the Bitterroot River during spring runoff could potentially deliver about 40 cfs of water to Mitchell Slough.

Scenario 2—Near-River Irrigation Wells

High-capacity pumping wells (modeled as collector wells using MODFLOW’s WEL Package), located

A Low K Model Results



B High K Model Results

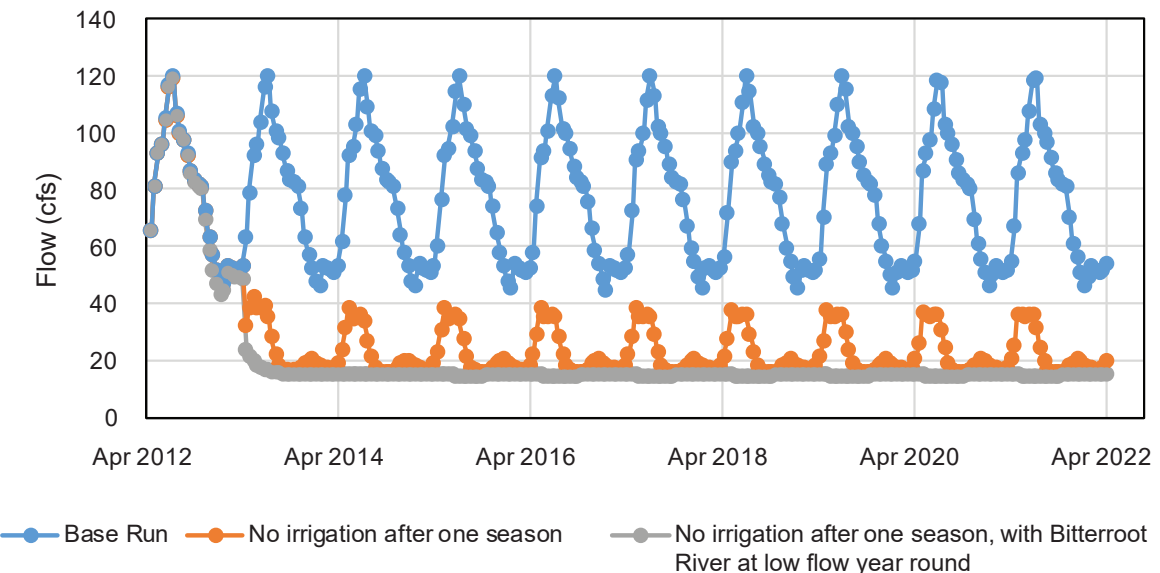


Figure 23. This 10-yr scenario eliminates all diversions, ditch leakage, and recharge from irrigated fields in the valley floor after the first irrigation season. The flows in the east branch of Mitchell Slough show large decreases in flow from the base run. The annual rise in the hydrographs reflects high stage in the Bitterroot River during spring runoff.

along the east side of the East Channel, were used to evaluate the potential effects of replacing irrigation water diverted from the East Channel with groundwater as the direct source of water into Mitchell Slough. This scenario was implemented in the 10-yr transient low and high K model versions. The maximum summer pumping rate for these wells totaled 60 cfs (26,923 gpm; the amount of water needed for high-demand summer irrigation at the Tucker Headgate into Mitchell Slough—see appendix E). Although not simulated, this water could be conveyed from the wells to the Tucker Headgate in a pipeline, or delivered in the current channel or an improved, lined open channel.

In the high K version of the model, this scenario converged but some wells in cells adjacent to the Bitterroot River had excessive drawdown. These wells were moved to model cells that include river reaches (fig. 24). This simulation suggests that six high-capacity wells next to the river can deliver the demands of average summer diversion amounts. This simulates a direct connection between these wells and the river, so that the river meets demand through groundwater withdrawals. Since this scenario captures river water through wells, it avoids the engineering challenges with maintaining flow in the East Channel.

These high-capacity collector wells simulate pumping 10 cfs each. A typical high-capacity well delivers 2 to 5 cfs, if aquifer sediments are sufficiently transmissive. The simulated high-capacity wells are similar to a Ranney collector well, a more substantial structure with radiating horizontal collector screens that can be installed within or near the river channel. These wells are designed to draw river water through shallow aquifer materials. Cost estimates for this approach need to also consider the conveyance of water from the collector wells to Tucker Headgate.

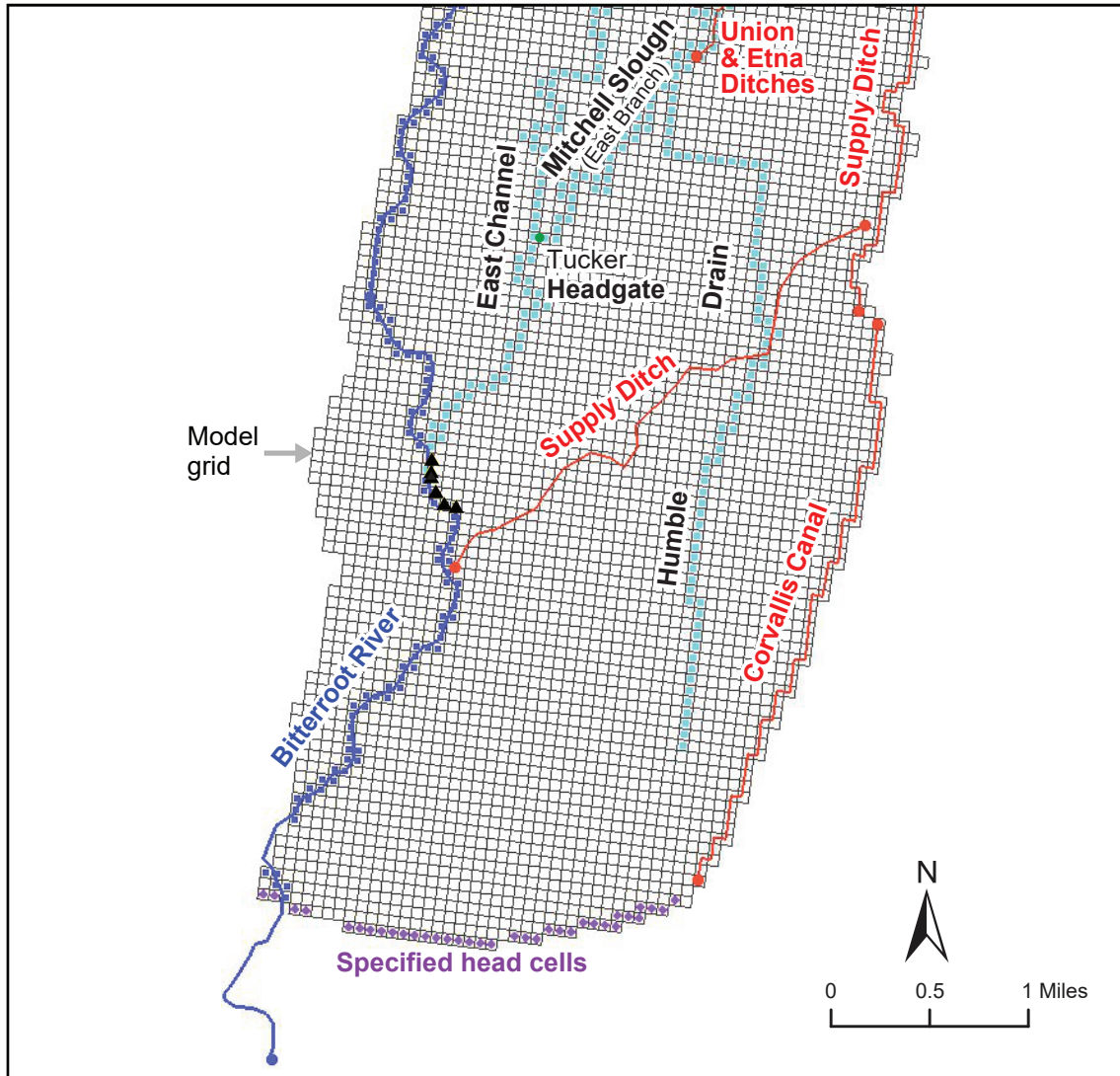
The low K version of the model would not converge using these groundwater withdrawal rates, indicating that upper aquifer transmissivity may not be sufficient to supply such a design. The model converged with an equivalent total groundwater withdrawal, with pumping rates set to $\frac{1}{4}$ of those used in the high K model using 24 wells spaced along a 2-mi reach of the East Channel and Bitterroot River (fig. 25). This demonstrates that in areas of low hydraulic conductivity, well interference could be overcome by using more wells at greater spacing.

Groundwater pumping next to the river is comparable to a direct surface-water diversion. Because groundwater in storage must be removed to propagate drawdown that allows river water to flow into the subsurface, some portion of water pumped will come from groundwater. The high K version of the model indicates that with pumping starting April 1, about 83 percent of the total water extracted is river water by June 10. By November 24, after pumping has ended, the river continues to lose flow to groundwater, replenishing aquifer storage. The lower hydraulic conductivity model indicates about 36 percent of the total water extracted is river water by June 10, and by November 24, the river continues to replenish groundwater to aquifer storage.

The model cell size limits the proximity of a simulated well next to the river. In reality, wells can be placed very near to the river to maximize the connection. This may simplify regulatory and legal issues related to changing the point of diversion for a surface-water right to a well-water right.

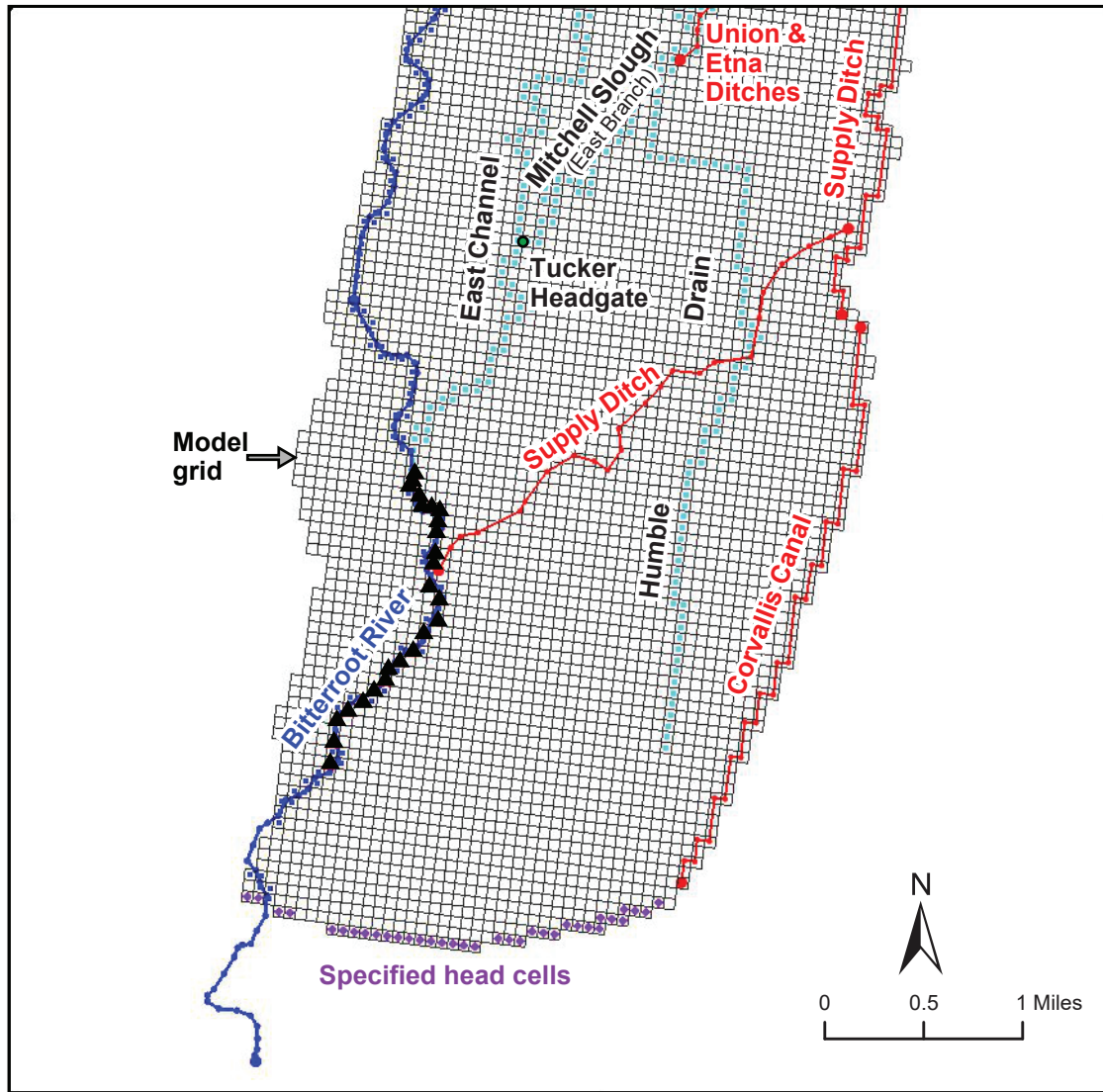
In this scenario, neither model simulates flow to the East Channel of the Bitterroot River below Tucker Headgate. However, the models show some groundwater discharge in the East Channel at Victor Crossing. In the high K model, discharge is 10 to 20 cfs during the irrigation season. Flows at the same location are lower in the low K model, ranging from about 2 to 5 cfs. Thus, in both models, limited water is available for diversions downstream of Tucker Headgate, affecting the Strange and Gerlinger Ditches. Additional water must be delivered to meet those needs. During this project, measured flows in Gerlinger Ditch ranged from zero to about 55 cfs. Flows were not measured in Strange Ditch because of access issues.

Just upstream of Tucker Crossing, the East Channel receives flow from two sources: the Bobby Smyth Ditch and the East Channel diversion from the Bitterroot River that has been dredged in recent years (fig. 7). The contribution of these two sources was not measured, but a visual inspection indicated that about half comes from each source. Since the Bobby Smyth source does not require dredging and thus no dredging permit, this half of the flow might continue under any of these scenarios. The Bobby Smyth source could supply flow to decrease water demand from wells, deliver water past Tucker Headgate, or some combination of the two.



-  Model river arc and nodes
-  Model specified flux arc and nodes
-  Model river cells
-  Model SFR2 cells
-  Model specified head cells
-  Modeled pumping wells near river
-  Tucker Headgate

Figure 24. Six high-capacity wells are placed upstream of the East Channel diversion from the Bitterroot River in cells that include river reaches. Groundwater pumped from the wells directly replaced surface water from the East Channel as a source for water to Mitchell Slough.



-  Model river arc and nodes
-  Model specified flux arc and nodes
-  Model river cells
-  Model SFR2 cells
-  Model specified head cells
-  Modeled pumping wells near river
-  Tucker Headgate

Figure 25. Twenty-four high-capacity wells were placed upstream of the East Channel diversion from the Bitterroot River in model cells that include river reaches. Groundwater pumped from the wells directly replaced surface water from the East Channel as a source for water to Mitchell Slough.

Scenario 3—Irrigation Wells across the Area Provide All East Channel Irrigation Water

In this scenario, all East Channel diversions and ditches were eliminated and 51 irrigation wells placed across the irrigated lands pumped groundwater to irrigate 3,946 acres. This scenario used the low and high K versions of the 13-mo model. The number of wells was based on each well producing less than 500 gpm and delivering water to areas ranging from 70 to 82 acres. The calculations for this irrigation well scenario, along with the diversions and ditches affected, are provided in appendix E (table E-11). Results from both the high and low K versions suggest that wells can deliver the required water.

As discussed in the model sensitivity analysis (appendix E), Mitchell Slough flows at Bell Crossing are directed to the east branch of Mitchell Slough (fig. 2; designated as E. Mitchell Sl). The west branch of the slough, as modeled and in reality, is influenced by nearby lands that are primarily sprinkler irrigated. Since the east branch typically contributes 90 percent or more of the irrigation return flows to Mitchell Slough, we considered only the east branch flow to characterize simulated changes on irrigation return flows in this scenario (fig. 26).

In this scenario, we implemented incremental changes to several elements of the model. The results of the low and high K versions are generally similar, but differ with respect to the magnitude of Mitchell Slough flow, because of the difference in the hydraulic conductivity of layer 1. Figures 26A and 26B show the “base runs” that simulate current conditions.

The response of flows to the incremental changes, as indicated by flow from Mitchell Slough east branch to the Bitterroot, show the following (fig. 26):

- a. Base run—existing conditions.
- b. Converting lands flood irrigated with water from the East Channel to sprinkler irrigation.
- c. This change is simulated by reducing the excess water available for groundwater recharge from flood-irrigated fields (1.5 ft) to the value used for sprinkler-irrigated fields (0.5 ft). Modest declines in flow were associated with this change from the base run.

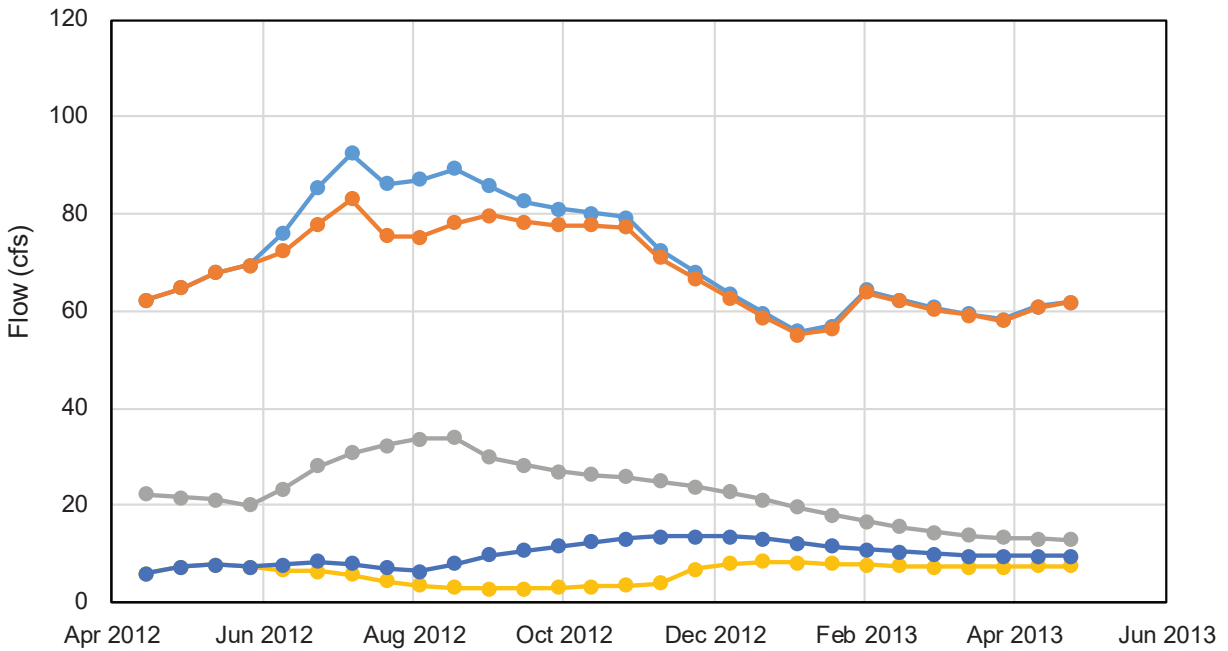
- d. Turning off all diversions from the East Channel and eliminating recharge from leaking canals. However, leakage was continued from the Supply Ditch and Corvallis Canal because these do not derive water from Mitchell Slough. This causes a large decline in flows in the east branch of Mitchell Slough throughout the year. Sprinkler irrigation recharge is applied (as in b) in this step.
- e. All diversions off (as above) and sprinkler irrigation recharge also turned off from fields serviced by the East Channel.
- f. Fifty-one wells were added to the above changes and pumping was simulated from June 1 through August 15. This results in the greatest diminishment of flows out of the east branch of Mitchell Slough. The sprinkler recharge rates are applied to all East Channel irrigated fields in these scenarios.

Of the steps applied in developing scenario 3, removing the diversions of water into leaky canals (c, above) creates the greatest single change in flows out of the east branch of Mitchell Slough compared to the base run.

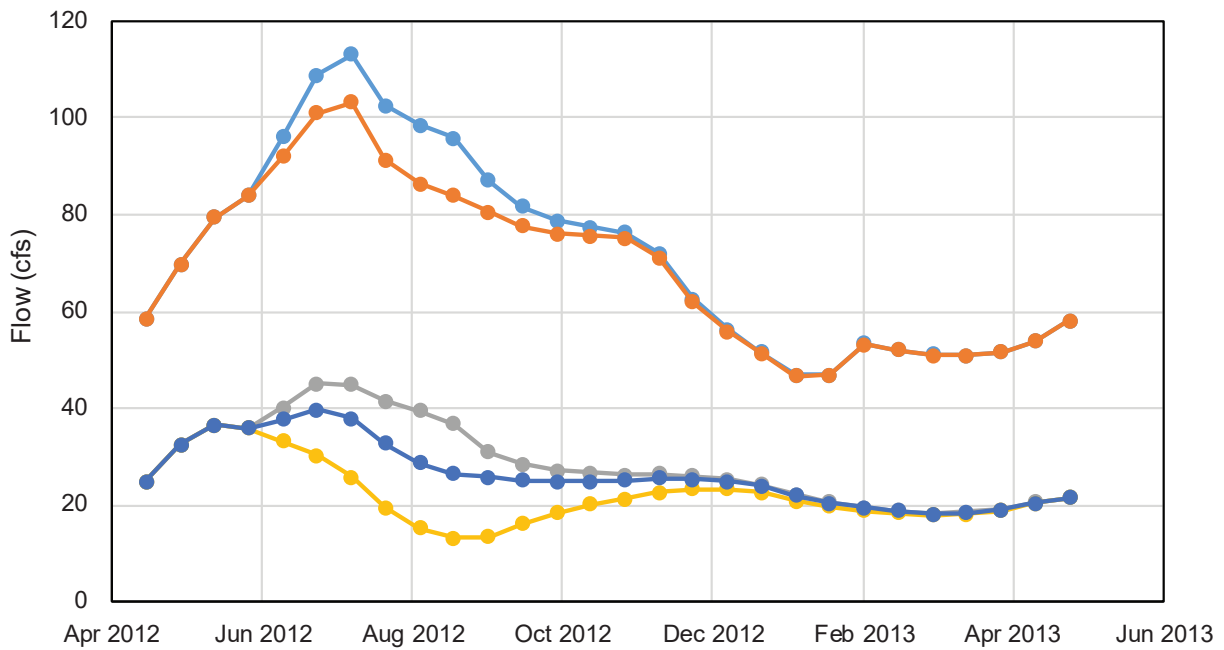
Seasonal drawdown of the water table associated with the 51 wells was the greatest in the low terrace on the east side of the domain (figs. 27, 28). The drawdown contours illustrate locations of the simulated irrigation wells; however, a few wells are located close to the canals and are difficult to discern. The drawdown was calculated by comparing a simulation with irrigation wells to the same model without irrigation wells. This scenario reflects only the drawdown caused by pumping wells, and does not include groundwater-level declines from recharge lost due to the lack of leaking ditches and excess recharge from flood-irrigated fields.

The low K model generates more drawdown (fig. 27) compared to the high K model (fig. 28), as expected. These figures illustrate the simulated groundwater head with irrigation wells compared to the baseline simulation that includes the diversions, leaking ditches, and flood irrigation recharge. Using the low K model, which generates higher drawdown estimates, the groundwater head in the model with irrigation wells was compared to baseline conditions. The results indicate that the total difference in head from both

A Low K Model Results



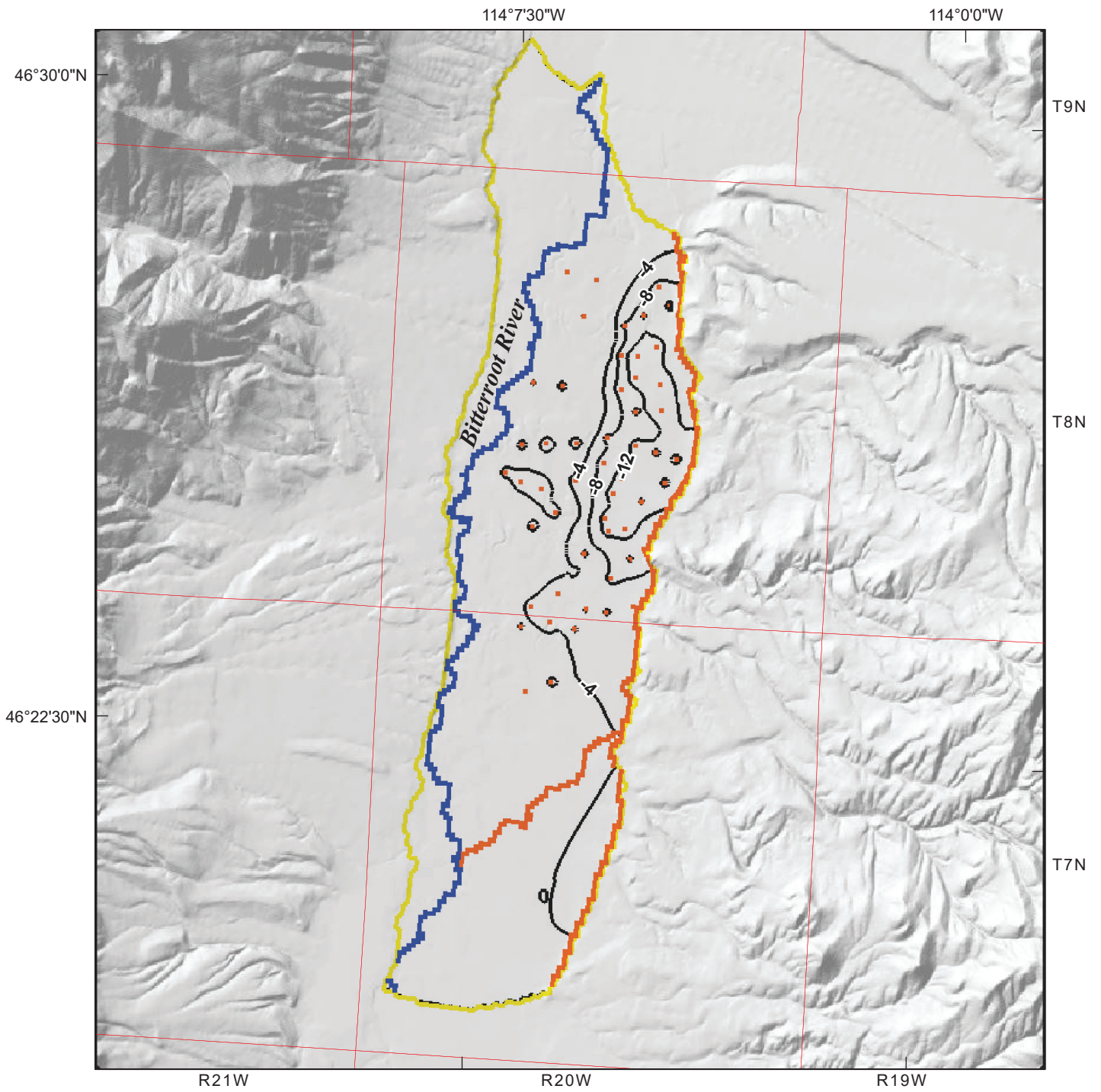
B High K Model Results



Explanation

- a. Base Runs—April 1, 2012 to April 30, 2013
- b. Converted flood-irrigated areas to sprinkler
- c. Diversions and East Channel ditch leakage off
- d. Same as c but no recharge from East Channel irrigated lands
- e. Wells service 3,946 acres of irrigated lands

Figure 26. The flow out of the east branch of Mitchell Slough as changes are applied cumulatively to irrigation activities in the valley floor area. The results of the low and high K models are similar, with changes in magnitudes and timing of flows out of the Slough.



Explanation

- Modeled area
 - Bitterroot River
 - Drawdown contours
- Features modeled using the wells package
- Modeled leaking irrigation canal
 - Modeled individual irrigation well

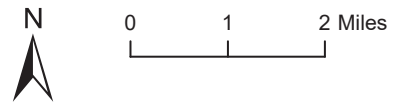


Figure 27. In the low K version of the model, drawdown from irrigation well pumping is greatest near well locations on the east edge of the model.

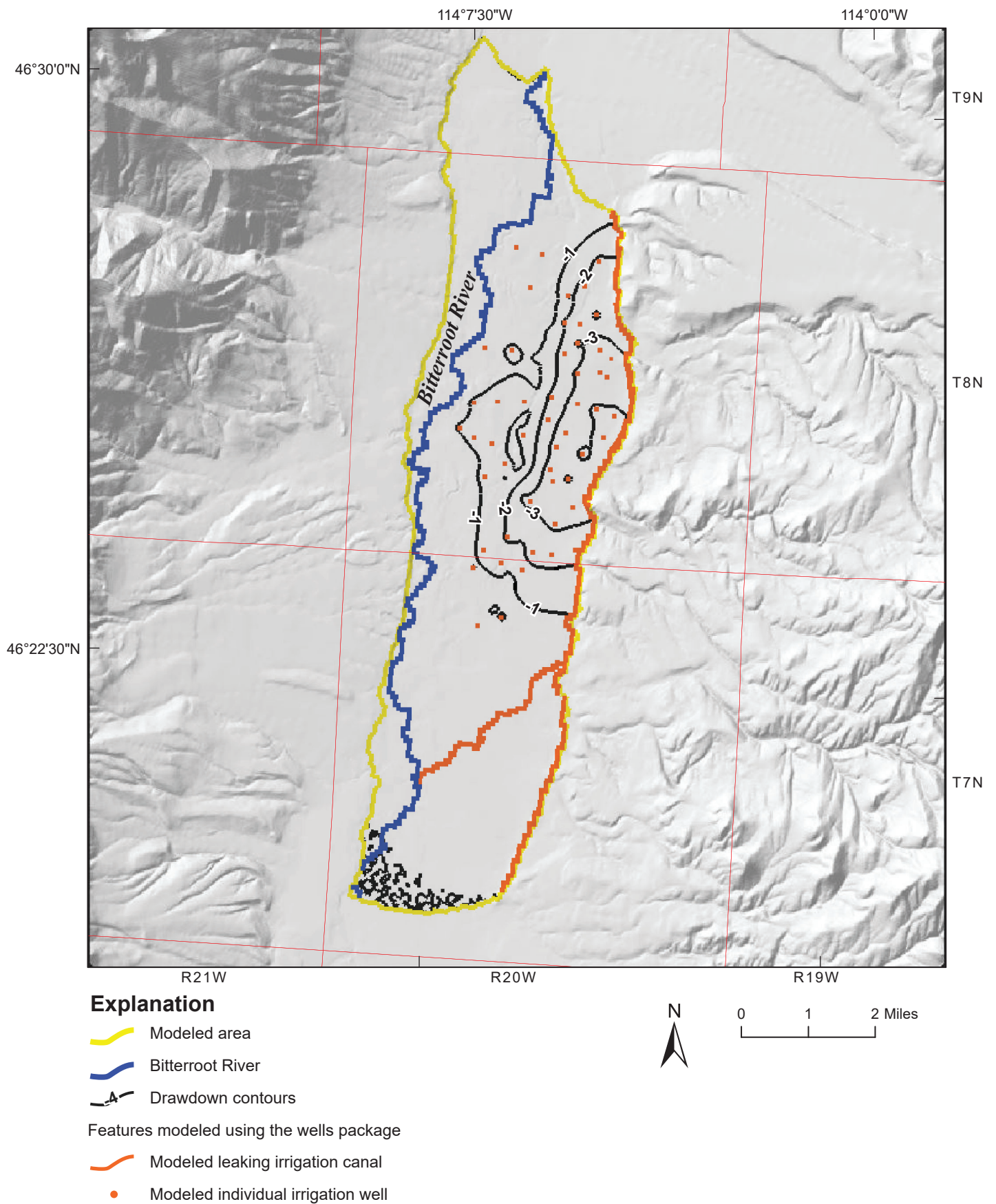


Figure 28. In the high K version of the model, drawdown from irrigation well pumping decreases by about 75% compared to the low K version (fig. 27).

the diminishment of irrigation recharge and pumping irrigation wells looks similar to the drawdown shown in figure 27; only the magnitude of the declines is increased. For the 4 and 12 ft contours shown in figure 27, the values are about 8 and 20 ft. These results show the calculated change from current conditions to a situation where all diversions and ditches sourced by the East Channel are off and all the fields irrigated with water derived from the East Channel are now sprinkler irrigated with groundwater.

These irrigation wells were generally operated in layer 1 of the model, representing the shallow alluvial aquifer. This assumes that wells producing up to nearly 500 gpm can be constructed in most areas. If in reality two or more closely spaced wells are needed to obtain this rate, the overall system response would be similar. In an additional simulation, wells were simulated in layer 3, which represents the deep sand and gravel aquifer. This simulation showed the effect on Mitchell Slough flows was virtually unchanged from wells pumping from model layer 1.

Scenario 4—Irrigation Wells across the Area Provide All East Channel Irrigation Water

This scenario used the 10-yr low and high K models to convert only sprinkler-irrigated lands from surface-water source to groundwater wells in three increments. This scenario differed from the previous simulation by preserving some flood irrigation. Sprinkler-irrigated lands were divided into three groups based on their location in relation to the ditch water they were serviced by. Wells were added to incrementally to replace fields currently irrigated by: (1) the Webfoot Ditch, (2) the Gehrlinger Ditch and Mitchell Slough, and (3) the Union, Etna, Victor, and Spooner Ditches. These irrigated lands were converted in the above three increments to evaluate the response of flows out of the Mitchell Slough east branch. Table E-12 lists the sprinkler-irrigated fields involved in this scenario; locations are shown in figure E-4 (appendix E).

Results of these incremental changes are shown in figure 29. Although only a 13-mo result is shown in the graphs, this exercise was also conducted using 10-yr transient simulations. The results show that flows are virtually unaffected by these changes in irrigation practices after early November, following the irrigation season. In this exercise, all diversions and canal

leakage remain unchanged. As shown in the graphs for both versions of the model, the decreases in flow out the Mitchell Slough east branch in the late summer are about 20 cfs. The simulated flows for 2021 are also shown on this graph (fig. 29; line e).

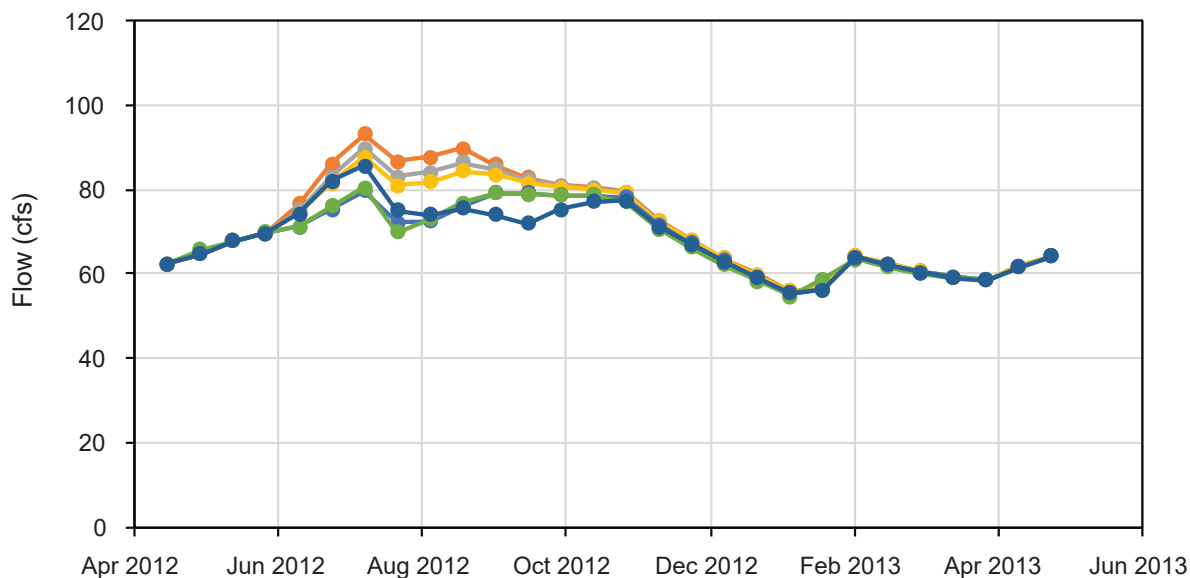
The model was also used to test the effect of shifting the irrigation season from June 1 through August 15, to July 1 through September 14, both 76 days in length. These simulations (fig. 29; line f) show that flow in the Mitchell Slough east branch is not affected in June, but is reduced by about 10 cfs compared to the base run in September, as one might expect. Simulated flows return to baseline levels by early November.

Diversions could be reduced by the amount that sprinkler irrigation withdraws from canals. Operators would need to make sure all diversion structures still function adequately for the flood irrigation diversions. The water savings are calculated based on the simulated demand of 2 ft of irrigation water for sprinkler-irrigated fields, applied evenly over 76 days from June 1 through August 15 of each irrigation season. For the 1,958 acres involved, about a 26 cfs reduction in diversions directly from the East Channel would occur. The permissible reduction in flow under this scenario, based on the lesser diversions needed to satisfy sprinkler irrigation, at the Tucker Headgate for Mitchell Slough, Union, Etna, and Webfoot Ditches, is about 9 cfs. Although about 26 cfs could be saved by converting all East Channel serviced canals to sprinkler irrigation, late summer return flows in the Mitchell Slough would diminish by 20 cfs, largely during the irrigation season. The primary benefit of this scenario would be retaining 26 cfs in the mainstem of the Bitterroot River (or the East Channel if desired) between the East Channel diversions and where Mitchell Slough discharges to the Bitterroot River. Downstream of that area, the change in flow would be minimal, on the order of a few cfs during the irrigation season. This is because at the point that all Mitchell Slough flows have rejoined the Bitterroot River, any water savings in the river are largely offset by the diminishment of Mitchell Slough flows.

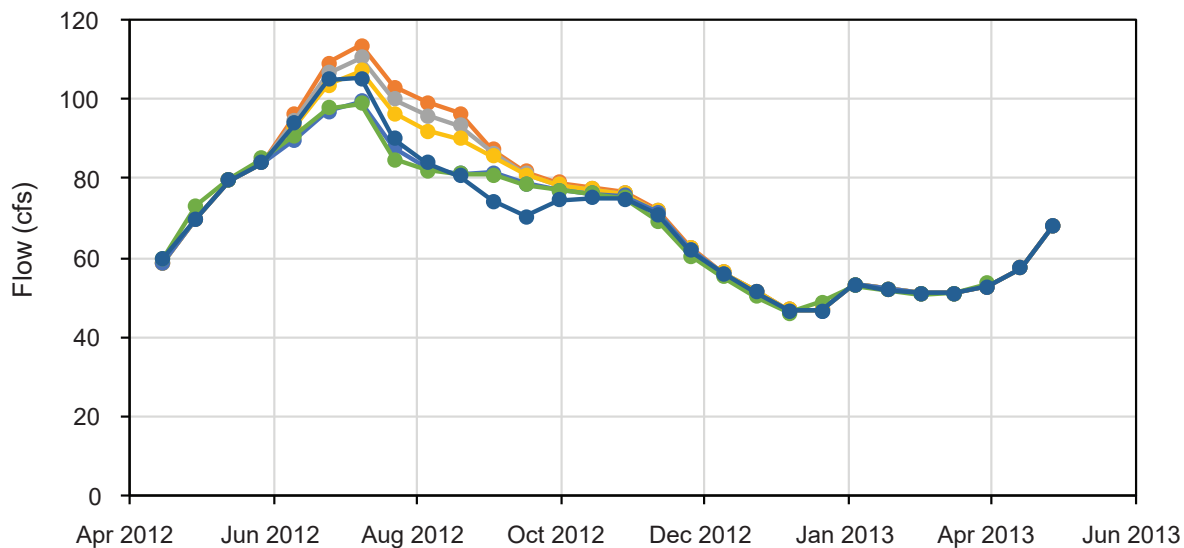
SUMMARY

The purpose of this investigation was to evaluate the feasibility of using groundwater to supplement or replace surface-water irrigation in the study area. We characterized the groundwater and surface-water sys-

A Low K Model Results



B High K Model Results



Explanation

- a. Base Runs—April 1, 2012 to April 30, 2013
- b. Convert Webfoot-serviced sprinkler-irrigated fields to wells
- c. Additionally convert sprinkler-irrigated fields serviced by Gerlinger Ditch and Mitchell Slough to wells
- d. Additionally convert sprinkler-irrigated fields serviced by Union, Etna, Victor and Spooner Ditches; Birch Creek Ditch to wells
- e. Year 2021—The flows calculated for year 2021 are plotted using the 2012–2013 time scale
- f. Shift irrigation from wells 1 mo later (for all sprinkler-irrigated lands serviced by wells) Irrigation recharge from these lands is also shifted 1 mo later (from July 1 instead of June 1).

Figure 29. The water sources for sprinkler-irrigated lands are incrementally converted to groundwater wells in the low (A) and high K (B) 13-mo transient models.

tems in the valley floor by conducting a 13-mo field study that included monitoring groundwater levels and stream, canal, and ditch flows. We developed a groundwater budget to provide reasonable estimates of irrigation canal leakage, irrigation drain gains, and recharge to shallow aquifers from excess irrigation water applied to fields.

Using these data and results from previous studies, we developed groundwater flow models to evaluate a variety of potential changes to irrigation and how those changes would affect groundwater levels and irrigation return flows. The flows of Mitchell Slough are of special interest, because the slough carries most of the irrigation return flows out of the study area.

The groundwater budget suggests that leaking irrigation canals are the primary source of seasonal recharge to shallow aquifers, followed by excess irrigation water applied to fields (table 2). This is reflected in groundwater model results, where the elimination of canal leakage creates the largest magnitude declines in irrigation return flows in Mitchell Slough. Converting sprinkler-irrigated lands from surface-water to groundwater sources has modest impacts to irrigation return flows in Mitchell Slough (fig. 29), but also results in less water diverted at the headgates. Diverting less water would make more surface water available for downstream users. The Bitterroot River mainstem is also a significant source of seasonal groundwater recharge as it supplies water to bank storage in the shallow aquifer that is discharged back to the river during low-flow conditions.

CONCLUSIONS AND RECOMMENDATIONS

The groundwater models developed for this project provide a tool to test scenarios involving irrigation activities in the central Bitterroot Valley. These models are available at: http://www.mbmgeology.mtech.edu/mgcat/public/ListCitation.asp?pub_id=32329&. The groundwater models simulate changes to the irrigation systems, such as replacing surface-water sources with groundwater sources, and effects of different irrigation methods or infrastructure on irrigation recharge to groundwater. Although there is adequate groundwater available to supply irrigation needs, there are options that avoid dredging of the East Channel and still use surface water as a source for irrigation.

Just above Tucker Crossing, the East Channel gets flow from two sources: the Bobby Smyth Ditch and the East Channel diversion from the Bitterroot River. The Bobby Smyth Ditch source is a diversion on the Supply Ditch. If surface water continues to be the major source of irrigation and if dredging of the East Channel is problematic, physical improvement of the Bobby Smyth Ditch might support diversion of more water into the ditch to compensate for the loss of water diverted into the East Channel.

Several practical concerns affect changes to using the Bobby Smyth Ditch to supply water to the East Channel. These include regulatory issues related to moving the point of diversion from the East Channel to where Bobby Smyth Ditch is diverted from Supply Ditch. Also an additional diversion from Supply Ditch might be required to allow about 60 cfs (the amount of water needed for high-demand summer irrigation at the Tucker Headgate into Mitchell Slough) of additional flow. Concerns also relate to gaining approval and funding to increase the flow of the Bobby Smyth Ditch by an additional 60 cfs to a total flow of about 120 cfs. Such changes would allow discontinuing dredging of the uppermost East Channel while generally preserving the irrigation and groundwater systems as they currently exist.

Another option to address concerns related to the current system includes improvements to the upper end of the East Channel to reduce annual maintenance needs. A more adequate and permanent diversion and conveyance channel may require less annual maintenance. An engineering study would be needed to determine a workable design and associated cost for such improvements.

Model results indicate that wells could provide irrigation water for lands currently irrigated with surface water derived from the East Channel. The scenario that least influences the current groundwater and surface-water conditions involves converting lands that are currently irrigated with sprinkler or pivot irrigation systems to groundwater sources (scenario 4; fig. 29). This scenario shows that converting from surface-water to groundwater sources generally does not affect irrigation return flows after November when compared to existing irrigation conditions.

Although conversion from flood to sprinkler irrigation would reduce the volume of water diverted to

fields, it would also reduce irrigation return flows. Various canals that use water from the East Channel service about 1,988 acres of flood-irrigated lands. Flood irrigation requires at least 1 ft more of water delivered to fields than sprinkler irrigation, so converting flood to sprinkler irrigation could save 1,988 acre-ft. For the 5-mo period from May through September, diversions would be reduced by about 6.6 cfs. The models show that flows exiting Mitchell Slough, due to the related reduction in irrigation return flows, would diminish by up to 10 cfs during the middle of the irrigation season, from late June through August, and by lesser amounts in early June and September (fig. 26).

Model results suggest that the complete conversion to a groundwater source of all lands serviced by a particular canal, and abandonment of the canal, lead to large reductions in the flows out of Mitchell Slough. For each canal abandoned, the previously diverted water is left in the source channel, either the East Channel or the mainstem of the Bitterroot River, and provides higher flows in the midsummer. Toward late summer, diminished irrigation return flows out of Mitchell Slough reduce river flow downstream of Mitchell Slough by amounts proportional to the midsummer flow savings.

The groundwater models are simplified approximations of a complex system. The diversion and irrigation rates used in the simulations are based on estimates of highly variable diversion rates and applications of water by individual users, introducing uncertainty into the results. These models are suitable tools for evaluating how major changes in irrigation practices affect the groundwater conditions and stream flow in the study area. For certain applications, the models may be updated with information about variations in irrigation practices, local-scale geologic conditions, and water use rates at existing wells, to improve simulations in key areas of interest.

The models developed for the Stevensville area may be modified to address other questions of interest. If used to analyze system response to a proposed well, an evaluation of the geologic materials between the potential well site and the nearest stream features could provide a basis for refining the model in the area of interest. For example, the hydraulic conductivity of layer 1 could be adjusted to reflect a locally important bed of coarse stream cobbles. Low and high K versions of these models can be used to simulate a rea-

sonable range of potential effects of proposed wells.

This modeling effort involved the use of GMS processing software. GMS files released with the native MODFLOW files provide the names of irrigated fields and canals within the model domain. This capacity simplifies modifying the model to simulate additional scenarios of interest.

All of the predictive simulations in this project used both the low K and high K model versions. The results agree within about 20% and provide a good indication of how the system would respond to changes in irrigation practices.

ACKNOWLEDGMENTS

This study is the result of Bitterroot River Water Commissioner Al Pernicelle's interest in the possibility of using groundwater resources to replace or supplement surface-irrigation sources in the central Bitterroot Valley. Many area landowners and residents allowed access to groundwater wells and surface-water features. Ravalli County provided court records, elevation data, and drain field test information. The Bitterroot Water Forum and the Bitterroot Conservation District provided a variety of reports and publications relevant to the study. The Bitterroot National Forest Service and Montana Department of Natural Resources and Conservation provided information and meeting space. The Montana Department of Transportation and Ravalli County supported installation of staff gages on bridges, which greatly benefited this work. MBMG staff provided reviews of the model and the overall report. Many thanks to MBMG staff Ali Gebril, Mary Sutherland, and Cam Carstarphen for their comments that helped improve the report.

REFERENCES

- Anderson, M.P., Woessner, W.W., and Hunt, R.J., 2015, *Applied groundwater modeling: Simulation of flow and advective transport*, 2nd ed.: San Diego, Academic Press, 564 p.
- Bobst, A., Waren, K., Swierc, J., and Madison, J., 2014, *Hydrogeologic investigation of the North Hills study area*, Lewis and Clark County, Montana, Technical Report: Montana Bureau of Mines and Geology Open-File Report 654, 376 p.
- Briar, D.W., and Dutton, D., 2000, *Hydrogeology and aquifer sensitivity of the Bitterroot Valley*, Ravalli

- County, Montana: U.S. Geological Survey Water-Resources Investigations Report 99-4219, 114 p.
- Carstarphen, C.A., Mason, D.M., Smith, L.N., LaFave, J.I., and Richter, M.G., 2003, Data for water wells visited during the Lolo-Bitterroot Area Ground-Water Characterization Study (open-file version): Montana Bureau of Mines and Geology Montana Ground-Water Assessment Atlas 4B-01, 1 sheet, scale 1:250,000.
- Driscoll, F.G. 1986, Groundwater and wells: St. Paul, Minn., Johnson Division, 1089 p.
- Fetter, C.W., 1980, Applied hydrogeology: Columbus, Ohio: Charles E. Merrill Publishing Company, 488 p.
- Finstick, S.A., 1986, Hydrogeology of the Victor and Bing quadrangles, Bitterroot Valley, Montana: Missoula, University of Montana, M.S. thesis, 150 p.
- Freeze, R.A, and Cherry, J.A., 1979, Groundwater: Englewood Cliffs, N.J., Prentice Hall, 604 p.
- Groundwater Information Center (GWIC), 2014, Montana Bureau of Mines and Geology Ground Water Information Center database, <http://mbmaggwic.mtec.edu> [Accessed September 2020].
- Groundwater Information Center (GWIC), 2016, Montana Bureau of Mines and Geology Ground-Water Information Center database, Recommended maximum concentrations for inorganic constituents in water, <http://mbmaggwic.mtech.edu/sqlserver/v11/help/reports/WQStandards.asp> [Accessed September 2020].
- Hackett, O.M., Visher, F.N., McMurtrey, R.G., and Steinhilber, W.L., 1960, Geology and ground-water resources of the Gallatin Valley, Gallatin County, Montana: U.S. Geological Survey Water-Supply Paper 1482, 282 p.
- Heath, R.C., 1983, Basic ground-water hydrology: U.S. Geological Survey Water Supply Paper 2220, 86 p.
- Hem, J.D., 1992, Study and interpretation of the chemical characteristics of natural water: U.S. Geological Survey Water Supply Paper 2254, 263 p.
- Kendy, E., and Tresch, R.E., 1996, Geographic, geologic, and hydrologic summaries of intermontane basins of the Northern Rocky Mountains, Montana: U.S. Geological Survey Water Resources Investigation Report 96-4025, 233 p.
- LaFave, J.I., 2006a, Potentiometric surface of the shallow basin-fill, deep basin-fill, and bedrock aquifers, Bitterroot Valley, Missoula and Ravalli counties, western Montana (open-file version): Montana Bureau of Mines and Geology Montana Ground-Water Assessment Atlas 4B-08, 1 sheet, scale 1:500,000.
- LaFave, J.I., 2006b, Ground-water quality in shallow basin-fill, deep basin-fill, and bedrock aquifers, Bitterroot Valley, Missoula and Ravalli counties, southwest Montana (open-file version): Montana Bureau of Mines and Geology Montana Ground-Water Assessment Atlas 4B-09, 1 sheet, scale 1:500,000.
- Lautz, L.K., 2008, Estimating groundwater evapotranspiration rates using diurnal water-table fluctuations in semi-arid riparian zone: Hydrogeology Journal, v. 16, p. 483-497.
- Lonn, J.D., and Sears, J.W., 2001a, Geology of the Bitterroot Valley on a topographic base: Montana Bureau of Mines and Geology Open-File Report 441-A, 1 sheet, scale 1:100,000.
- Lonn, J.D., and Sears, J.W., 2001b, Geology of the Bitterroot Valley, shaded relief, no topography: Montana Bureau of Mines and Geology Open-File Report 441B, 1 sheet, scale 1:100,000.
- Lonn, J.D., and Sears, J.W., 2001c, Geology of the Bitterroot Valley, shaded relief, no topography: Montana Bureau of Mines and Geology Open-File Report 441C, 1 sheet, scale 1:48,000.
- McMurtrey, R.G., Konizeski, R.L., Stermitz, F., and Swenson, H.A., 1959, Preliminary report on the geology and water resources of the Bitterroot Valley: Montana Bureau of Mines and Geology Bulletin 9, 45 p.
- McMurtrey, R.G., Konizeski, R.I., Johnson, M.V., and Bartells, J.H., 1972, Geology and water resources of the Bitterroot Valley, southwestern Montana: U.S. Geological Survey Water-Supply Paper W 1889, 80 p.
- Montana State Engineer's Office, 1958, Water Resources Survey, Ravalli County, Montana, Helena, Montana, 81 p.
- Montana Department of Environmental Quality (MDEQ), 2010, Montana numeric water quality standards: Circular DEQ-7, 61 p.

- Montana Department of Revenue (MT-DOR), 2012, Revenue final land unit (FLU) classification, http://nris.mt.gov/nsdi/nris/mdb/revenue_flu.zip [Accessed May 2013].
- Montana Department of Natural Resources and Conservation (MT-DNRC), 2007, Digitized ditch reference data from Montana's Water Resources Survey, http://www.dnrc.mt.gov/wrd/water_rts/survey_books/default.asp, based on the State Engineer's Office WRS publication for Ravalli County, June 1958 [Accessed June 2009].
- Montana Department of Natural Resources and Conservation (MT-DNRC), 2016, DNRC Water right query system, <http://wr.msl.mt.gov/> [Accessed February 2016].
- National Agricultural Imagery Program (NAIP), 2011, Natural-color aerial photos of Montana, 2011, <http://nris.mt.gov/gis/> [Accessed May 2014].
- National Resources Conservation Service (NRCS), 2014, Snow surveys and water supply forecasting, Snow Telemetry (SNOTEL) and Snow Course Data and Products: USDA Agriculture Information Bulletin 536, 1988, <http://www.wcc.nrcs.usda.gov/factpub/aib536.html> [Accessed February 2014].
- Norbeck, P.M., 1980, Preliminary evaluation of deep aquifers in the Bitterroot and Missoula valleys in western Montana: Montana Bureau of Mines and Geology Open-File Report 46, 160 p., 1:250,000.
- Natural Resource Information System (NRIS), 2010, Revenue final land unit (flu) classification, 2010, <http://geoinfo.msl.mt.gov/> [Accessed February 2013].
- Smith, L.N., 2006a, Altitude of the bedrock surface in the Bitterroot Valley: Missoula and Ravalli Counties, Montana (open-file version): Montana Bureau of Mines and Geology Montana Ground-Water Assessment Atlas 4B-05, 1 sheet, scale 1:125,000.
- Smith, L.N., 2006b, Thickness of quaternary unconsolidated deposits in the Lolo-Bitterroot area, Mineral, Missoula, and Ravalli Counties, Montana (open-file version): Montana Bureau of Mines and Geology Montana Ground-Water Assessment Atlas 4B-03, 1 sheet, scale 1:125,000.
- Smith, L.N., 2006c, Patterns of water-level fluctuations, Lolo-Bitterroot area, Mineral, Missoula and Ravalli Counties, Montana (open-file version): Montana Bureau of Mines and Geology Montana Ground-Water Assessment Atlas 4B-10, 1 sheet, scale 1:125,000.
- Smith, L.N., LaFave, J.I., and Patton, T.W., 2013, Groundwater resources of the Lolo-Bitterroot area: Mineral, Missoula, and Ravalli Counties, Montana: Part A—Descriptive overview and water-quality data: Montana Bureau of Mines and Geology Montana Ground-Water Assessment Atlas 4A, 96 p.
- Sonnichsen, R.P., 1993, Seepage rates from irrigation canals: Water Resources Program, Department of Ecology, Washington State Open-File Technical Report OFTR 93-3, 10 p.
- Stevensville COOP, 2014, National Climate Data Center NCDC COOP Station name: STEVENSVILLE, Station number 247894-1, data accessed 2/2/2014.
- Stiff, H.A., Jr. 1951, The interpretation of chemical water analysis by means of patterns: Journal of Petroleum Technology, v. 3, no. 10, 3 p.
- Stewart, A.M., 1998, Groundwater quantity and quality of the Eight Mile, Ravalli County, Montana: Missoula, University of Montana, M.S. thesis, 48 p.
- Sutherland, M., Michalek, T., and Wheaton, J., 2014, Hydrogeologic investigation of the Four Corners study area, Gallatin County, Montana, groundwater modeling report: Montana Bureau of Mines and Geology Open-File Report 652, 76 p.
- U.S. Department of the Interior Bureau of Reclamation (USBR), 1977, Ground water manual: Denver, Colo., United States Government Printing Office, 480 p.
- U.S. Department of Agriculture (USDA), 2011, Environmental Technical Note No. MT-1 (Rev.2), https://www.nrcs.usda.gov/Internet/FSE_DOCUMENTS/nrcs144p2_051302.pdf [Accessed September 2020].
- U.S. Geological Survey (USGS), 2010, LANDFIRE Existing Vegetation Type (LANDFIRE_US_110EVT), <http://www.landfire.gov/vegetation.php> [Accessed August 2015].
- U.S. Geological Survey (USGS), 2014, Water-resources data for the United States, Water Year 2013: U.S. Geological Survey Water-Data Report WDR-US-2013, site 12350250, <http://wdr.water>

[usgs.gov/wy2013/pdfs/12350250.2013.pdf](https://www.usgs.gov/wy2013/pdfs/12350250.2013.pdf) [Accessed May 2015].

U.S. Geological Survey (USGS), 1967, Hamilton North 1:24,000, Accessed at <https://catalog.data.gov/dataset/usgs-1-24000-scale-quadrangle-for-hamilton-north-mt-1967>.

Uthman, W., 1988, Hydrogeology of the Hamilton north and Corvallis quadrangles, Bitterroot Valley, southwestern Montana: Missoula, University of Montana, M.S. thesis, 232 p.

APPENDIX A:
GROUNDWATER MONITORING NETWORK

Appendix A
Table A-1
Groundwater Monitoring Network

GWIC Id	Latitude	Longitude	Township	Range	Section	Tract	Ground Surface Elevation (ft)	Static Water Level (SWL) Date	SWL-Ground (ft)	SWL-Elevation (feet Above Mean Sea Level)	Aquifer	Total Depth (ft)	Yield (gpm)	Well Use	Depth Water Enters and Top of	Depth to Bottom of Screen (ft)
56064	46.39138600	-114.14110700	07N	20W	6	DBAA	3431.37	6/28/2012	39.4	3391.97	112TRRC	57	20	DOMESTIC	49	54
56169	46.37698290	-114.07439277	07N	20W	10	DAAA	3550.13	3/7/2013	152.96	3397.17	120SNGR	245	25	DOMESTIC	185	245
56384	46.33394920	-114.12272926	07N	20W	29	DBBA	3448.88	3/7/2013	8.72	3440.16	110TRRC	39	12	DOMESTIC	39	39
56528	46.31398456	-114.11453346	07N	20W	32	DDDA	3476.71	3/7/2013	13.44	3463.27	111ALVM	40	20	FIRE PROTECTION	40	40
56843	46.35956460	-114.18223299	07N	21W	14	DBCC	3655.50	3/7/2013	55.97	3599.53	120SDMS	125	20	DOMESTIC	NR	NR
57128	46.31320039	-114.15802060	07N	21W	36	DDCC	3488.49	3/7/2013	13.88	3474.69	112TRRC	31	20	DOMESTIC	23	28
57607	46.42800263	-114.05323247	08N	20W	26	AAAB	3557.24	3/7/2013	192.48	3364.76	120SDMS	219	15	DOMESTIC	211	216
57723	46.47158705	-114.12797737	08N	20W	8	BAAB	3334.88	3/6/2013	26.16	3308.72	111ALVM	50	15	DOMESTIC	30	50
57788	46.47171305	-114.04148249	08N	20W	12	BAAA	3808.60	3/6/2013	52.98	3755.62	120SDMS	108	25	DOMESTIC	100	100
57790	46.47169295	-114.04151035	08N	20W	12	BAAA	3808.60	3/6/2013	38.73	3769.87	120SDMS	87	40	DOMESTIC	NR	NR
57844	46.45399709	-114.08928809	08N	20W	15	BCDD	3332.28	3/6/2013	11.38	3320.09	112TRRC	39	100	DOMESTIC	34	39
57848	46.44369352	-114.08325518	08N	20W	15	CDCC	3351.46	3/6/2013	20.13	3331.33	111ALVM	39	30	DOMESTIC	34	39
57905	46.43365303	-114.11438112	08N	20W	21	CBCB	3341.19	3/7/2013	4.89	3336.3	111ALVM	120	60	DOMESTIC	115	120
58019	46.41449421	-114.14156159	08N	20W	30	CDCC	3397.70	3/6/2013	22.9	3374.8	111ALVM	42	40	DOMESTIC	42	42
58096	46.41789397	-114.14789464	08N	20W	30	CDAB	3409.61	3/6/2013	25.8	3383.81	112ALVF	39	20	DOMESTIC	34	39
58222	46.41252484	-114.11288168	08N	20W	33	BBBD	3362.21	3/7/2013	3.77	3358.44	111ALVM	29	100	DOMESTIC	24	29
58226	46.40767816	-114.09843997	08N	20W	33	ADCC	3370.23	3/7/2013	6.17	3364.06	111ALVM	30	NR	DOMESTIC	NR	NR
60137	46.51214495	-114.08171861	09N	20W	26	BACC	3367.76	3/6/2013	81.97	3285.789	120SNGR	552	218	MONITORING	310	332
128772	46.43284310	-114.09484482	08N	20W	21	DADD	3345.93	3/6/2013	7.78	3338.15	111ALVM	40	500	DOMESTIC	35	40
136050	46.31161068	-114.18645643	06N	21W	2	ABBC	3754.46	3/7/2013	59.59	3694.87	120SDMS	83.9	NR	DOMESTIC	NR	NR
136174	46.47404466	-114.07412256	08N	20W	2	DDAD	3456.29	3/6/2013	140.54	3315.75	120SNGR	162	30	UNKNOWN	154	159
136183	46.44046486	-114.11518973	08N	20W	20	AADD	3335.78	3/7/2013	5.88	3329.9	120SNGR	105	375	IRRIGATION	85	105
136969	46.44120848	-114.14735724	08N	20W	19	BADA	3395.64	3/6/2013	18.84	3376.8	112ALVF	52	NR	UNUSED	NR	NR
136970	46.46367792	-114.02969839	08N	19W	7	CBDD	3892.78	3/6/2013	95.31	3797.47	120SDMS	112	NR	DOMESTIC	NR	NR
144577	46.39884079	-114.15634132	07N	21W	1	AAAD	3504.24	3/7/2013	39.83	3464.41	120SNGR	80	50	DOMESTIC	NR	NR
148985	46.50365208	-114.10079582	09N	20W	27	CDAB	3399.46	3/15/2013	19.95	3279.51	112TRRC	80	100	DOMESTIC	NR	NR
148986	46.50403027	-114.10118325	09N	20W	27	CDBA	3290.14	3/15/2013	12.71	3277.43	120SNGR	97	100	IRRIGATION	97	97
149726	46.42558954	-114.15710548	08N	21W	25	AADD	3423.01	3/7/2013	10.8	3412.21	120SNGR	120	10	DOMESTIC	120	120
152085	46.41504894	-114.08051311	08N	20W	27	DCDB	3392.25	3/21/2012	34.87	3358.9	111ALVM	138	50	DOMESTIC	138	138
154007	46.32344821	-114.22809913	07N	21W	33	ACBB	4220.48	3/6/2013	163.39	4057.09	211DBTL	300	8	DOMESTIC	150	160
158828	46.34553563	-114.11072079	07N	20W	21	CBDC	3433.98	3/7/2013	7.27	3426.71	112TRRC	50	40	DOMESTIC	50	50
161907	46.47246842	-114.08802950	08N	20W	3	CDCC	3319.45	3/6/2013	12.7	3306.75	112TRRC	61	50	PWS*	52	58
164754	46.50175287	-114.07878426	09N	20W	26	CDCC	3398.20	3/7/2013	17.29	3380.91	112ALVF	28	NR	UNUSED	NR	NR
166051	46.32596220	-114.11283729	07N	20W	33	BBBC	3466.03	3/7/2013	15.86	3450.17	111ALVM	51	18	DOMESTIC	51	51
170634	46.44160868	-114.10269819	08N	20W	21	ABAB	3336.88	3/6/2013	8.05	3328.83	111ALVM	63	NR	DOMESTIC	NR	NR
170952	46.33876349	-114.16837004	07N	21W	25	BADD	3475.02	3/7/2013	16.35	3458.67	112TRRC	60	NR	DOMESTIC	NR	NR
174634	46.42316409	-114.07204075	08N	20W	26	BCBC	3431.12	3/8/2013	67.92	3363.2	120SNGR	92	10	DOMESTIC	NR	NR
207831	46.34629824	-114.04328494	07N	20W	24	CACD	4092.43	3/7/2013	114.03	3978.4	120PLNC	180	NR	UNUSED	NR	NR
232344	46.44105904	-114.11199938	08N	20W	21	BBDB	3336.73	3/7/2013	7.6	3329.13	111ALVM	60	35	DOMESTIC	55	60
244362	46.32278439	-114.05103115	08N	20W	35	ADAA	3863.38	3/7/2013	123.14	3740.24	120SNGR	193	15	DOMESTIC	128	193
246207	46.34638991	-114.04474901	07N	20W	24	CACA	4061.76	3/7/2013	135.04	3926.72	120PLNC	440	6	UNKNOWN	207	438
260539	46.42785881	-114.04529854	08N	20W	25	BABB	3645.67	3/7/2013	65.15	3580.52	400BELT	340	15	DOMESTIC	310	340
266065	46.43420831	-114.11419778	08N	20W	25	CBBC	3340.44	3/7/2013	4.8	3335.64	111SNGR	24	NR	DOMESTIC	21	24
266087	46.43421867	-114.11418954	08N	20W	21	CBBC	3340.44	3/7/2013	4.72	3335.72	111SNGR	16	NR	MONITORING	13	16
266088	46.43421259	-114.11418637	08N	20W	21	CBBC	3340.44	3/7/2013	4.68	3335.76	111SNGR	8	NR	MONITORING	5	8
266089	46.43276172	-114.11495108	08N	20W	21	CBCC	3340.20	3/7/2013	3.18	3337.02	111SNGR	21	NR	MONITORING	18	21
266090	46.43276884	-114.11495559	08N	20W	21	CBCC	3340.80	3/7/2013	3.76	3337.04	111SNGR	8	NR	MONITORING	5	8
266796	46.41497604	-114.08050022	08N	20W	21	CCDD	3392.76	3/7/2013	10.39	3382.37	111ALVM	21	NR	MONITORING	NR	NR
266824	46.46609421	-114.09172646	08N	20W	27	DCDB	3314.93	3/7/2013	5.76	3309.17	111ALVM	NR	NR	UNUSED	NR	NR
266829	46.47320677	-114.12519745	08N	20W	10	BCCA	3309.73	3/7/2013	5.06	3304.67	111ALVM	18	NR	DOMESTIC	NR	NR
266835	46.36723900	-114.09712703	08N	20W	5	DCCB	3409.64	3/7/2013	4.25	3405.39	111SNGR	NR	NR	UNUSED	NR	NR
266837	46.41753881	-114.09897750	07N	20W	16	AACC	3361.53	3/7/2013	8.12	3353.41	111ALVM	NR	NR	IRRIGATION	NR	NR
266838	46.40967500	-114.08326500	08N	20W	34	BDAE	3375.65	9/21/2012	6.94	3368.71	120SNGR	NR	NR	DOMESTIC	NR	NR
266842	46.40003479	-114.08870077	08N	20W	34	CCDD	3383.06	3/7/2013	10.51	3372.55	111ALVM	39	NR	DOMESTIC	NR	NR
267988	46.38600000	-114.09550000	07N	20W	4	DDDC	3390.41	3/6/2013	8.88	3384.6	111ALVM	5	NA	OLD GRAVEL PIT	NA	NA

*PWS, Public Water Supply

Aquifer Codes

- 110TRRC TERRACE DEPOSITS (QUATERNARY)
- 111ALVM ALLUVIUM (HOLOCENE)
- 111SNGR SAND AND GRAVEL (HOLOCENE)
- 112ALVF ALLUVIAL FAN DEPOSITS - PLEISTOCENE
- 112TRRC TERRACE DEPOSITS (PLEISTOCENE)
- 120PLNC PLUTONIC ROCKS (TERTIARY - CRETACEOUS)
- 120SDMS SEDIMENTS (TERTIARY)
- 120SNGR SAND AND GRAVEL (TERTIARY)
- 211DBTL IDAHO BATHOLITH
- 400BELT BELT SUPERGROUP

Table A-2

Reported water well information from valley floor wells within the modeled area, and estimated hydraulic properties.

Shallow alluvial aquifer

GWIC ID	TD (ft)	PERF (ft)	PERF TYPE	Q (gpm)	SWL (ft)	PWL (ft)	S (ft)	Q/S (gpm/ft)	EST T (ft ² /d)	EST K (ft/d)	
228646	34	29-34	Screen	50	5	NA	NA	NA	NA	NA	
182388	28	25-Oct	5-in Torch Cuts	30	6	16	10	3.0	602	27	
123115	37	32-37	Screen	100	4	30	26	3.8	762	23	
145759	63	55-60	5-in Torch Cuts	80	28	32	4	20.0	4011	115	
161907	61	52-58	5-in Torch Cuts	50	13	25	12	4.2	842	18	
57738	39	31-36	5-in Slots	50	3	30	27	1.9	381	11	
134667	38	30-35	5-in Torch Cuts	80	8	12	4	20.0	4011	134	
262400	39	34-39	Screen	100	12	NA	NA	NA	NA	NA	
57848	39	34-39	Screen	30	20	34	14	2.1	421	22	
57847	39	34-39	Screen	100	8	34	26	3.8	762	25	
156175	38	33-38	Screen	100	18	30	12	8.3	1664	83	
57849	42	42	Open Hole	15	28	*	29	1	15.0	3008	215
173377	42	34-39	5-in Torch Cuts	60	22	NA	NA	NA	NA	NA	
57954	45	37-42	5-in Slots	25	29	42	13	1.9	381	24	
57922	55	60-65	5-in Slots	50	5	50	45	1.1	221	4	
257820	34	29-34	Screen	50	5	NA	NA	NA	NA	NA	
136193	28	20-25	5-in Torch Cuts	70	5	9	4	17.5	3509	153	
58222	29	24-29	5-in Slots	100	5	27	22	4.5	902	38	
58006	40	40	Open Hole	15	6	25	19	0.8	160	5	
58227	19	15-19	5-in Slots	30	3	17	14	2.1	421	26	
147610	38	38	Open Hole	50	11	33	22	2.3	461	17	
56150	41	41	Open Hole	20	4	25	21	1.0	201	5	
239904	37	29.5-34.5	5-in Torch Cuts	60	6	NA	NA	NA	NA	NA	
56233	40	40	Open Hole	30	15	22	7	4.3	862	34	
56209	40	40	Open Hole	25	7	20	13	1.9	381	12	
192843	32	27-32	Screen	100	3	NA	NA	NA	NA	NA	
248993	34	29-34	5-in Torch Cuts	20	6	NA	NA	NA	NA	NA	
154840	47	42-47	Screen	100	16	40	24	4.2	842	27	
167219	43	43	Open Hole	35	8	23	15	2.3	461	13	
56272	35	35	Open Hole	100	15	NA	NA	NA	NA	NA	
56289	31	26-31	5-in Slots	20	8	15	7	2.9	582	25	
164588	43	43	Open Hole	NA	8	20	12	NA	NA	NA	
56271	40	40	Open Hole	10	15	35	20	0.5	100	4	
56388	41	41	Open Hole	50	4	7	3	16.7	3349	91	
56391	40	40	Open Hole	20	3	12	9	2.2	441	12	
122159	20	20	Open Hole	30	6	15	9	3.3	662	47	
56384	39	39	Open Hole	12	7	*	8	1	12.0	2406	75
186653	30	25-30		35	6	NA	NA	NA	NA	NA	
186655	30	25-30		35	10	25	15	2.3	461	23	
139119	38	30-35	5-in Torch Cuts	150	6	15	9	16.7	3349	105	
Avg. TD	38.2			avg. SWL	9.925						

Deep sand and gravel aquifer

GWIC ID	TD (ft)	PERF (ft)	PERF TYPE	Q (gpm)	Shallow Aquifer				S (ft)	Q/S (gpm/ft)	EST T (ft ² /d)	EST K (ft/d)
					SWL (ft)	Bottom (ft)	FM TOP (ft)	PWL (ft)				
155427	163	163	Open Hole	20	-4.62	20	162	100	104.62	0.2	53	53
169584	73	53-73	Screen	100	4	37	50	50	46	2.2	588	26
142201	126	126	Open Hole	90	6	32	118	NA	NA	NA	NA	NA
126199	58	50-55	5-in Torch Cuts	60	35	38	50	42	7	8.6	2299	287
215365	79	79	Open Hole	40	30	18	36	NA	NA	NA	NA	NA
136183	105	85-105	5-in Torch Cuts	375	9	42	50	85	76	4.9	1310	24
232344	60	55-60	Screen	35	6	45	45	NA	NA	NA	NA	NA
57921	130	125-130	5-in Slots	30	6	40	116	60	54	0.6	160	11
122170	88	88	Open Hole	10	55	73	75	NA	NA	NA	NA	NA
164586	88	88	Open Hole	15	45	70	85	60	15	1.0	201	67
152085	138	138	Open Hole	50	32	15	100	110	78	0.6	160	4
58223	58	50-55	5-in Slots	40	6	48	51	NA	NA	NA	NA	NA
157399	69	69	Open Hole	15	10	12	30	NA	NA	NA	NA	NA
251072	60	55-60	5-in Torch Cuts	15	34	26	54	NA	NA	NA	NA	NA
128727	67	62-67	Screen	30	5	52	60	40	35	0.9	241	34
173169	126	126	Open Hole	50	6	58	125	80	74	0.7	187	187
173170	123	123	Open Hole	50	8	90	122	100	92	0.5	134	134
					Avg 17		42*		Avg 58			

*Reported pumping water level same as static, so 1 ft added to PWL to avoid division by zero.

Explanations (basic data from water well logs; drawdown, specific yield, transmissivities, and hydraulic conductivities estimated as indicated):

Column Explanation

- GWIC ID, MBMG GWIC database well identification number
- TD (ft), Total depth
- PERF (ft), Perforated interval
- TYPE, Type of perforations
- Q (gpm), Yield of the well in gallons per minute
- SWL (ft), Static water level in ft below ground surface
- FM TOP (ft), Depth to the top of the producing zone in the deep aquifer
- PWL (ft), Pumping water level in feet below ground surface
- S (ft), Drawdown (PWL minus SWL, in ft)
- Q/S (gpm/ft), Specific yield (yield/drawdown, in gpm/ft)

*Average shallowaquifer bottom

EST T (ft²/d), Estimated transmissivity in ft-squared/day: (from Driscoll, 1986)

$$\text{Shallow Aquifer T (ft-squared/d)} = (Q/S \text{ (gpm/ft)} * 1500)/7.48 \text{ gal/ft-cubed}; \text{ Deep Aquifer T (ft-squared/d)} = (Q/S \text{ (gpm/ft)} * 2000)/7.48 \text{ gal/ft}^3$$

EST K (ft/d), Estimated hydraulic conductivity in ft/day = T/b; aquifer thickness (b) is calculated by: (shallow aquifer: b=TD-SWL); (deep aquifer b=TD-FM TOP)

APPENDIX B:
SURFACE WATER MONITORING NETWORK

Appendix B

Surface-Water Monitoring Network

GWIC Id	Site Name	Lat	Lon	Geomethod	Point* ft, AMSL	Altitude of Measuring				Q	Sec	Type	First	Last	Readings
						Rng	Sec	Rng	Sec						
266793	BITTERROOT RIVER * VICTOR CROSSING * WEST BRANCH (BR-VIC-W)	46.41474573	-114.13274729	SUR-GPS	3371.61	08N	20W	29	29	29	29	29	3/2/2012	4/17/2013	28
266799	BITTERROOT RIVER * WOODSIDE CROSSING (BR-WOOD-N)	46.31276766	-114.14548186	SUR-GPS	3473.06	06N	20W	6	6	6	6	6	4/4/2012	9/15/2014	9067
266801	BITTERROOT RIVER * WOODSIDE CROSSING (BR-WOOD-S)	46.31266654	-114.14548488	SUR-GPS	3473.09	06N	20W	6	6	6	6	6	3/2/2012	4/17/2013	25
266804	BITTERROOT RIVER * TUCKER CROSSING WEST (BR-TUCK-W)	46.37111255	-114.14011027	SUR-GPS	3397.79	07N	20W	7	7	7	7	7	3/28/2012	4/16/2013	9228
266805	BITTERROOT RIVER * TUCKER CROSSING EAST (BR-TUCK-E)	46.37029792	-114.12167802	SUR-GPS	3399.05	07N	20W	17	17	17	17	17	3/28/2012	4/17/2013	9121
266806	MITCHELL SLOUGH * HEADGATE (MS-THAD)	46.37452159	-114.12256608	SUR-GPS	3394.90	07N	20W	8	8	8	8	8	4/12/2012	4/18/2013	8674
266807	BITTERROOT RIVER * VICTOR CROSSING * MIDDLE BRANCH (BR-VIC-M)	46.41447409	-114.12683994	SUR-GPS	3354.46	08N	20W	29	29	29	29	29	3/2/2012	4/16/2013	9559
266814	BITTERROOT RIVER * VICTOR CROSSING * EAST BRANCH (BR-VIC-E)	46.41449040	-114.12103106	SUR-GPS	3353.03	08N	20W	29	29	29	29	29	3/2/2012	4/16/2013	9861
266815	SPOONER DITCH * VICTOR CROSSING (SPD-VIC)	46.41439975	-114.11933372	SUR-GPS	3365.30	08N	20W	29	29	29	29	29	4/4/2012	4/17/2013	22
266816	UNNAMED SLOUGH * VICTOR CROSSING (US-VIC)	46.41570452	-114.10845992	SUR-GPS	3358.27	08N	20W	28	28	28	28	28	4/4/2012	4/17/2013	21
266817	MITCHELL SLOUGH * VICTOR CROSSING (MS-VIC)	46.41571822	-114.10670925	SUR-GPS	3352.85	08N	20W	28	28	28	28	28	3/27/2012	4/17/2013	9152
266818	WEBFOOT DITCH * VICTOR CROSSING (WD-VIC)	46.41579233	-114.10174647	SUR-GPS	3357.29	08N	20W	28	28	28	28	28	3/27/2012	4/17/2013	9165
266819	BIRCH CREEK * SPOONER CREEK LN (BC-VIC)	46.41058648	-114.09430663	SUR-GPS	3366.62	08N	20W	33	33	33	33	33	6/27/2012	4/17/2013	12
266820	BITTERROOT RIVER * BELL CROSSING (BR-BELL)	46.44353091	-114.12372502	SUR-GPS	3320.20	08N	20W	17	17	17	17	17	DCCC STREAM	7/1/2008	180000+
266828	ETNA DITCH * VICTOR CROSSING (ED-VIC)	46.41066684	-114.08214818	SUR-GPS	3371.81	08N	20W	34	34	34	34	34	3/27/2012	4/17/2013	5585
266839	UNION DITCH * VICTOR CROSSING (UD-VIC)	46.41067291	-114.08201941	SUR-GPS	3372.31	08N	20W	34	34	34	34	34	3/27/2012	4/17/2013	6519
266841	UNNAMED SLOUGH-1 * BELL CROSSING (US1-BELL)	46.44346873	-114.11934236	SUR-GPS	3343.37	08N	20W	17	17	17	17	17	DCCC STREAM	4/4/2012	20
266843	GEHLINGER DITCH * BELL CROSSING (GD-BELL)	46.44338829	-114.11187702	SUR-GPS	3329.80	08N	20W	16	16	16	16	16	3/26/2012	4/17/2013	6759
266844	UNNAMED SLOUGH-2 * BELL CROSSING (US2-BELL)	46.44336489	-114.10087875	SUR-GPS	3331.42	08N	20W	16	16	16	16	16	DCCC STREAM	5/1/2012	17
266845	MITCHELL SLOUGH * BELL CROSSING (MS-BELL)	46.44330171	-114.09827379	SUR-GPS	3328.20	08N	20W	16	16	16	16	16	DCCC STREAM	3/22/2012	9308
266846	WEBFOOT DITCH * BELL CROSSING (WD-BELL)	46.44339909	-114.08905568	SUR-GPS	3335.26	08N	20W	15	15	15	15	15	DCCC STREAM	3/26/2012	2512
266847	UNION DITCH * BELL CROSSING (UD-BELL)	46.44329889	-114.07452615	SUR-GPS	3366.57	08N	20W	15	15	15	15	15	DDDD STREAM	3/26/2012	8176
266848	WILLOUGHBY CREEK * BELL CROSSING (WC-BELL)	46.44481717	-114.06805849	SUR-GPS	3400.29	08N	20W	14	14	14	14	14	CCDA STREAM	4/6/2012	8436
266849	BITTERROOT RIVER * STEVENSVILLE (BR-STV)	46.52075476	-114.10756675	SUR-GPS	3264.23	09N	20W	22	22	22	22	22	BCBA STREAM	3/22/2012	9291
266850	UNION DITCH * STEVENSVILLE (UD-STV)	46.48665276	-114.08729461	SUR-GPS	3353.87	09N	20W	35	35	35	35	35	CCCC STREAM	3/26/2012	6276
266851	ETNA DITCH * DOUBLE FORK RANCH (ED-DF)	46.39228869	-114.10502236	SUR-GPS	3381.26	07N	20W	4	4	4	4	4	CAAA STREAM	4/20/2012	5025
266852	UNION DITCH * DOUBLE FORK RANCH (UD-DF)	46.38943376	-114.10599905	SUR-GPS	3382.60	07N	20W	4	4	4	4	4	CADC STREAM	4/26/2012	4882
267520	GEHLINGER DITCH (GD-BRN) * GD-BRN	46.43270657	-114.11502578	SUR-GPS	3338.06	08N	20W	21	21	21	21	21	CBCC DITCH	4/5/2012	5375
268245	BITTERROOT RIVER * TUCKER CROSSING WEST II (BR-TUCK-WII)	46.36989654	-114.13980568	SUR-GPS	3397.52	07N	20W	18	18	18	18	18	AABB STREAM	7/25/2012	6373
268246	WEBFOOT DITCH * EASTSIDE HIGHWAY (WD-EH)	46.42554798	-114.09521700	SUR-GPS	3353.87	08N	20W	28	28	28	28	28	AADD DITCH	5/2/2012	12
268247	COMBO DITCH * EASTSIDE HIGHWAY (CD-EH)	46.43962449	-114.09427880	SUR-GPS	3335.35	08N	20W	22	22	22	22	22	BBCC DITCH	5/2/2012	12
269370	BITTERROOT IRRIGATION DISTRICT CANAL AT EAST TAMMANY TRAIL	46.24430000	-114.06520000	SUR-GPS	3895.17	06N	20W	26	26	26	26	26	CACC DITCH	9/13/2012	10000+
269371	BITTERROOT IRRIGATION DISTRICT CANAL AT SKALKAKO HWY	46.18210000	-114.07970000	SUR-GPS	3909.72	05N	20W	22	22	22	22	22	ABBA DITCH	9/13/2012	10000+
269727	MITCHELL SLOUGH (MS-NICH)	46.46802421	-114.09427026	SUR-GPS	3306.86	08N	20W	10	10	10	10	10	BCBB STREAM	4/12/2012	8869

*0.00 ft on all staff gages.

**APPENDIX C:
WELL LOG LITHOLOGIC CATEGORIES**

Appendix C

Materials Key for Well Log Data

This appendix lists the 18 material codes used in the Groundwater Modeling System software to identify geologic materials. The resulting borehole products are included in the steady state models.

Adjusted material codes

Material	Code
Topsoil	1
M	2
Ash	3
Ash, S, G	4
C & Ash	5
C	6
C & G/C, S, & G	7
C & S	8
S	9
S & C	10
S & M	11
S & G	12
S, G, Cb/S, G, Bld	13
G/Cb	14
Conglom.	15
Sed. Rock	16
Granite	17
Bedrock/Rock	18

C, clay; S, sand; M, silt; Bld, boulders; Cb, cobbles; Sed. Rock, sedimentary rock.

18 materials

Clay & gravel combined w/ clay, sand, and gravel. Sand, gravel & cobbles combined w/ sand, gravel, & boulders. Some ash categories combined.

APPENDIX D:
SURFACE WATER AND GROUNDWATER QUALITY DATA

Appendix D
Water-Quality Data
Surface Water

GWIC ID	Site Name	Sample ID	Latitude	Longitude	Twn	Range	Section	Tract	Site Type	Sample Date	Water Temp (°F)	pH	Specific Conductance (µS/cm)	Ca (mg/L)	Mg (mg/L)	Na (mg/L)	K (mg/L)	Fe (mg/L)	Mn (mg/L)
266799	Bitterroot River @ Woodside	202526	46.312768	-114.145482	06N	20W	6	BAAA	STREAM	8/8/12	67.5	7.18	55	9.94	2.20	3.48	1.13	0.029 J	0.004 J
266852	Union Ditch @ Double Fork Ranch	202527	46.389434	-114.105999	07N	20W	4	CADC	STREAM	8/8/12	20.5	8.21	89	16.08	3.51	4.66	1.52	0.032 J	0.016 J
266806	Mitchell Slough @ Tucker Headgate	202518	46.374522	-114.122566	07N	20W	8	DBCD	STREAM	8/8/12	67.8	8.08	91	14.13	3.04	3.58	1.34	0.017 J	0.003 J
267501	Fred Burr Creek FBC-93	202523	46.349900	-114.148000	07N	20W	19	BBCD	STREAM	8/8/12	NA	6.83	50	6.07	1.49	4.69	1.01	0.033 J	0.002 J
266848	Willoughby Creek @ Bell Crossing	202521	46.444817	-114.068058	08N	20W	14	CCDA	STREAM	8/8/12	73.2	7.99	333	30.80	9.34	27.94	6.07	0.032 J	<0.002 U
266845	Mitchell Slough @ Bell Crossing	202524	46.443302	-114.098274	08N	20W	16	DDCD	STREAM	8/7/12	67.6	8.24	298	38.91	7.53	12.11	4.15	<0.015 U	0.002 J
266818	Webfoot Ditch @ Victor	202525	46.415792	-114.101746	08N	20W	28	DCCA	STREAM	8/8/12	67.3	7.81	185	26.32	5.05	7.11	2.54	0.016 J	0.004 J
266819	Birch Creek @ Victor	202532	46.410586	-114.094307	08N	20W	33	ADAA	STREAM	8/8/12	57.0	7.35	343	46.17	8.76	18.50	4.13	<0.015 U	<0.002 U
267499	Kootenai Creek @ Kootenai Creek Road	202522	46.530200	-114.137200	09N	20W	17	ABAB	STREAM	8/9/12	64.4	6.69	122	1.64	0.34	1.13	0.43	<0.015 U	<0.002 U
266849	Bitterroot River @ Stevensville	202517	46.520755	-114.107567	09N	20W	22	CBCA	STREAM	8/8/12	18.9	8.07	122	18.24	3.67	5.83	1.87	0.016 J	0.006 J
266850	Union Ditch @ Stevensville	202520	46.486653	-114.087295	09N	20W	35	CCCC	STREAM	8/8/12	66.4	7.51	109	16.81	3.62	4.97	1.98	0.027 J	0.002 J
271965	Webfoot Ditch @ East Side Highway	202529	46.467500	-114.093170	08N	20W	10	BCBB	CANAL	8/7/12	NA	8.26	277	40.06	7.93	13.11	4.26	<0.015 U	<0.002 U
267500	BRID @ Drift Lane	202519	46.472000	-114.037700	08N	20W	12	ABAB	CANAL	8/8/12	70.7	7.34	25	4.37	0.89	0.55	0.37	<0.015 U	<0.002 U
267522	Gerlinger Ditch	202530	46.433600	-114.113900	08N	20W	21	CBCB	CANAL	8/9/12	68.9	7.89	89	14.69	3.21	4.51	1.50	0.019 J	<0.002 U
268247	Combo Ditch @ East Side Highway	202531	46.433624	-114.094279	08N	20W	22	BBCC	CANAL	8/8/12	57.4	7.51	300	42.11	8.30	13.20	4.81	0.027 J	0.003 J

Notes: Latitude and Longitude values were acquired by Survey grade GPS or identification on aerial photo. Datum WGS84.

NA, Not Available

Sample ID	Site Name	SiO ₂ (mg/L)	HCO ₃ (mg/L)	CO ₂ (mg/L)	SO ₄ (mg/L)	Cl (mg/L)	F (mg/L)	OPO4-P (mg/L)	Total Arsenic (AsT) (µg/L)	Lead (Pb) (µg/L)	Uranium (U) (µg/L)	Nitrate-N (NO ₃ -N) (mg/L)	Nitrite-N (NO ₂ -N) (mg/L)	Total Nitrogen (mg/L)	TDS (mg/L)	Alkalinity (mg/L CaCO ₃)	SAR	Procedure
202526	Bitterroot River @ Woodside	10.0	45.8	0.00	0.0	1.5	0.13	<0.020 U	0.00	<0.040 U	0.00	<0.010 U	<0.010 U	<1.000 U	51	38	0.22	DISSOLVED
202527	Union Ditch @ Double Fork Ranch	11.6	74.5	0.00	2.7	1.8	0.14	<0.020 U	0.63	<0.040 U	0.76	<0.010 U	<0.010 U	<1.000 U	81	62	0.29	DISSOLVED
202518	Mitchell Slough @ Tucker Headgate	11.8	63.1	0.00	2.7	1.7	0.14	<0.020 U	0.00	<0.040 U	0.62	0.06	<0.010 U	<1.000 U	70	52	0.25	DISSOLVED
202523	Fred Burr Creek FBC-93	14.6	35.6	0.00	0.0	1.5	0.1	<0.020 U	0.00	<0.040 U	0.00	<0.010 U	<0.010 U	<1.000 U	47	30	0.47	DISSOLVED
202521	Willoughby Creek @ Bell Crossing	19.7	194.0	0.00	9.1	5.1	0.36	0.090 J	3.85	<0.040 U	3.78	<0.010 U	<0.010 U	<1.000 U	204	159	1.13	DISSOLVED
202524	Mitchell Slough @ Bell Crossing	20.7	175.9	0.00	3.4	2.2	0.2	<0.020 U	2.28	<0.040 U	3.53	0.44	<0.010 U	1.13	179	144	0.46	DISSOLVED
202525	Webfoot Ditch @ Victor	16.5	117.4	0.00	3.7	2.5	0.17	<0.020 U	1.33	<0.040 U	1.21	0.11	<0.010 U	<1.000 U	121	96	0.33	DISSOLVED
202532	Birch Creek @ Victor	26.3	208.9	0.00	7.2	4.2	0.21	0.050 J	3.29	<0.040 U	4.93	1.19	<0.010 U	1.8	219	171	0.67	DISSOLVED
202522	Kootenai Creek @ Kootenai Creek Road	5.7	9.9	0.00	3.1	0.0	0.050 J	<0.020 U	0.00	<0.040 U	0.00	0.08	<0.010 U	<1.000 U	17	8	0.19	DISSOLVED
202517	Bitterroot River @ Stevensville	13.7	82.9	0.00	3.3	2.1	0.14	<0.020 U	0.65	<0.040 U	1.05	0.09	<0.010 U	<1.000 U	90	68	0.34	DISSOLVED
202520	Union Ditch @ Stevensville	11.6	80.0	0.00	2.8	1.8	0.15	<0.020 U	0.73	<0.040 U	0.68	<0.010 U	<0.010 U	1.08	84	66	0.29	DISSOLVED
202529	Webfoot Ditch @ East Side Highway	21.6	182.4	0.00	6.1	3.4	0.21	0.080 J	2.85	<0.040 U	3.41	0.42	<0.010 U	1.01	186	149	0.49	DISSOLVED
202519	BRID @ Drift Lane	5.0	21.5	0.00	0.0	0.0	0.06	<0.020 U	0.00	<0.040 U	0.00	<0.010 U	<0.010 U	<1.000 U	22	17	0.11	DISSOLVED
202530	Gerlinger Ditch	10.2	68.9	0.00	2.8	1.7	0.13	<0.020 U	0.00	<0.040 U	0.64	<0.010 U	<0.010 U	<1.000 U	74	57	0.31	DISSOLVED
202531	Combo Ditch @ East Side Highway	24.2	193.3	0.00	6.1	3.3	0.2	0.060 J	2.89	<0.040 U	3.54	0.64	<0.010 U	1.54	197	158	0.48	DISSOLVED

Appendix D—Water-Quality Data

Groundwater

GWIC ID	Sample ID	Latitude	Longitude	Township	Range	Section	Tract	Site Type	Aquifer	Total Depth (ft)	Sample Date	Water Temperature (°F)	pH	Specific Conductance (µS/cm)	Ca (mg/L)	Mg (mg/L)	Na (mg/L)	K (mg/L)	Fe (mg/L)
56169	202499	46.376983	-114.074393	07N	20W	10	DAAA	WELL	120SNGR	245	8/7/12	54.3	7.63	475	68.66	12.72	11.53	11.45	<0.015 U
158828	202478	46.345536	-114.110721	07N	20W	21	CBDC	WELL	112TRRC	50	8/7/12	52.5	7.11	327	47.32	9.60	12.61	3.32	<0.015 U
56384	202491	46.333949	-114.122729	07N	20W	29	DBBA	WELL	110TRRC	39	8/7/12	51.3	7.08	291	44.68	9.07	9.18	3.15	<0.015 U
56528	202488	46.313985	-114.114533	07N	20W	32	DDDA	WELL	111ALVM	40	8/6/12	52.7	7.21	323	45.65	11.21	11.38	3.39	<0.015 U
144577	202494	46.398841	-114.156341	07N	21W	1	AAAD	WELL	120SNGR	80	8/9/12	49.5	6.52	86	11.40	3.08	5.64	1.10	0.217
57128	202489	46.313220	-114.158023	07N	21W	36	DDDD	WELL	112TRRC	31	8/8/12	60.3	6.25	58	3.87	0.80	2.74	1.28	0.036J
136970	202500	46.463678	-114.029698	08N	19W	7	CBBD	WELL	120SDMS	112	8/6/12	49.6	7.98	782	45.17	21.40	121.23	1.93	<0.015 U
136174	202495	46.474045	-114.074123	08N	20W	2	CC	WELL	120SNGR	162	8/7/12	54.0	7.34	514	68.64	14.49	17.49	5.91	<0.015 U
161907	202483	46.472468	-114.088030	08N	20W	3	CDCC	WELL	112TRRC	61	8/6/12	54.3	7.29	255	36.81	5.98	11.79	3.49	<0.015 U
266829	202502	46.473207	-114.125197	08N	20W	5	DCCB	WELL	111ALVM	0	8/7/12	49.8	6.79	159	21.68	4.76	8.54	1.23	2.372
57723	202609	46.471587	-114.127977	08N	20W	8	BAAB	WELL	111ALVM	0	8/22/12	54.7	6.39	116	17.33	5.48	5.39	1.48	0.019J
266824	202498	46.466094	-114.091726	08N	20W	10	BCCA	WELL	111ALVM	0	8/7/12	52.5	7.39	381	56.57	11.15	14.07	5.67	<0.015 U
57788	202484	46.471713	-114.041482	08N	20W	12	BA	WELL	120SDMS	108	8/6/12	49.8	7.76	720	57.60	53.33	32.22	4.87	<0.015 U
57844	202477	46.453997	-114.089288	08N	20W	15	BCDD	WELL	112TRRC	39	8/6/12	52.9	7.25	398	55.23	11.34	19.71	6.36	<0.015 U
57848	202481	46.443694	-114.083255	08N	20W	15	CDCC	WELL	111ALVM	39	8/7/12	51.3	7.24	407	53.77	10.61	19.18	6.32	<0.015 U
136969	202946	46.441208	-114.147357	08N	20W	19	BADA	WELL	112ALVF	52	10/19/12	48.2	7.03	172	27.05	9.52	4.46	2.07	0.13
170634	202480	46.441609	-114.102698	08N	20W	21	ABAB	WELL	111ALVM	63	8/7/12	52.5	7.31	227	38.47	5.66	5.23	1.92	<0.015 U
232344	202490	46.441059	-114.111999	08N	20W	21	BB	WELL	111ALVM	60	8/7/12	54.7	6.59	99	17.20	3.24	5.24	1.20	0.807
57905	202492	46.433653	-114.114381	08N	20W	21	CBGB	WELL	111ALVM	120	8/9/12	55.8	7.41	242	38.17	6.93	8.06	2.48	<0.015 U
128772	202486	46.432843	-114.094845	08N	20W	21	DADD	WELL	111ALVM	40	8/7/12	51.4	7.25	438	64.04	11.11	18.02	5.05	<0.015 U
266065	202496	46.434208	-114.114198	08N	20W	21		WELL	111ALVM	24	8/9/12	51.8	6.62	114	16.78	3.37	4.94	1.83	0.754
260539	202610	46.427859	-114.045299	08N	20W	25	BABB	WELL	400BELT	340	8/23/12	59.7	7.61	286	27.03	6.43	40.34	3.59	0.043J
130860	204312	46.427364	-114.064786	08N	20W	26	BAAC	WELL	120SDMS	440	7/23/13	60.8	7.13	466	30.60	8.13	56.45	7.39	<0.015 U
174634	202509	46.423164	-114.072041	08N	20W	26	BCBC	WELL	120SNGR	92	8/10/12	52.2	7.35	651	73.33	16.57	40.91	10.78	<0.015 U
152085	202506	46.415049	-114.080513	08N	20W	27	DCD	WELL	120SDMS	138	8/9/12	58.1	7.50	425	59.40	8.92	19.45	6.44	<0.015 U
266796	202505	46.414976	-114.080500	08N	20W	27	DCDB	WELL	111ALVM	0	8/9/12	56.1	7.19	197	25.40	5.04	12.99	5.20	<0.015 U
266837	202507	46.417539	-114.098978	08N	20W	28	DC	WELL	111ALVM	0	8/10/12	57.6	7.40	372	50.99	9.45	16.30	5.32	<0.015 U
58019	202497	46.414494	-114.141562	08N	20W	30	DCDD	WELL	111ALVM	42	8/7/12	50.9	6.30	59	7.12	2.20	3.03	2.07	0.019J
58226	202482	46.407678	-114.098440	08N	20W	33	AD	WELL	111ALVM	30	8/7/12	52.0	7.09	335	49.27	7.87	13.04	3.21	<0.015 U
58222	202501	46.412525	-114.112882	08N	20W	33	BBBD	WELL	111ALVM	29	8/6/12	49.6	6.95	196	27.79	5.50	8.15	1.75	<0.015 U
266838	202508	46.409675	-114.083265	08N	20W	34	BAAA	WELL	120SDMS	0	8/11/12	55.8	7.67	433	56.57	10.52	21.30	9.67	<0.015 U
266842	202503	46.400035	-114.088701	08N	20W	34	CCDD	WELL	111ALVM	0	8/9/12	52.3	7.42	465	62.40	12.43	21.09	6.77	<0.015 U

Notes:
Latitude and Longitude values were acquired by Survey grade GPS or identification on aerial photo. Datum WGS84.

APPENDIX E:
GROUNDWATER MODEL DETAILS

GROUNDWATER MODEL DETAILS

We developed steady-state, 13-mo, and 10-yr transient groundwater flow models to evaluate the effect of various irrigation changes on groundwater levels and surface-water flows. This appendix includes details about these models, providing potential users with descriptions of the software, the model files, model use, grid and layer construction, sources and sinks, calibration, and sensitivity analysis results. Calculations are included at the end of the appendix to document development of model inputs.

OVERVIEW OF GROUNDWATER MODELS

The Stevensville groundwater models consist of three layers that simulate conditions in the valley floor of the Bitterroot Valley. Hydrogeologic units include a shallow alluvial aquifer, an underlying silt and clay aquitard, and a deep sand and gravel aquifer. The models extend from about 2 mi north of Corvallis (upstream end) generally downstream of the Supply Ditch and east of the mainstem of the Bitterroot River to the Stevensville area (downstream end), where the east branch of Mitchell Slough discharges to the Bitterroot River (fig. E-1). We developed a steady-state model, available in two versions, which uses average annual rates and stages for dynamic features. One version applies a low K of 200 ft/d and the other applies a higher K of 2,000 ft/d. Both versions can be used to estimate long-term effects of changes to the hydrologic system.

High K and low K versions of a transient model were calibrated to the 13-mo period from April 2012 through April 2013. This corresponds to the monitoring period for this project. Finally, a 10-yr transient model expands the 13-mo transient model, in both the low and high K versions. This model repeats the 2012 irrigation season activities for all subsequent years. The 10-yr model can be used as a base case, to compare results to those from model runs that simulate changes in irrigation practices or groundwater withdrawals.

These groundwater models are designed to assess the effect of changes in irrigation practices, such as using groundwater wells to supplement or replace surface water for irrigation, on the hydrologic system in the valley floor area. Scenarios provide an indication of the hydrogeologic response of reducing or elimi-

nating irrigation recharge to groundwater and return flows. The model files are provided so that other users may adapt or modify this work to investigate other features of the hydrologic system.

GROUNDWATER MODELING SOFTWARE

We used the U.S. Geological Survey (USGS) MODFLOW code, version 1.19.01 (Harbaugh and others, 2000) with Groundwater Modeling System software (GMS version 9.2.9; Aquaveo, 2014) as a graphical user interface. GMS facilitates the use of maps, images, and geographical information system (GIS) products for groundwater modeling. GMS includes a subsurface characterization capability to analyze and correlate lithologic information reported on well logs.

BOREHOLE ANALYSIS

We completed an analysis with GMS, assembling well log data for selected wells in the study area with locations verified by cadastral data. Cadastral data verification involved matching a landowner or lot number from the Montana Cadastral website with a well log record. Elevation and project codes were assigned to the selected well logs. Data were exported from MBMG's Groundwater Information Center (GWIC) database using a GMS Export tool. The borehole data are embedded in GMS files related to the steady-state models.

GROUNDWATER FLOW MODEL CONSTRUCTION

The model grid was created in GMS using the North American Datum (NAD) 1983 State Plane coordinates (fig. E-1), with dimensional units of international feet. A grid frame was created with an x origin of 787,400 ft, y origin of 787,050 ft, and z origin of 3,125 ft (table E-1). A rotation angle of 353° was specified to align the grid in the direction of the Bitterroot Valley. This angle effectively rotates the model clockwise 7°. The surface of the model represents the land-surface elevation and was developed from the National Elevation Dataset (USGS, 1999) accessed on February 26, 2013, with the GMS online maps function. The active model grid covered about 32 mi².

Model Boundaries

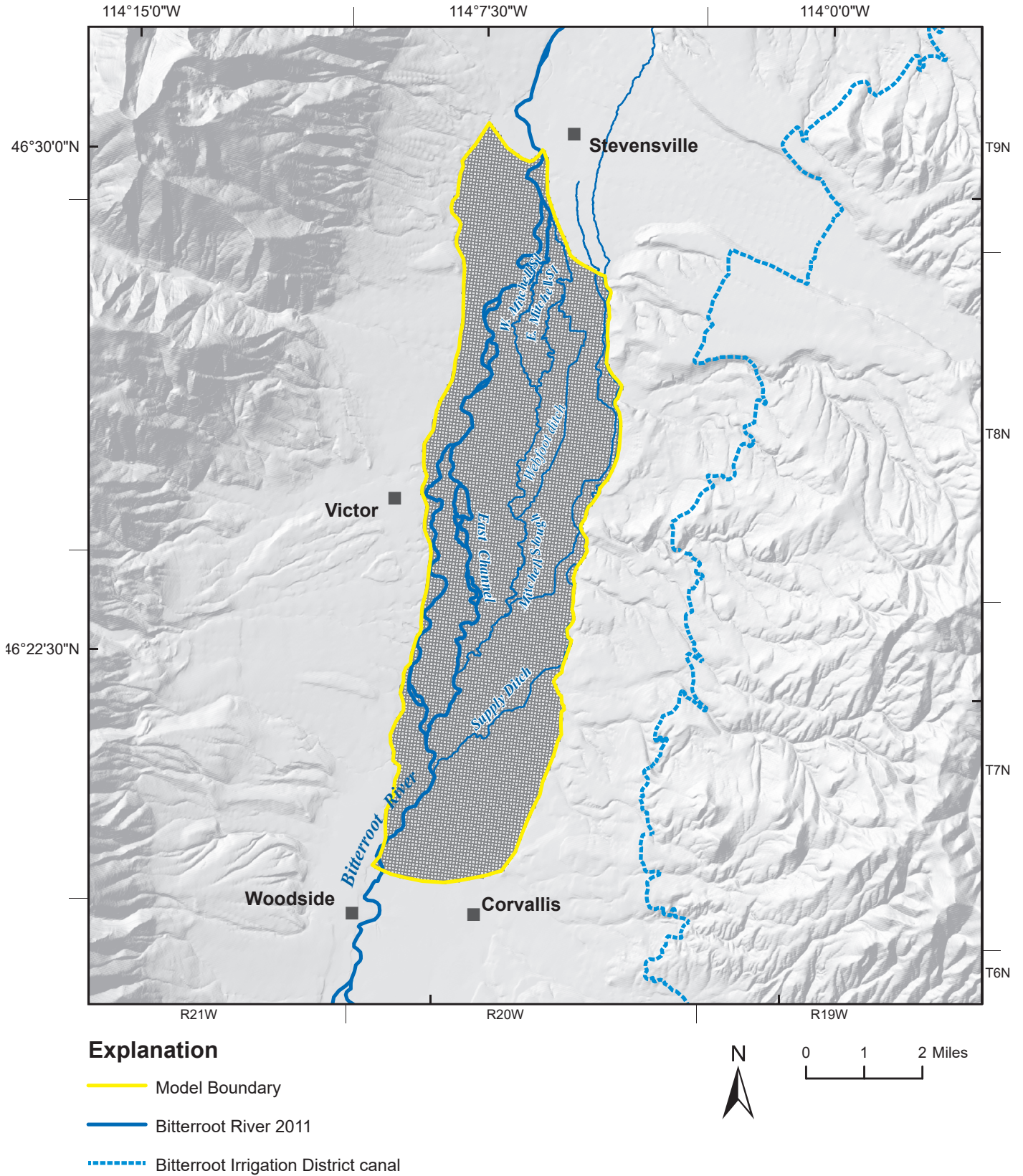


Figure E-1. The model grid is located in the valley floor portion of the study area. Its north and south boundaries are defined using modified potentiometric contours.

Table E-1. Model grid information.

Grid type:	Cell Centered
X origin:	787,400.0 (ft)
Y origin:	787,050.0 (ft)
Z origin:	3125.0 (ft)
Length in X:	27,600.0 (ft)
Length in Y:	77,100.0 (ft)
Length in Z:	375.0(ft)
Rotation angle:	353.0
AHGW X origin:	796,796.12637654 (ft)
AHGW Y origin:	863,575.30829155 (ft)
AHGW Z origin:	3,500.0 (ft)
AHGW Rotation angle:	97.0
Minimum scalar:	3,275.0
Maximum scalar:	3,450.0
Num cells i:	257
Num cells j:	92
Num cells k:	3
Number of nodes:	95,976
Number of cells:	70,932
No. Active cells:	29,541
No. Inactive cells:	41,391

The active area of the domain was determined with selected potentiometric contours at the north and south ends. The domain extends to east and west boundaries formed by the edge of the valley floor.

The west edge of the domain is a no-flow boundary set at the edge of the shallow alluvial aquifer. Although beyond the focus area for this model, setting the boundary at the western valley edge permits simulation of flux on both sides of the Bitterroot River. This allows consideration of groundwater storage in aquifer sediments west of the river.

The east boundary is a flux-dependent boundary, where groundwater flow is added using the MODFLOW wells package. This represents groundwater entering the system from the eastern high terraces. The flux rate was adjusted in the transient models to simulate leaking irrigation ditches located at the eastern boundary.

Specified head cells provide boundaries at the north and south edges of the model. Based on the potentiometric surface contours from March 2013 (fig. 12, main report), the south boundary head is set at 3,450 ft and the north boundary head is set at 3,275 ft. A part of this project involved simulating the

groundwater system without any irrigation activities. For these model scenarios, the specified head at the southern boundary was adjusted to allow groundwater levels to reflect the stage of the Bitterroot River. By changing the specified heads at the south edge cells to an east–west trending line, the model no longer reflected the rise in water levels from the previous irrigation season.

Model Layers and Hydraulic Properties

The active model grid includes 230 rows and 59 columns with a 300 ft x 300 ft cell size. We generated the top and bottom layers beneath the surface using the mapped potentiometric surface for January 2013. We created a triangular integrated network (TIN) based on the potentiometric surface. Horizontal and vertical conductivity of the three layers is included in table E-2. In general vertical conductivity is set at 1/10 horizontal conductivity; however, because of the lack of fine sediments in the sands and gravel, the vertical conductivity was set at 1/3 of the horizontal conductivity.

Layer 1 is the top layer and represents the shallow alluvial aquifer across the domain, in the floodplain and low terraces. Layer 1 varies in thickness because the cell tops represent the land-surface elevation, as

Table E-2. Aquifer properties assigned to model layers.

	Hydraulic Conductivity Horizontal ($K_x=K_y$; ft/day)	Hydraulic Conductivity Vertical* (K_z; ft/day)	Storage**
Layer 1	200 2,000	66.7 557	0.2 (specific yield) 0.2 (specific yield)
Layer 2	1	0.33	0.0003 (storage coefficient) 0.20 (specific yield)
Layer 3	50	16.7	0.0003 (storage coefficient) 0.20 (specific yield)

*Vertical conductivity is 1/3 of horizontal conductivity.

**Storage is necessary for the transient model. Layers 2 and 3 are convertible layer types; this type allows the cells in the layer to be confined or unconfined depending on whether the head is above or below the top of the cells.

derived from the USGS digital elevation model. The average depth of layer 1 is about 40 ft, but varies due to seasonal water-level changes and other stresses that may be applied to the model. The bottom of layer 1 is the groundwater surface TIN shifted downward to 40 ft below the groundwater surface.

The horizontal hydraulic conductivity (K_h) of layer 1 was initially set at 200 ft/d. Sensitivity analysis (explained below) showed that assigning a hydraulic conductivity of 2,000 ft/d to layer 1 improved the calibration to groundwater levels. However, many surface-water flows were calibrated reasonably with both K values, and the match to some surface-water measurements was improved with the lower K value. Values of 200 to 2,000 ft/d fall within the range of literature values for clean sand and gravel (Bureau of Reclamation, 1985).

Layer 2, the middle layer, represents the silt and clay aquitard that underlies the alluvium. Layer 2 is assigned a thickness of 20 ft with the bottom set at 60 ft lower than the water table. Layer 2 was assigned a K_h of 1 ft/day.

Layer 3 represents the deep sand and gravel aquifer. It is 80 ft thick, extending to depths of 150 ft from the groundwater surface. K_h for layer 3 was set to 50 ft/day.

Storage parameters are required in transient

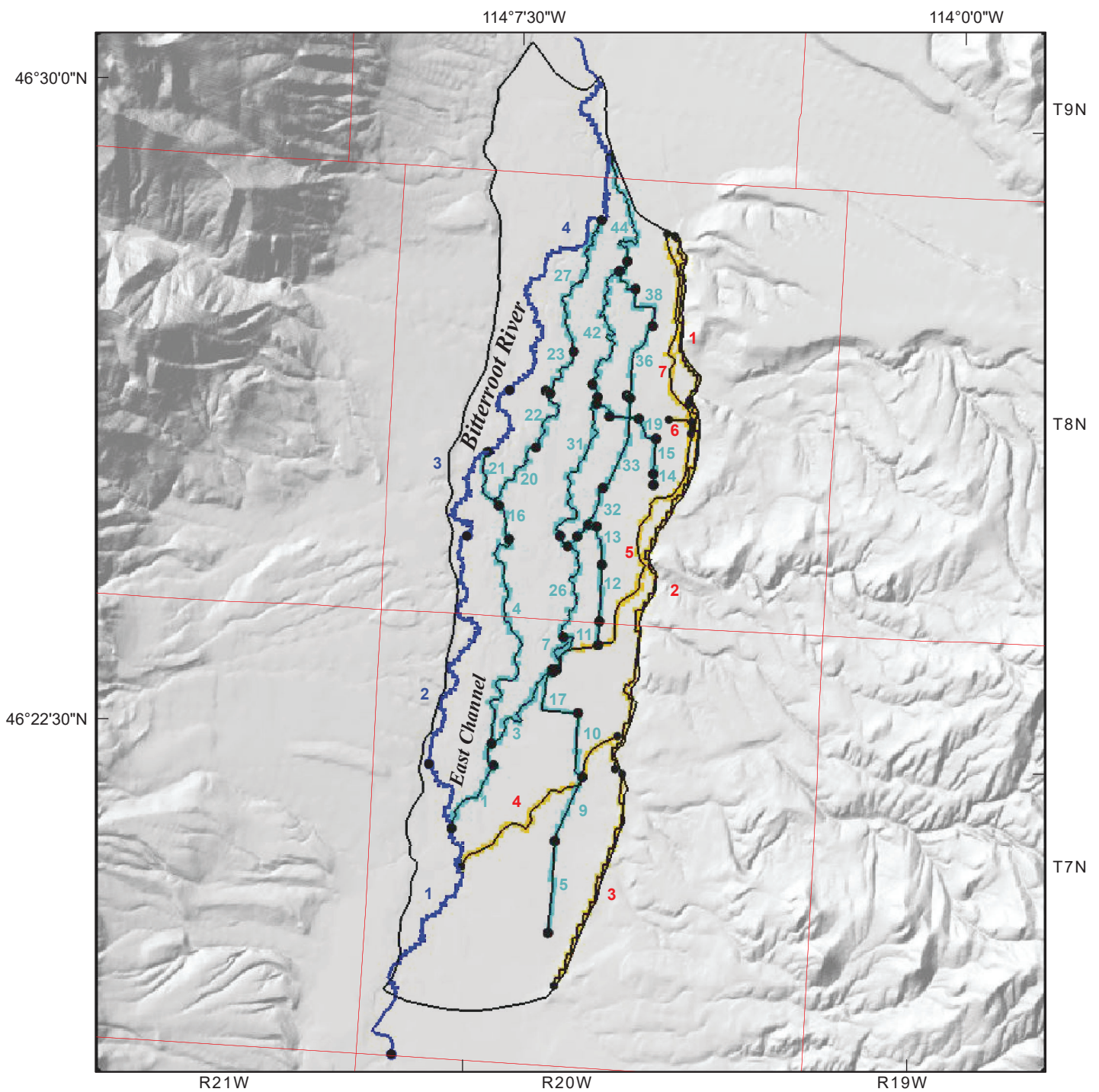
versions of the models. Layer 1 was defined as an unconfined layer (type 1 in MODFLOW) and was assigned a specific yield of 0.2. Layers 2 and 3 were both convertible confined/unconfined layers (type 3 in MODFLOW). These convertible layer types require a confined storage coefficient and a secondary storage coefficient, specific yield, which is applied only if the simulated head in a cell falls below the top of the layer. Layers 2 and 3 have a storage coefficient of 0.0003, and a specific yield of 0.2 (table E-2).

Sources and Sinks

Sources and sinks include boundary conditions within the model domain. These features include the Bitterroot River and its East Channel, simulated irrigation ditches, irrigated fields, and groundwater flux from the Tertiary aquifer east of the valley floor. These features are simulated with various MODFLOW packages (fig. E-2).

Bitterroot River

The Bitterroot River is simulated with the MODFLOW river package (fig. E-2). The package calculates gains and losses to the river based on streambed conductance, aquifer properties, and the relationship between river stage and groundwater head. However, the river package does not track accumulated surface flow in the river. Five staff gage sites provide river stage elevations (table E-3). Each staff gage site is



Explanation

-  Modeled area
-  Bitterroot River arcs
-  SFR Module arcs
-  Specified flux arcs



Figure E-2. The main stem of the Bitterroot River is modeled with the river (RIV) package. The East Channel and numerous canals are modeled using the stream-flow routing (SFR) package. A few canals on the low terrace or east edge of the model area are modeled as specified-flux features. Numbers correspond to stream segments in table E-4.

Table E-3. Stage measurements at five Bitterroot River sites applied in the steady-state model. Sites are listed from downstream to upstream.

Site	GWIC ID	Date	Stage
Woodside Crossing	266799	12/12/12	3464.63
Tucker Crossing West II	268245	1/24/13	3398.56
Victor Crossing - West Branch	266793	1/23/13	3358.20
Bell Crossing	266820	1/20/13	3327.12
Stevensville	266849	12/14/12	3265.75

represented by a node and stages are assigned to each node. The Woodside Crossing and Stevensville staff gage sites are outside the MODFLOW model, but were entered into the GMS software. The three sites within the model domain represent data from Tucker, Victor, and Bell crossings. GMS interpolates intermediate MODFLOW river cells with stage data based on the node locations, elevation values, and the river arc geometry (in GMS, lines drawn are termed “arcs”). Four river arcs connect the five nodes and follow the approximate course of the river in the 2011 National Agricultural Imagery Program (NAIP) aerial imagery (NAIP, 2011).

The steady-state model uses wintertime stage measured during December 2012 and January 2013 (table E-3). Some stages were affected by ice, hence the variable dates. The riverbed top elevation is set to 3 ft below the stage at each river node. For the 13-mo transient model, stages recorded or estimated at the beginning of each stress period are used so that the model simulates changes in stage over time.

In GMS, river conductance is entered in terms of conductance per unit length of an arc. The conductance assigned is 100 ft²/d/ft, representing a hydraulic conductivity of 2 ft/d, a stream width of 50 ft, and a unit streambed thickness. The hydraulic conductivity of 2 ft/d is in the range of fine sand (U.S. Bureau of Reclamation, 1977).

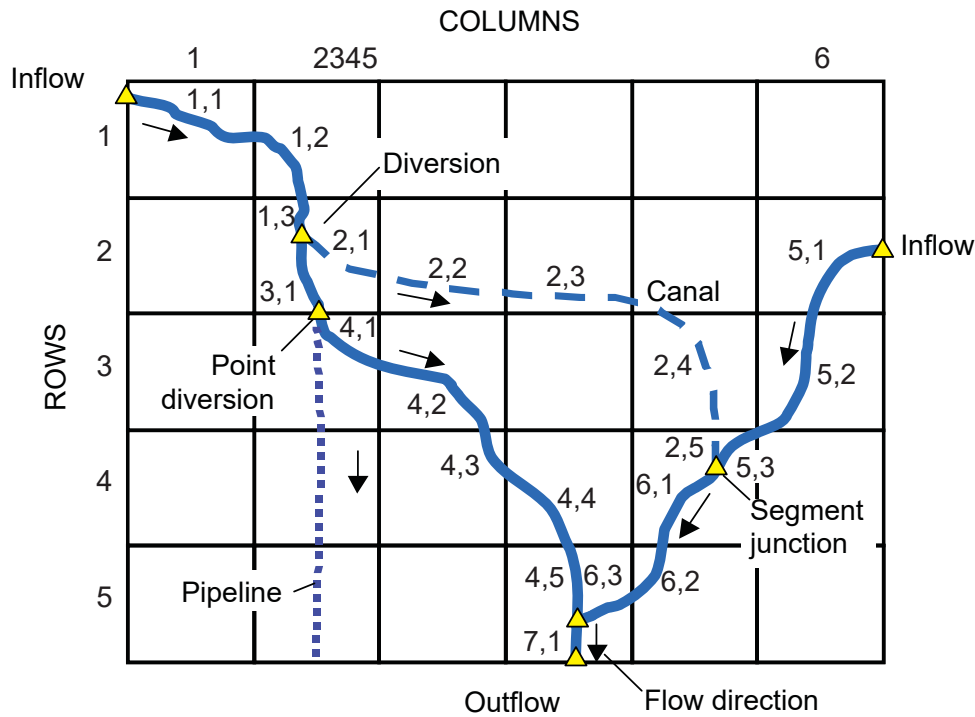
Other Streams and Canals

The MODFLOW stream flow routing (SFR2) package routes surface-water flow along channels in the model, allowing users to designate flows in stream reaches. The SFR2 package is used to model streams and canals east of the mainstem of the Bitterroot River that were expected to interact with the water table. The diversion flows assigned in the model are simplified from reality, and were designed in the model to deliver sufficient flow to service downstream diversions.

The basic element of the SFR2 package is the stream segment, which may include one or more segments. Each segment has a variety of input data pertaining to its upstream and downstream ends and includes streambed and stream stage elevations at both ends. When overlaid onto the groundwater model grid, segments are divided into reaches. There is one reach for each groundwater model cell that the segment spans (fig. E-3). MODFLOW uses the streambed top elevation data assigned for the end of a segment to map the streambed elevations for each stream reach. Reaches are used by the model to calculate groundwater surface-water interactions on a cell-by-cell basis. Flow may be assigned at the upstream end of a segment; the model calculates the flow at the downstream end by applying the gains or losses calculated for each reach of the segment.

The flow in the simulated streams interacts with the groundwater system. If the stream stage is above the saturated zone of the aquifer, the stream loses water and recharges the underlying aquifer. If heads in the aquifer exceed the level of the stream, the stream gains water from groundwater. In general, the stream reach loses or gains water depending on the gradient between the stage in the stream reach and the head in the adjacent cell.

The SFR2 package was used to model the East Channel of the Bitterroot River, Mitchell Slough, Gerlinger Ditch, Webfoot Ditch, Humble Drain, Birch Creek (drain), and the Combo Ditch. The numbers in figure E-2 correspond to the segment numbers shown in table E-4. These sloughs, ditches, and drains are generally at or near the water table in many locations and the SFR package simulates gain or loss of water from these features. Measurements of stage during winter months, which constitutes low-flow conditions, were used as streambed top elevations at staff gage locations.



Explanation

- 1,1 Segment number and reach number
- Stream

Figure E-3. This schematic (modified from Prudic and others, 2004) illustrates a stream flow (SFR) network of segments and reaches, indicated by the first and second numbers in each pair, respectively. Segments define arcs between specified nodes (yellow triangles). Each segment is subdivided into reaches where segments intersect the model grid, such that there is one reach per model cell. Diversions and junctions can be incorporated into the network as illustrated.

The SFR2 package requires values for the streambed hydraulic conductivity, a Manning’s roughness coefficient, and streambed thickness. We assigned a hydraulic conductivity of 4 ft/d, roughness coefficient of 0.03, and streambed thickness of 1 ft to all segments. The hydraulic conductivity is in the range of fine sand (U.S. Bureau of Reclamation, 1977) and the roughness coefficient is representative of natural channels (Linsley and others, 1982).

Figure E-2 shows the stream segments with labels for the longer segments along the Bitterroot River and East Channel. Stage was estimated with elevation from LiDAR at other sites, such as diversions, outflow locations, and intermediate elevation control points along long stream segments. The GMS arcs were converted to stream segments in MODFLOW, and the terms arc and stream segment are used interchangeably here. Each stream segment begins and ends at nodes in GMS, and for the steady-state model are listed in tables E-4 and E-5. The transient models include the same features, but the stream segment num-

bering varies slightly. MODFLOW writes the results of the stream flow routing package to the “.istcb2” file extension. The segment numbers in table E-4 can be used with this file to find results for any given stream segment. If stream segments are changed during other model applications, this numbering system will no longer apply.

In the models, Mitchell Slough is designated to follow the slough’s east branch north of Bell Crossing. As modeled, the Mitchell Slough west branch starts where Gerlinger Ditch empties into it, and carries the flow simulated in Gerlinger Ditch back to the Bitterroot River.

Humble Drain, Union and Etna Canals, Birch Creek, and Combo Ditch

From south to north, SFR segments (other than the East Channel and Mitchell Slough) are assigned flow values as follows: Humble Drain has no flow assigned to any segments, acting as a drain that removes excess shallow groundwater from the system. In the

Table E-4. Stream flow routing (SFR) segments for the steady-state model.

NSEG	Reach Description	OUTSEG	IUPSEG	FLOW	ROUGHCH	HCOND1	THICKM1	ELEV.UP	WIDTH1	DEPTH1	HCOND2	THICKM2	ELEV.DN	WIDTH2	DEPTH2
1	East Channel diversion	2	0	8,029,700	0.03	4	1	3,417.80	50	0	4	1	3,400.62	50	0
2	East Channel BR-TUCK-E to MS-THEAD	4	0	0	0.03	4	1	3,400.62	50	0	4	1	3,396.00	50	0
3	Mitchell Slough diversion (MS-THEAD) to UD/Etna diversion	6	2	5,439,474	0.03	4	1	3,396.00	50	0	4	1	3,383.80	50	0
4	East Channel MS-THEAD to BR-VIC-E	16	0	0	0.03	4	1	3,396.00	50	0	4	1	3,354.53	50	0
5	Humble Drain first reach	9	0	0	0.03	4	1	3,441.06	10	0	4	1	3,417.54	10	0
6	Mitchell Slough from UD/Etna diversion to bend at Double Fork	7	0	0	0.03	4	1	3,383.80	50	0	4	1	3,381.80	50	0
7	Mitchell Slough from Bend at Double Fork to junction Humble Drain	26	0	0	0.03	4	1	3,381.80	50	0	4	1	3,374.62	50	0
8	Union/Etna diversion	0	3	1,750,472	0.03	4	1	3,383.80	10	0	4	1	3,383.50	10	0
9	Humble Drain second reach	10	0	0	0.03	4	1	3,417.54	10	0	4	1	3,404.70	10	0
10	Humble Drain third reach	17	0	0	0.03	4	1	3,404.70	10	0	4	1	3,392.43	10	0
11	Birch Creek first reach	12	0	0	0.03	4	1	3,379.18	6	0	4	1	3,371.28	6	0
12	Birch Creek second reach	13	0	0	0.03	4	1	3,371.28	6	0	4	1	3,362.21	6	0
13	Birch Creek third reach	18	0	0	0.03	4	1	3,362.21	6	0	4	1	3,359.20	6	0
14	Combo Ditch first reach	15	0	0	0.03	4	1	3,362.65	8	0	4	1	3,354.68	8	0
15	Combo Ditch second reach	19	0	0	0.03	4	1	3,354.68	8	0	4	1	3,343.50	8	0
16	East Channel BR-VIC-E to Gerlinger Ditch diversion	21	0	0	0.03	4	1	3,354.53	50	0	4	1	3,348.45	50	0
17	Humble Drain fourth reach ends at Double Fork	25	0	0	0.03	4	1	3,392.43	10	0	4	1	3,384.01	10	0
18	Birch Creek fourth reach (junction Webfoot Ditch)	33	0	0	0.03	4	1	3,359.20	6	0	4	1	3,355.99	6	0
19	Combo Ditch third reach	30	0	0	0.03	4	1	3,343.50	8	0	4	1	3,339.42	8	0
20	Gerlinger Ditch diversion to GD-JB	22	16	809,948	0.03	4	1	3,348.45	8	0	4	1	3,338.28	8	0
21	East Channel from Gerlinger Diversion to Bitterroot River	0	0	0	0.03	4	1	3,348.45	50	0	4	1	3,338.11	50	0
22	Gerlinger Ditch GD-JB to GD-BELL	23	0	0	0.03	4	1	3,338.28	8	0	4	1	3,329.92	8	0
23	Gerlinger Ditch GD-BELL to Mitchell Slough West	27	0	0	0.03	4	1	3,329.92	8	0	4	1	3,323.28	8	0
24	Gerlinger irrigation extraction at Bell Crossing	0	22	151,003	0.03	4	1	3,329.92	8	0	4	1	3,329.62	8	0
25	Humble Drain fourth reach Double Fork to Mitchell Slough	26	0	0	0.03	4	1	3,384.01	10	0	4	1	3,374.62	10	0
26	Mitchell Slough Humble outlet to Webfoot diversion	29	0	0	0.03	4	1	3,374.62	50	0	4	1	3,358.14	50	0
27	Mitchell Slough West from Gerlinger junction to Bitterroot River	0	0	0	0.03	4	1	3,323.28	8	0	4	1	3,298.06	8	0
28	Webfoot Ditch diversion to WD-BELL	32	26	1,244,609	0.03	4	1	3,358.14	10	0	4	1	3,357.76	10	0
29	Mitchell Slough from Webfoot diversion to MS-VIC	31	0	0	0.03	4	1	3,358.14	50	0	4	1	3,353.34	50	0
30	Combo Ditch fourth reach crossing Webfoot Ditch	35	0	0	0.03	4	1	3,339.42	8	0	4	1	3,333.91	8	0
31	Mitchell Slough MS-VIC to Combo Ditch outflow	40	0	0	0.03	4	1	3,353.34	50	0	4	1	3,329.20	50	0
32	Webfoot Ditch from WD-BELL to Birch CR outflow	33	0	0	0.03	4	1	3,357.76	10	0	4	1	3,355.99	10	0
33	Webfoot Ditch Birch Cr outflow to WD-EH	34	0	0	0.03	4	1	3,355.99	10	0	4	1	3,349.75	10	0
34	Webfoot Ditch from WD-EH crossing Combo Ditch to WD-BELL	36	0	0	0.03	4	1	3,349.75	10	0	4	1	3,335.71	10	0
35	Combo Ditch fifth reach to junction Mitchell Slough	40	0	0	0.03	4	1	3,333.91	8	0	4	1	3,329.20	8	0
36	Webfoot Ditch first reach after WD-BELL	38	0	0	0.03	4	1	3,335.71	10	0	4	1	3,332.26	10	0
37	Webfoot irrigation extraction near Bell Crossing	0	34	151,547	0.03	4	1	3,335.71	8	0	4	1	3,335.41	8	0
38	Webfoot Ditch second reach after WD-BELL	39	0	0	0.03	4	1	3,332.26	10	0	4	1	3,316.65	10	0
39	Webfoot Ditch last reach to junction with Mitchell Slough East	44	0	0	0.03	4	1	3,316.65	10	0	4	1	3,305.96	10	0
40	Mitchell Slough from Combo Ditch outlet to MS-BELL	41	0	0	0.03	4	1	3,329.20	50	0	4	1	3,329.14	50	0
41	Mitchell Slough from MS-BELL to East-West split	42	0	0	0.03	4	1	3,329.14	50	0	4	1	3,326.16	50	0
42	Mitchell Slough from East-West split to MS_NICH	43	0	0	0.03	4	1	3,326.16	50	0	4	1	3,307.12	50	0
43	Mitchell Slough from MS_NICH to Webfoot outlet	44	0	0	0.03	4	1	3,307.20	50	0	4	1	3,305.96	50	0
44	Mitchell Slough from Webfoot outlet to Bitterroot River	0	0	0	0.03	4	1	3,305.96	50	0	4	1	3,288.18	50	0

Notes: All modeled stream flow segments used a streambed hydraulic conductivity of 4 ftd, a streambed thickness of 1 ft, and a roughness coefficient of 0.03. NSEG numbers are the same numbers shown in figure E-2. Numbering of segments can sometimes vary slightly, so the stream flow routing table within any particular model should be verified.

Table 5. Model SFR nodes by elevation.

Site Description	Water Feature	GWIC ID	X	Y	Elevation	Elevation Source
(elevation control)	Humble Drain		806999	795480	3441.06	LIDAR
East Channel Diversion	East Channel		800120	802946	3417.80	LIDAR
(elevation control)	Humble Drain		807467	802034	3417.54	LIDAR
(elevation control)	Humble Drain		809478	806585	3404.70	LIDAR
BR_TUCK_E	East Channel	266805	803102	807417	3400.62	11/15/2012
MS_THEAD	East Channel/Mitchell Slough	266806	802969	808967	3396.00	1/23/2013
(elevation control)	Humble Drain		809154	811137	3392.43	LIDAR
(elevation control)	Humble Drain		807373	814053	3384.01	LIDAR
Union/Etna Diversion	Mitchell Slough at UD		807353	814102	3383.80	LIDAR
(elevation control)	Union/Etna Extraction		807628	814229	3383.50	arbitrary
(elevation control)	Mitchell Slough		807299	814248	3381.80	LIDAR
(elevation control)	Birch Cr		810589	815966	3379.18	LIDAR
Humble Drain Outflow	Humble Drain/Mitchell Slough		808079	816526	3374.62	LIDAR
(elevation control)	Birch Cr		810684	817647	3371.28	LIDAR
(elevation control)	Combo Ditch		814529	827342	3362.65	LIDAR
(elevation control)	Birch Cr		810859	821677	3362.21	LIDAR
(elevation control)	Birch Cr		810490	824395	3359.20	LIDAR
Webfoot Ditch Diversion	Webfoot Ditch/Mitchell Slough		808407	822992	3358.14	LIDAR
WD-VIC	Webfoot Ditch at Victor Crossing	266818	809110	823681	3357.76	1/24/2013
(elevation control)	Birch Cr/Webfoot Ditch		809901	824516	3355.99	LIDAR
(elevation control)	Combo Ditch		814518	828123	3354.68	LIDAR
BR-VIC-E	East Channel at Victor Crossing	266814	804214	823487	3354.53	1/23/2013
MS-VIC	Mitchell Slough at Victor Crossing	266817	807845	823721	3353.34	1/24/2013
WD-EH	Webfoot Ditch at Eastside Highway	268246	810941	827133	3349.75	1/24/2013
Gerlinger Ditch Diversion	Gerlinger Ditch/East Channel		803496	825878	3348.45	LIDAR
(elevation control)	Combo Ditch		814708	830667	3343.50	LIDAR
(elevation control)	Combo Ditch		813492	832084	3339.42	LIDAR
GD-BROWN	Gerlinger Ditch at Jim Brown	267520	806123	830034	3338.28	4/13/2012
East Channel Outflow	East Channel/Bitterroot River		802718	829713	3338.11	LIDAR
(elevation control)	Webfoot Ditch		812876	833546	3335.71	LIDAR
(elevation control)	Webfoot Ditch Extraction		812620	833742	3335.41	arbitrary
(elevation control)	Combo Ditch		811411	832249	3333.91	LIDAR
(elevation control)	Webfoot Ditch		814473	838677	3332.26	LIDAR*
GD-BELL	Gerlinger Ditch at Bell Crossing	266843	807143	833879	3329.92	12/13/2012
(elevation control)	Gerlinger Ditch Extraction		806835	834086	3329.62	arbitrary
Combo Ditch Outflow	Combo Ditch/Mitchell Slough		810463	833137	3329.20	LIDAR
MS-BELL	Mitchell Slough at Bell Crossing	266845	810558	833633	3329.14	1/24/2013
(elevation control)	Mitchell Slough at East/West Split		810188	834531	3326.16	LIDAR*
Gerlinger Ditch Outflow	Gerlinger Ditch /Mitchell Slough West		808840	836868	3323.28	LIDAR
(elevation control)	Webfoot Ditch		813256	841311	3316.65	LIDAR*
MS-Nichols	Mitchell Slough at Ben Nichols	269727	812093	842570	3307.20	1/24/2013
Webfoot Ditch Outflow	Webfoot Ditch/Mitchell Slough		812673	843282	3305.96	LIDAR
Mitchell Slough West Outflow	Mitchell Slough West/Bitterroot River		810849	846193	3298.06	LIDAR*
Mitchell Slough East Outflow	Mitchell Slough East/Bitterroot River		811450	850610	3288.18	LIDAR*

*Some adjustments to the high-water LiDAR data were made at these locations. arbitrary elevations were used for modeled irrigation extractions to have the discharge end lower than the point of diversion. D:\D:\Documents2\GMS_STEVI_1\SV_SS_8pt6_for_STR_map_MODFLOW\SFR2_nodes_by_elev.xlsx

model, a single diversion simulates Union and Etna Ditch diversions from Mitchell Slough because in reality both headgates are located close to each other. A 40 cfs diversion was deemed adequate to simulate this diversion. This flow is removed from the model because of the way the Union and Etna Ditches are simulated downstream of the headgates. The Union and Etna Ditches are represented with GMS’s constant flux function, which converts to MODFLOW’s well package, as described below.

Birch Creek has no flow assigned to any segments, acting as a drain that removes excess shallow groundwater from the system. This is consistent with field ob-

servations. Webfoot Ditch flows were calculated based on the stages and flow recorded at Webfoot Ditch at Victor Crossing. A representative value for irrigation season flows in Webfoot Ditch is about 20 cfs, and is reduced to 6.5 cfs for the rest of the year. Flow calculations assume the diversions operate from April 1 to October 26.

Similar to Birch Creek, Combo Ditch has no flow assigned to any segments and acts as a drain that removes excess shallow groundwater from the system. Gerlinger and Webfoot Ditches tend to be above the water table, and mostly lose water rather than accruing appreciable gains from groundwater. These diversions

are intended to remove the approximate amount of water that needs to be delivered to irrigation systems connected to each canal, based on irrigated acreages and irrigation method. We provide the amounts and timing of diversions in the Calculation Details section, below.

Mitchell Slough and the East Channel

The East Channel of the Bitterroot River, Mitchell Slough, and a few drain ditches are in contact with the shallow water table, and gain and lose water to the aquifer in various reaches.

Determining the amount of water to assign in the model at Tucker Headgate, discharging into Mitchell Slough, was complex. The amount of water measured at Tucker Headgate was less than the flow measured 1.5 mi downstream in the Slough (this is where water is diverted from Mitchell Slough to the Union and Etna Ditches). This gain in flow is attributed to groundwater discharging into Mitchell Slough.

Flows in Mitchell Slough must be sufficient to supply flows to Union and Etna ditches, deliver 6.5 to 20 cfs to the Webfoot Ditch, and retain 30 to 40 cfs during the irrigation season at Victor Crossing. Considering the modest summer gains of 5 to 10 cfs simulated from Humble drain, we developed a flow scheme for Mitchell Slough at Tucker Headgate (table E-6). The measured flows are based on rating curves developed from stage and discharge relationships at Tucker Headgate, and are considered approximate due to measurement error. The flows we added to these features in the model were based on providing enough water to Mitchell Slough to simulate both the Webfoot diversion and continued flow downstream of the diversion.

The model diversions from the East Channel of the Bitterroot River were structured to deliver the water

needed for Mitchell Slough diversions and maintain the flows typically observed (i.e., 30 to 40 cfs) to the East Channel at Victor Crossing (table E-7). The modeled flows for the East Channel and for Mitchell Slough at Tucker Headgate are large but not extreme compared to flow estimates provided by the Bitterroot River Water Commissioner Al Pernicelle (oral commun., 2015). He estimates that flow in the East Channel during a typical water year is about 100 cfs. Thus, the maximum simulated East Channel diversion of 120 cfs is reasonable. The 75 to 90 cfs simulated in the model for flow at Tucker Headgate is comparable to the approximate low water year flow estimated by the Water Commissioner at 65 cfs. Additional flow was added to the model to account for the unknown augmentation by groundwater discharge to ditches.

In the model, the flow of Mitchell Slough at Bell Crossing is directed to the East Channel, because we had no information about the split of flow just north of Bell Crossing (fig. 2). The modeled flows out of the east branch of Mitchell Slough range from about 50 to 120 cfs. The tail water from Gerlinger Ditch becomes the west branch of the Mitchell Slough, and these flows as modeled are relatively low, between 0 and 13 cfs.

Corvallis, Supply, Union, and Etna Ditches

The Corvallis, Supply, Union, and Etna irrigation canals and ditches are located on the low terrace, at elevations that are above the water table for most of their length. These canals, modeled as specified fluxes with the MODFLOW well package, are expected to lose water to the aquifer. The specified flux applied in the model was based on the limited canal seepage data available from Union Ditch. Leakage estimates for each ditch segment were based on measurements indicating a 2 cfs/mi loss along a 2.18 mi segment of the Union Ditch (see the Calculation Details section,

Table E-6. Modeled Mitchell Slough flow rates at Tucker Headgate.

Date	Appx. Actual	Add	Augmented Flow	ft ³ /day	Days	Total for Duration (ft ³)
4/1-7/10	60 cfs	30 cfs	90 cfs	7,776,660	30+31+30+10	785,426,600
7/10-10/26	45 cfs	30 cfs	75 cfs	6,480,000	21+31+30+26	699,840,000
10/27-1/15	10 cfs	20 cfs	30 cfs	2,592,000	5+30+31+15	209,952,000
1/16-3/31	25 cfs	20 cfs	45 cfs	3,888,000	16+28+31	291,600,000
						1,986,818,600

Annual total: 1,986,818,600/365.25 ft³/yr = Steady-state value of 5,439,612 ft³/d or 62.96 cfs

Table E-7. Modeled East Channel diversion rates at Victor Crossing.

Date	Augmented Flow	Ft ³ /d	Days	Total for Duration
4/1-7/10	120 cfs	10,368,000	30+31+30+10	1,047,168,000 ft ³ /d
7/10-10/26	105 cfs	9,072,000	21+31+30+26	979,776,000 ft ³ /d
10/27-1/15	60 cfs	5,184,000	5+30+31+15	419,000,000 ft ³ /d
1/16-3/31	75 cfs	6,480,000	16+28+31	486,000,000 ft ³ /d
Annual total				2,932,848,000 ft ³ /d

2,932,848,000 ft³/d / 365.25 = steady state value of 8,029,700 ft³/d or 92.93 cfs

below). A leakage rate of 1 cfs/mi was used for the Etna Ditch, and 1.5 cfs/mi was used for the Supply and Corvallis ditches. We applied the average annual ditch leakage fluxes in the steady-state model. In the transient models, ditch leakage was active during the time steps simulating periods of seasonal use.

The easternmost arcs along the east edge of the model include a year-round groundwater flux from the Tertiary aquifer into the model domain. These are described in the Calculation Details section, below.

Groundwater Recharge from Irrigated Lands

Groundwater recharge from irrigated lands was applied in the model by developing polygons for irrigated fields (fig. E-4, table E-8). Each polygon represents irrigated lands with a single known or assumed water source (generally a canal or stream) and a single irrigation type, such as flood or sprinkler. This seasonal recharge was applied using the MODFLOW recharge package. Recharge generated from excess irrigation water is described in the Methods section of this report. The steady-state model applies 0.5 ft to sprinkler-irrigated fields and 1.5 ft to flood-irrigated fields over the period of a year, or the equivalent of 0.042 and 0.125 ft/mo, respectively. The transient models apply the same total amount of water, 0.5 ft and 1.5 ft, respectively, from June 1 to August 15 of each simulated irrigation season. Recharge was not applied outside of that time frame in the transient models. There is so little pivot irrigation in the study area that the sprinkler irrigation recharge rates were applied to pivot-irrigated fields; this simplification can be modified as appropriate by subsequent model users. Irrigated field polygons are identified in the map module of GMS.

STEADY-STATE CALIBRATION

Targets for the steady-state calibration included

water elevations from 23 wells measured during November 2012 within the model domain (table E-9). We chose this dataset because these groundwater levels reflect intermediate conditions, following initial recovery from the irrigation season, and yield a calibration based on annual average conditions. The files associated with the model calibration are available for download (Groundwater Model Product section; November 2012 SWLs BWIPMONST_ModelArea_Rev.csv).

The model objectives drove model construction with recharge polygons based on blocks of irrigated lands based on the likely source canal and irrigation method. Recharge from irrigation activities in the steady-state model applies annual irrigation recharge from all sources of 2.72 ft in the low K version and 3.97 ft in the high K version.

The steady-state calibration match of observed to modeled heads in the low K version has a mean residual of about -1.9 ft, mean absolute residual error of 3.0, and a root mean squared error of 4.4 ft (fig. E-5). Through the model sensitivity analysis (described below), we evaluated alternative K values in a trial and error approach to improve the steady-state calibration. This resulted in carrying forward low K and high K versions, because the match to heads is better for the high K version of the model, with a mean residual head of 0.8 ft, mean absolute error of 1.35 ft, and root mean squared error of 1.98 ft (fig. E-6). Modelers commonly attempt to achieve mean absolute errors and root mean squared errors within 5 or 10% of the range. In this model, the range of target heads is about 150 ft, so errors within 7.5 to 15 ft are acceptable. Thus, both the low and high K versions are reasonably well calibrated. The calibration is best in the high K version, in part because it generates better matches of seasonal flow in the east branch of Mitchell Slough, which collects the bulk of irrigation return flows from

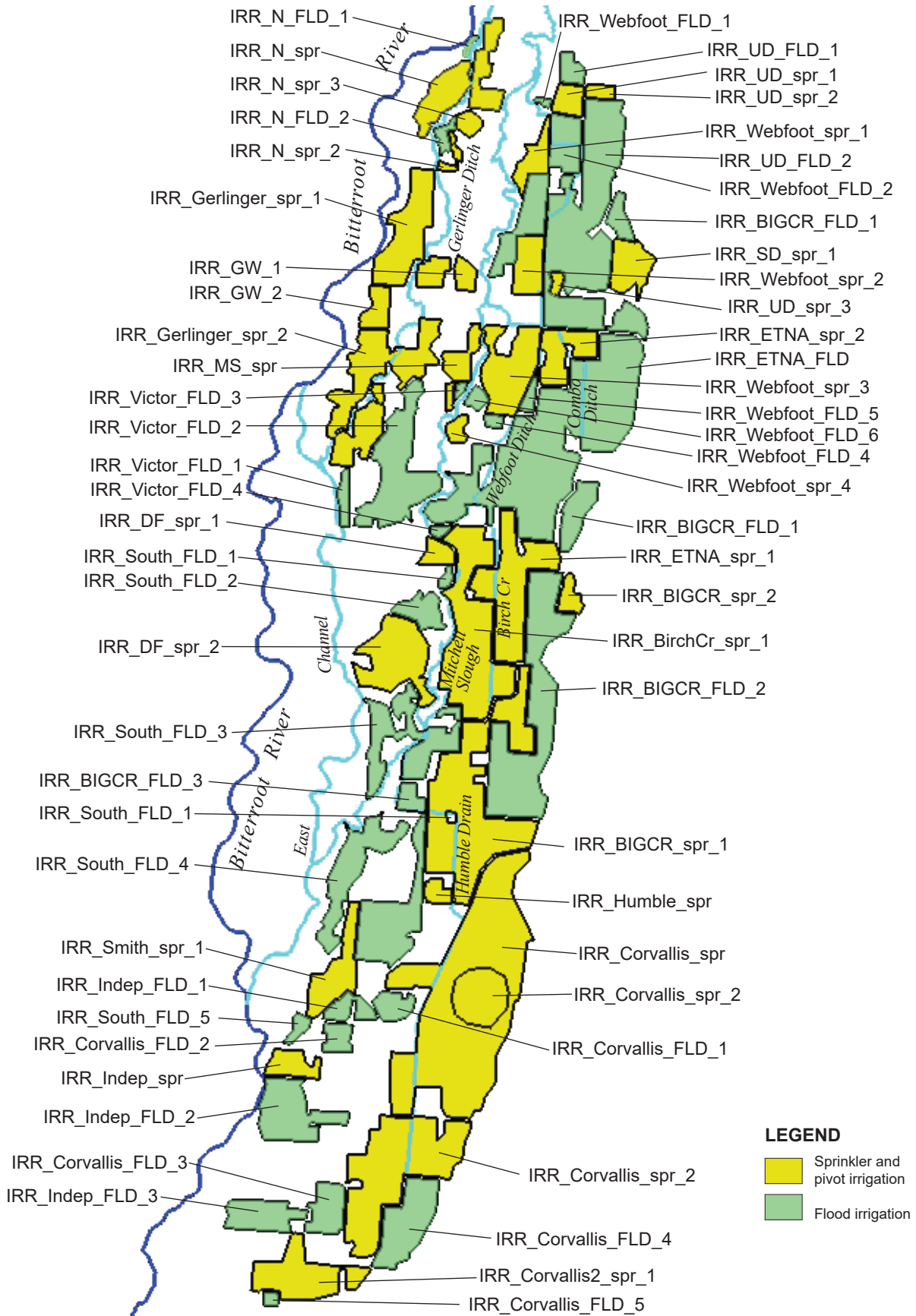


Figure E-4. This maps shows the polygons assigned to irrigated lands. The polygon names are generally derived from canals thought to be the sources of the irrigated areas and correspond to table E8.

Table E-8. Irrigated field polygons including area and recharge rates (ft/day).

Area name (in GMS)	Area (acres)	Steady-state recharge rate	Transient recharge rate
IRR_BIGCR_FLD_1	31	0.004107	0.01974
IRR_BIGCR_FLD_1	62	0.004107	0.01974
IRR_BIGCR_FLD_2	369	0.004107	0.01974
IRR_BIGCR_FLD_3	201	0.004107	0.01974
IRR_BIGCR_spr_1	474	0.001369	0.006579
IRR_BIGCR_spr_2	27	0.001369	0.006579
IRR_BirchCr_spr_1	339	0.001369	0.006579
IRR_Corvallis_FLD_1	39	0.004107	0.01974
IRR_Corvallis_FLD_2	32	0.004107	0.01974
IRR_Corvallis_FLD_3	66	0.004107	0.01974
IRR_Corvallis_FLD_4	143	0.004107	0.01974
IRR_Corvallis_FLD_5	8	0.004107	0.01974
IRR_Corvallis_spr	761	0.001369	0.006579
IRR_Corvallis_spr_2	114	0.001369	0.006579
IRR_Corvallis2_spr_1	376	0.001369	0.006579
IRR_Corvallis2_spr_2	161	0.001369	0.006579
IRR_DF_spr_1	29	0.001369	0.006579
IRR_DF_spr_2	177	0.001369	0.006579
IRR_ETNA_spr_1	232	0.001369	0.006579
IRR_ETNA_spr_2	89	0.001369	0.006579
IRR_Gerlinger_spr_1	198	0.001369	0.006579
IRR_Gerlinger_spr_2	283	0.001369	0.006579
IRR_GW_1	26	0.001369	0.006579
IRR_GW_2	41	0.001369	0.006579
IRR_Humble_spr	23	0.001369	0.006579
IRR_Indep_FLD_1	37	0.004107	0.01974
IRR_Indep_FLD_2	143	0.004107	0.01974
IRR_Indep_FLD_3	86	0.004107	0.01974
IRR_Indep_spr	50	0.001369	0.006579
IRR_MS_spr	56	0.001369	0.006579
IRR_N_FLD_1	5	0.004107	0.01974
IRR_N_FLD_2	16	0.004107	0.01974
IRR_N_spr	156	0.001369	0.006579
IRR_N_spr_2	14	0.001369	0.006579
IRR_N_spr_3	21	0.001369	0.006579
IRR_SD_spr_1	79	0.001369	0.006579
IRR_Smith_spr_1	108	0.001369	0.006579
IRR_South_FLD_1*	5	0.004107	0.01974
IRR_South_FLD_1	9	0.004107	0.01974
IRR_South_FLD_2	50	0.004107	0.01974
IRR_South_FLD_3	179	0.004107	0.01974
IRR_South_FLD_4	147	0.004107	0.01974
IRR_South_FLD_5	17	0.004107	0.01974
IRR_UD_FLD_1	27	0.004107	0.01974
IRR_UD_FLD_2	505	0.004107	0.01974
IRR_UD_spr_1	36	0.001369	0.006579
IRR_UD_spr_2	17	0.001369	0.006579
IRR_UD_spr_3	10	0.001369	0.006579
IRR_Victor_FLD_1	24	0.004107	0.01974
IRR_Victor_FLD_2	220	0.004107	0.01974
IRR_Victor_FLD_3	5	0.004107	0.01974
IRR_Victor_FLD_4	8	0.004107	0.01974
IRR_Webfoot_FLD_1	4	0.004107	0.01974
IRR_Webfoot_FLD_2	69	0.004107	0.01974
IRR_Webfoot_FLD_3	93	0.004107	0.01974
IRR_Webfoot_FLD_4	9	0.004107	0.01974
IRR_Webfoot_FLD_5	15	0.004107	0.01974
IRR_Webfoot_FLD_6	15	0.004107	0.01974
IRR_Webfoot_spr_1	52	0.001369	0.006579
IRR_Webfoot_spr_2	71	0.001369	0.006579
IRR_Webfoot_spr_3	158	0.001369	0.006579
IRR_Webfoot_spr_4	20	0.001369	0.006579
Total acreage irrigated lands:	7,576		

Table E-9. Steady-state model water-level calibration targets.

OBJECTID	GWIC	NAME	LATITUDE	LONGITUDE	X	Y	TD	DATE_	SWL	SWLELEV	METHOD
1	161907	GALILEE BAPTIST CHURCH	46.47246842	-114.0880295	813756.74	844094.825	61	11/16/2012 11:09	11.39	3308.06	SOUNDER
2	266829	EARTH AND WOOD	46.47320677	-114.1251975	804428.754	844913.659	0	11/16/2012 13:35	4.56	3305.17	SOUNDER
3	57723	EARTH AND WOOD	46.47158705	-114.1279774	803695.057	844365.637	50	11/16/2012 13:35	25.52	3309.36	SOUNDER
4	266824	NICHOLS, BEN	46.46609421	-114.0917265	812691.194	841829.978	0	11/15/2012 14:05	5.28	3309.65	SOUNDER
5	57844	VON ESCHEN, KEN	46.45399709	-114.0892881	813046.072	837392.238	39	11/16/2012 14:12	10.19	3322.09	SOUNDER
6	57848	STRANGE, BILL	46.44369352	-114.0832552	814343.623	833554.133	39	11/16/2012 13:50	18.53	3332.93	SOUNDER
7	266090	MONTANA BUREAU OF MINES AND GEOLOGY	46.43276884	-114.1149556	806135.519	830047.788	8	11/16/2012 12:00	2.11	3338.69	DIGITAL LOGGER
8	266089	MONTANA BUREAU OF MINES AND GEOLOGY	46.43276172	-114.1149511	806136.499	830045.13	21	11/16/2012 12:00	1.47	3338.73	DIGITAL LOGGER
9	266087	MONTANA BUREAU OF MINES AND GEOLOGY	46.43421867	-114.1141895	806359.367	830563.958	16	11/16/2012 12:00	3.05	3337.39	DIGITAL LOGGER
10	266088	MONTANA BUREAU OF MINES AND GEOLOGY	46.43421259	-114.1141864	806360.016	830561.699	8	11/16/2012 12:00	2.98	3337.46	DIGITAL LOGGER
11	266065	MONTANA BUREAU OF MINES AND GEOLOGY	46.43420831	-114.1141978	806357.057	830560.311	24	11/16/2012 12:00	3.16	3337.28	DIGITAL LOGGER
12	170634	HARDIN, DON	46.44160868	-114.1026982	809408.461	833082.638	63	11/16/2012 16:30	6.94	3329.94	SOUNDER
13	232344	SUNDERLAND, MICHEAL	46.44105904	-114.1119994	807057.059	833020.426	60	11/16/2012 14:05	5.5	3331.23	SOUNDER
15	57905	BROWN, JIM	46.43365303	-114.1143811	806299.027	830360.986	120	11/14/2012 17:00	3.43	3337.76	SOUNDER
16	128772	GALIHER, RICHARD AND KAREN	46.4328431	-114.0948448	811196.587	829777.011	40	11/16/2012 12:00	7.36	3338.57	ESTIMATE
17	152085	WHITE, TIM	46.41504894	-114.0805131	814423.123	823090.797	138	11/15/2012 15:05	32.08	3360.17	SOUNDER
19	58222	JOLLEY, TED AND LAURIE	46.41252484	-114.1128817	806222.955	822650.984	29	11/16/2012 10:45	3.58	3358.63	SOUNDER
20	266842	WHITE, TOM	46.40003479	-114.0887008	812042.128	817748.359	0	11/16/2012 14:27	9.49	3373.57	SOUNDER
21	267988	HENNEGAR, MIKE AND BEV	46.386	-114.0955	810030.565	812742.02	0	11/16/2012 15:45	7.82	3385.66	SOUNDER
22	266835	TURF FARM	46.367239	-114.097127	809219.764	805939.579	0	11/15/2012 14:08	3.39	3406.25	SOUNDER
23	158828	BENNETT, LINDA AND DANIEL	46.34553563	-114.1107208	805330.287	798244.013	50	11/16/2012 10:03	5.75	3428.23	SOUNDER
24	56384	BARTILL, STAN AND LEILA	46.3339492	-114.1227293	802055.241	794206.734	39	11/16/2012 12:00	7.4	3441.48	DIGITAL LOGGER
25	166051	SIMPSON, JERRY AND KAROLYN	46.3259622	-114.1128373	804377.04	791153.403	51	11/16/2012 9:45	12.68	3453.35	SOUNDER

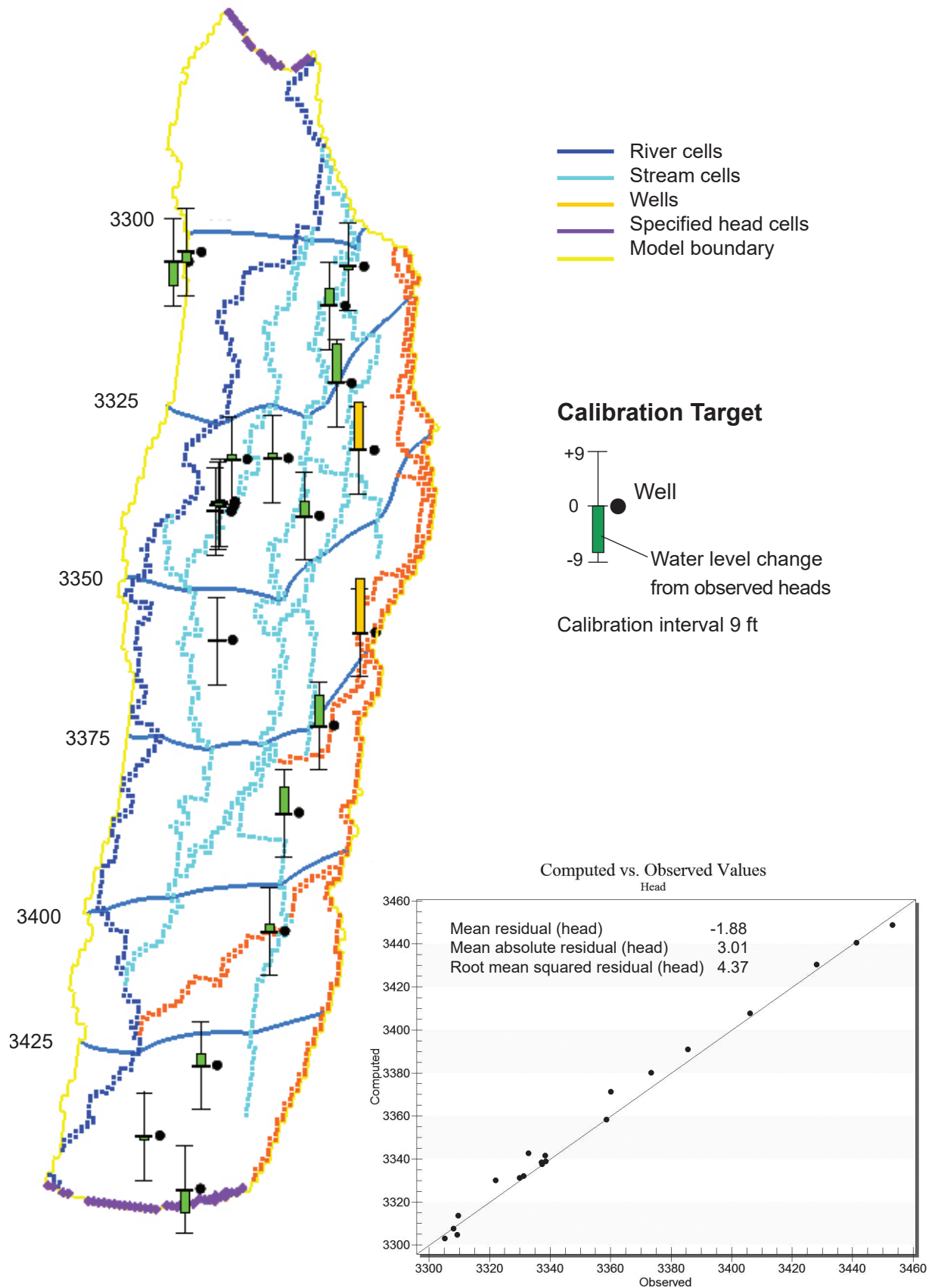


Figure E-5. Computed vs. observed heads in the low K version of the steady-state calibrated model. The calibration interval for this model run was set to 9 ft.

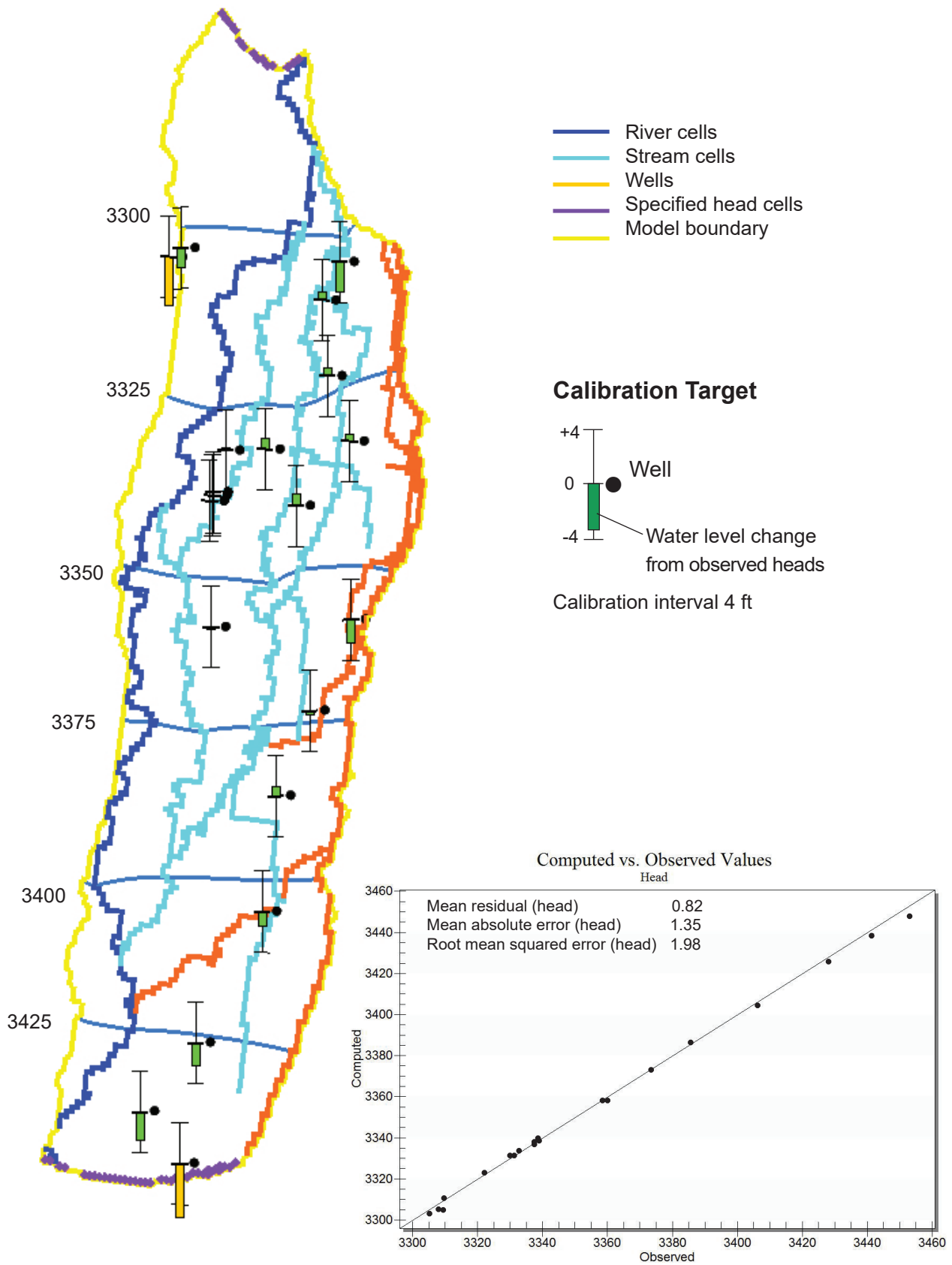


Figure E-6. Computed vs. observed heads in the high K version of the calibrated steady-state model. The calibration interval for this model run was set to 4 ft.

irrigated lands surrounding it.

The steady-state model budgets are comparable to the groundwater budgets developed for the conceptual model (table 2, main report). However, the flux into the aquifer from canal leakage is notably different, especially in the high K version of the model. This is attributed to several ditches modeled with the SFR package with a high conductivity streambed. Thus, the ditches deliver more water than originally estimated. However, this is reasonable because stream flow losses measured in Union Ditch were as high as 19 cfs. In the low K version of the steady-state model, the average annual rate of leakage from the Gerlinger Ditch is about 1.2 cfs/mi. In reality, the ditch is running water for 6 mo and its leakage rate is twice that, or 2.4 cfs/mi. In the high K model, the ditch leaks about 2.3 cfs, representing a 4.6 cfs/mi summer rate. Overall, the high K model produces more groundwater flux than the low K model (table 2, main report). This difference between the two versions is an expected result of higher flux facilitated in high K aquifer sediment.

TRANSIENT CALIBRATION

The 13-mo transient model spans April 1, 2012, through April 30, 2013. Sources of irrigation recharge are applied at the rates and time periods presented above, in the Sources and Sinks section.

The magnitude and timing of seasonal groundwater fluctuations observed in wells are reasonably achieved by the low K transient model (fig. E-7) and are improved somewhat in the high K transient model (fig. E-8). Irrigation return flows rendered by the model are in the expected magnitude in both versions, based on the simulated Mitchell Slough flows.

The comparison of measured, calculated, and modeled Mitchell Slough flows are provided to compare the low K model results to measured and calculated flows at several locations (figs. E-9, E-10, E-11). Measured flows, as shown in the figures, are stream flow measurements made in the field. Calculated flows were derived from rating curves. Similar high K model results indicate subtle differences in flows in Mitchell Slough (figs. E-12, E-13, E-14). The low K model provides improved simulation of flows in a few of the drains on the low terrace that drain irrigated lands. The augmented flows modeled (flow added to the first reach of the Mitchell Slough segment) are compared to the estimated and measured flows at Tucker Head-

gate (fig. E-9A). The simulated flows at Victor Crossing (figs. E-9B, E-12B) provide a reasonable match to the highly variable estimated and measured flows observed at that site.

The calibration at Mitchell Slough at Bell Crossing is less satisfactory. The simulated flow in the low K version of the transient model at the Crossing is less than the measured and calculated flow (fig. E-10A). The high K version produces a better match to observed conditions (fig. E-13A).

The comparison of simulated flow out of Mitchell Slough (presented as the sum from both simulated branches) to the Bitterroot River compares reasonably well with the Bell Crossing measured and calculated flows (figs. E-10B, E-13B). This is important for the model calibration because downstream of where Mitchell Slough was measured at Bells Crossing, Webfoot Ditch tailwater flows into the slough and additional gains occur. Thus, the modeled flows are somewhat higher (10 to 15 cfs) than the Bell Crossing measured flows, in both the low and high K models.

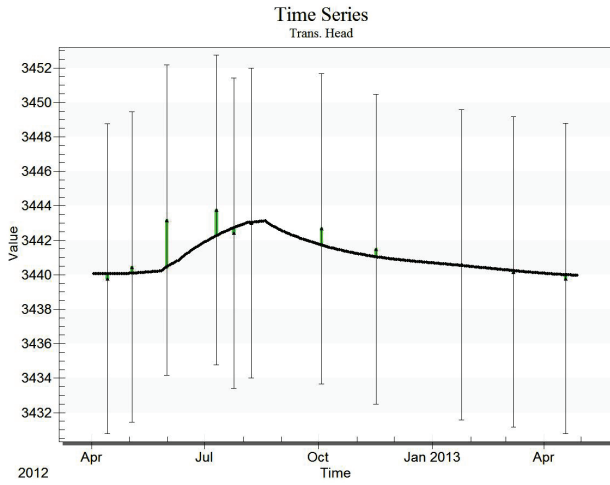
MODEL VERIFICATION

We compared an independent dataset to model results. These data consist of static water-level elevations measured in 19 wells by the USGS around March 1, 1958 (McMurtrey and others, 1972). We assumed that these measurements were based on the vertical datum North American Datum (NAVD) of 1929. Conversions of several locations in the study area indicated that the difference between the 1929 vertical datum and the 1988 vertical datum is around 3.6 ft, and we added 3.6 ft to each data point to compare to results of the high K steady-state model. The mean absolute error for the current observed versus simulated groundwater elevations was 1.35 ft. Using the 1958 USGS dataset, the mean absolute error increased slightly to 1.62 ft (fig. E-6). We consider this a reasonable verification of the model calibration.

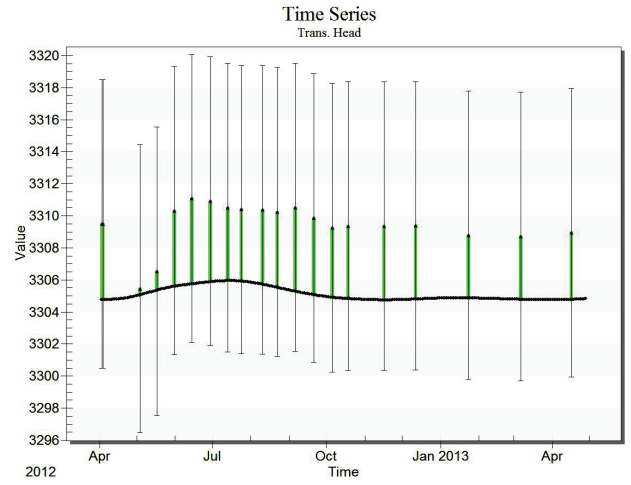
SENSITIVITY ANALYSIS

We conducted an initial sensitivity analysis by varying key model parameters in the steady-state model. In the analysis, one parameter is varied while all other parameters are kept at their assigned state. Parameters tested included hydraulic conductivity in each layer, ditch leakage, streambed conductance, riverbed conductance, irrigated fields recharge, and

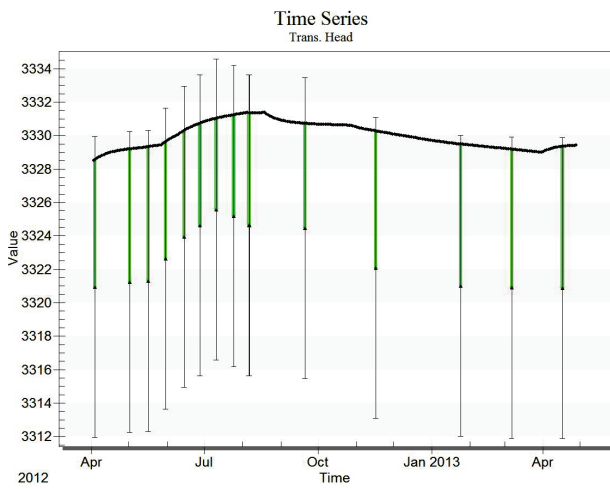
Well 56384



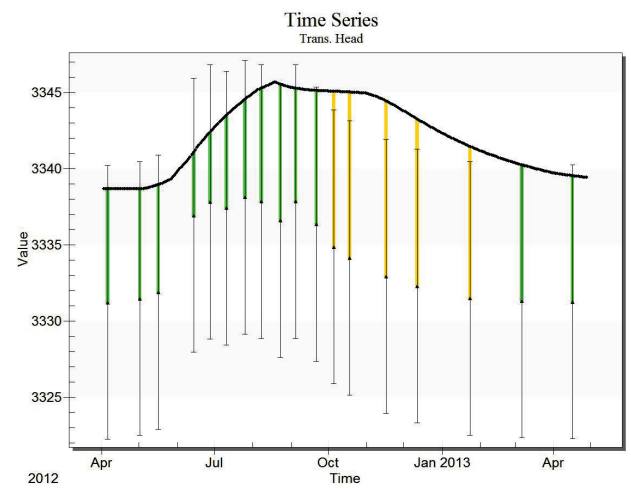
Well 57723



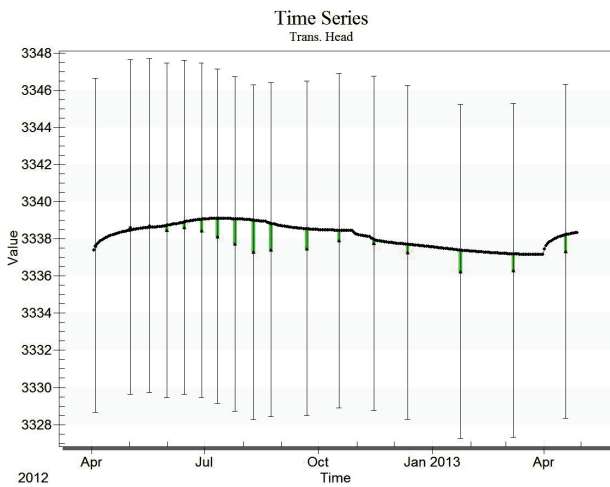
Well 57844



Well 57848



Well 57905



Well 58222

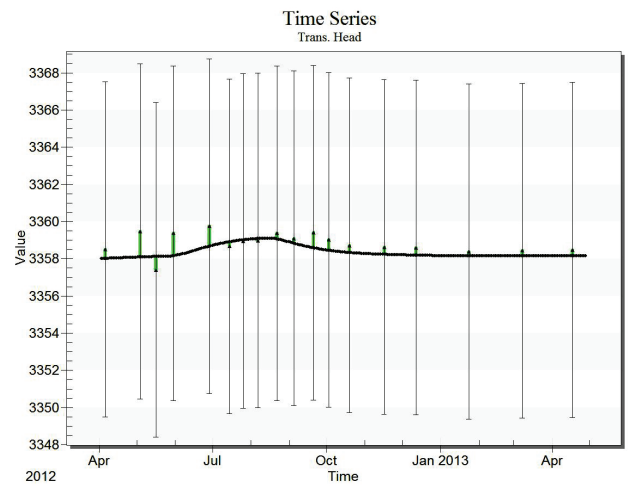
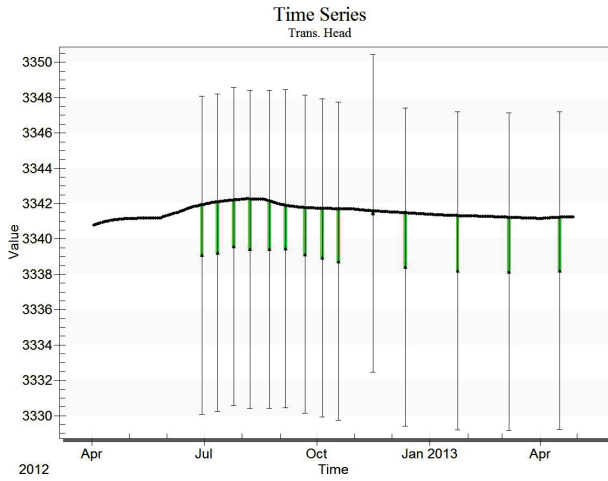
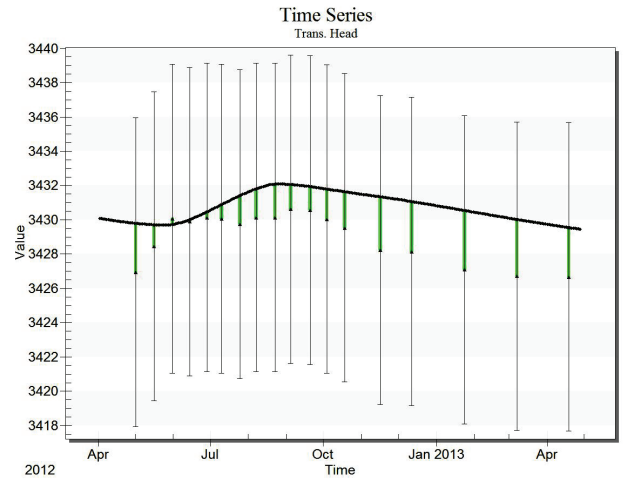


Figure E-7. Transient calibration hydrographs show observed water levels over time (middle value in each vertical hachure) vs. the simulated heads in the low K version (the dark line in each graph). The hachures encompass 9 ft of the observed value, referred to as the calibration interval.

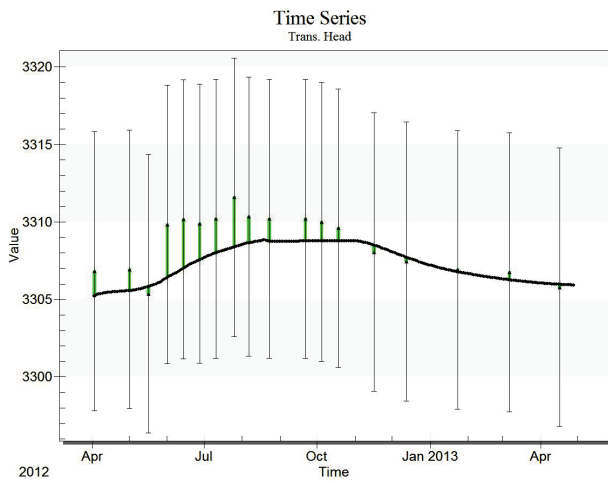
Well 128772



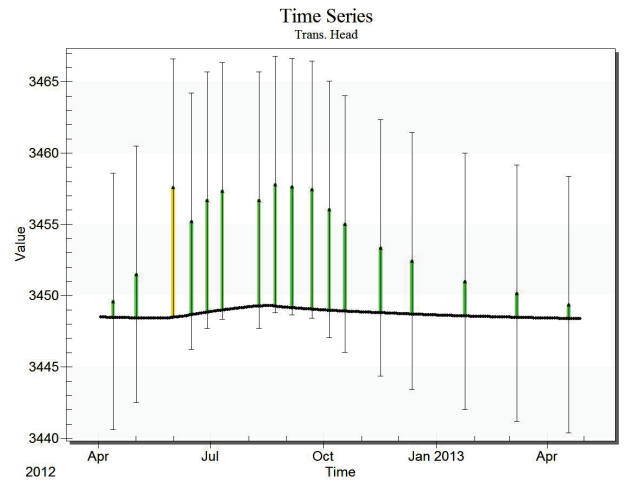
Well 158828



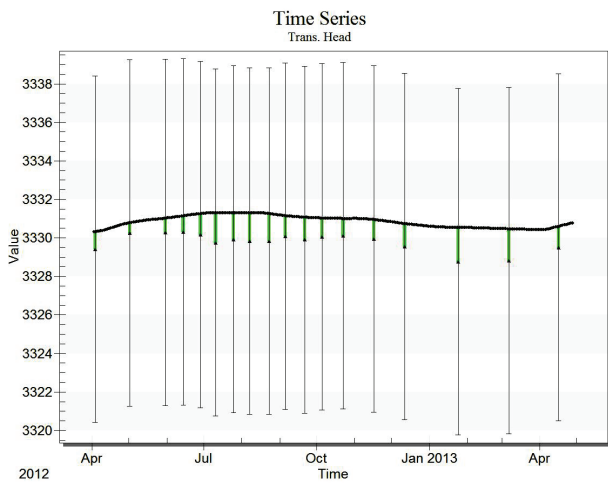
Well 161907



Well 166051



Well 170634



Well 232344

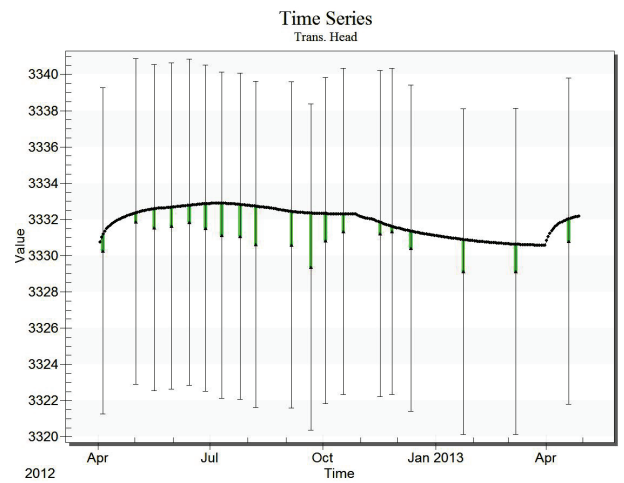
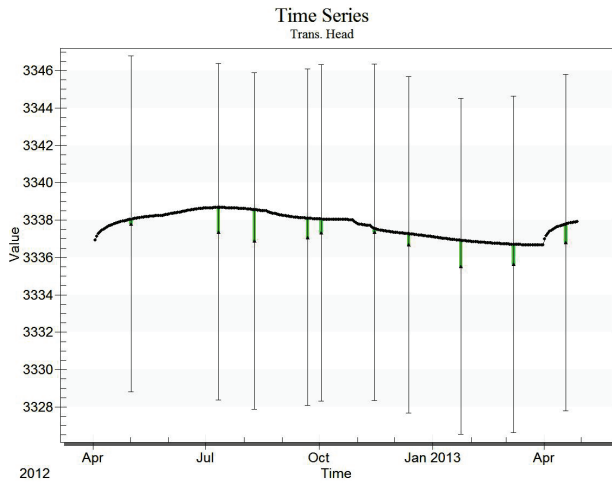
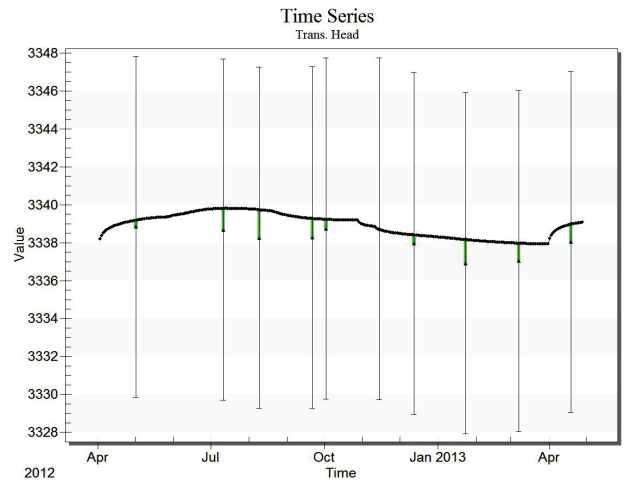


Figure E-7, Continued.

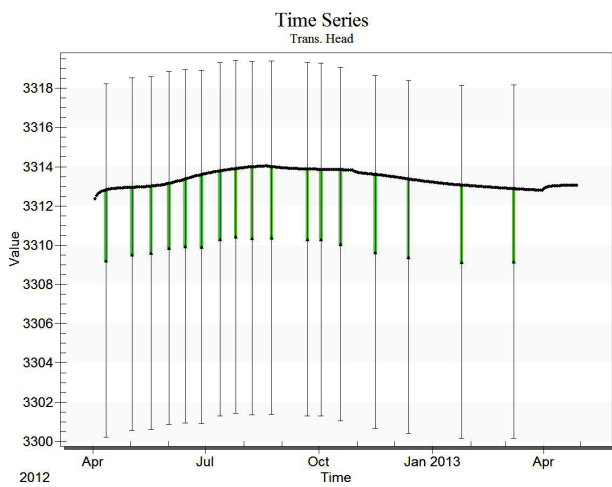
Well 266065



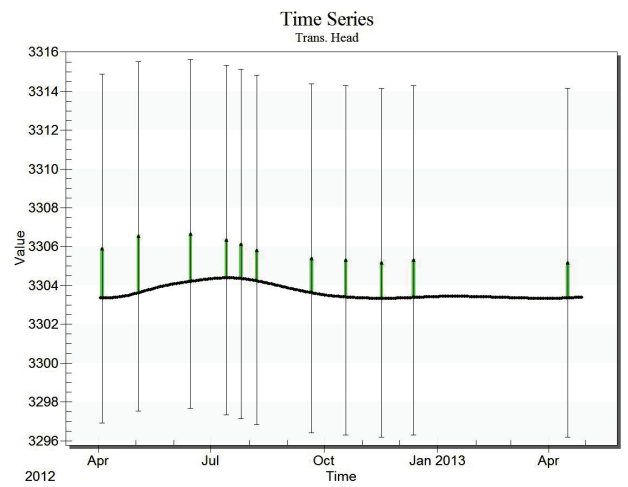
Well 266090



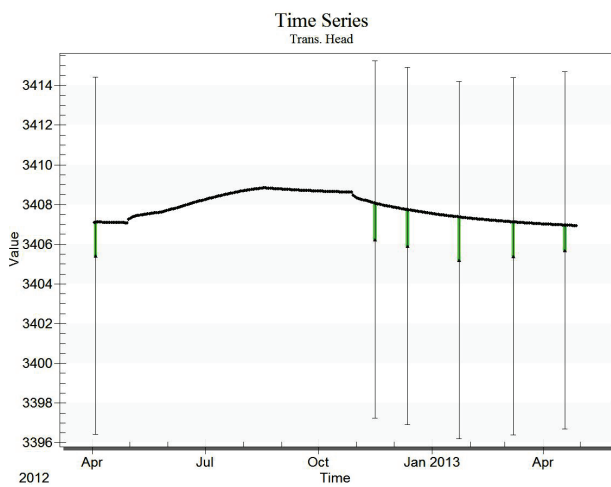
Well 266824



Well 266829



Well 266835



Well 266842

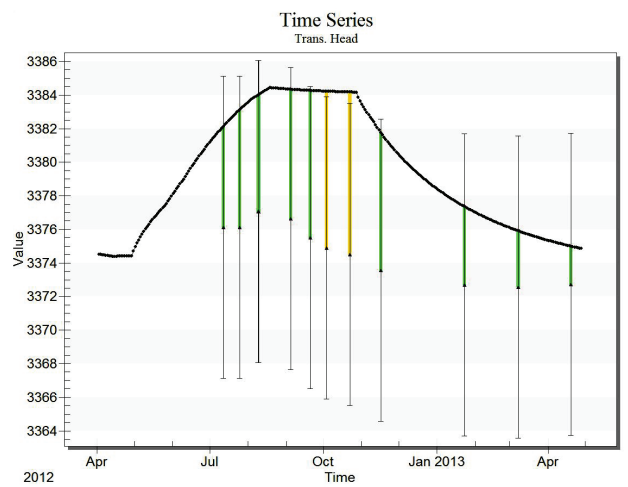


Figure E-7, Continued.

Well 267988

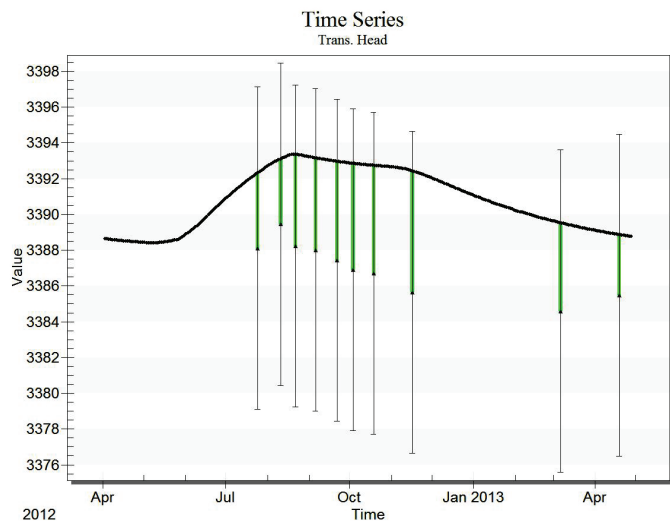
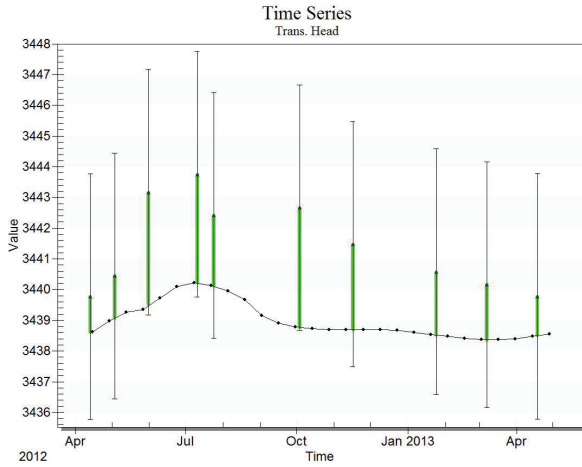
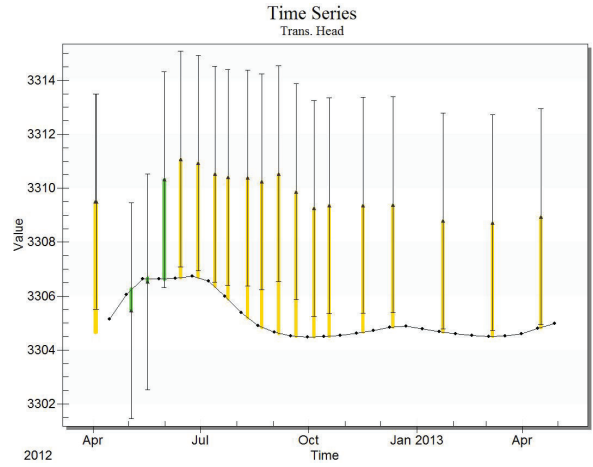


Figure E-7, Continued.

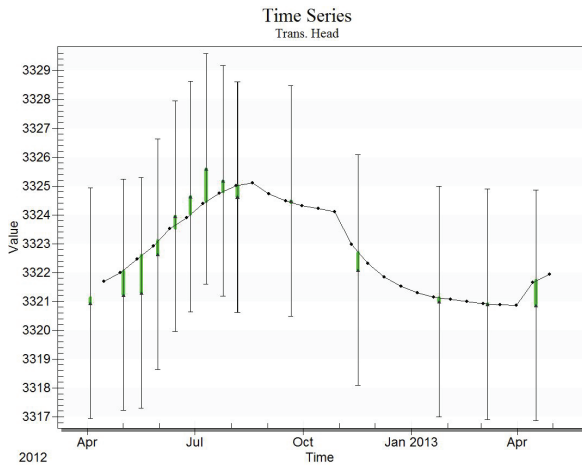
Well 56384



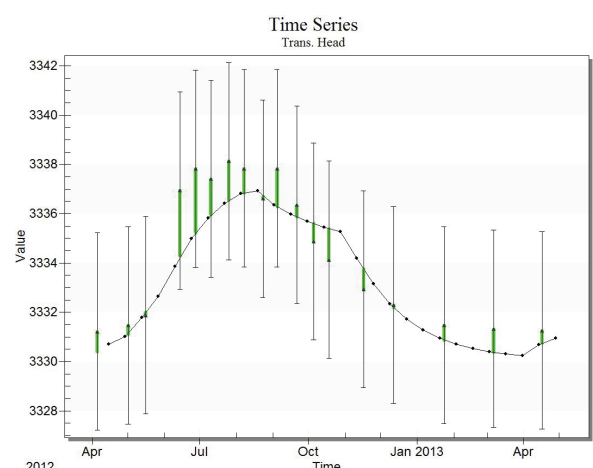
Well 57723



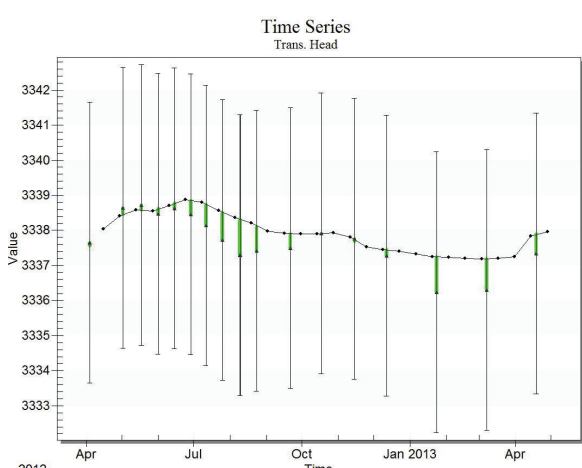
Well 57844



Well 57848



Well 57905



Well 58222

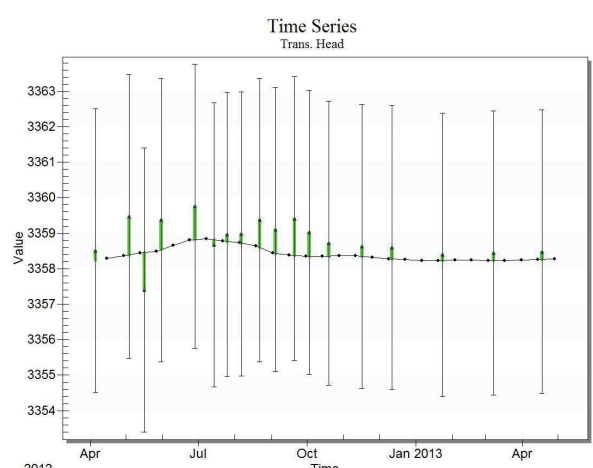
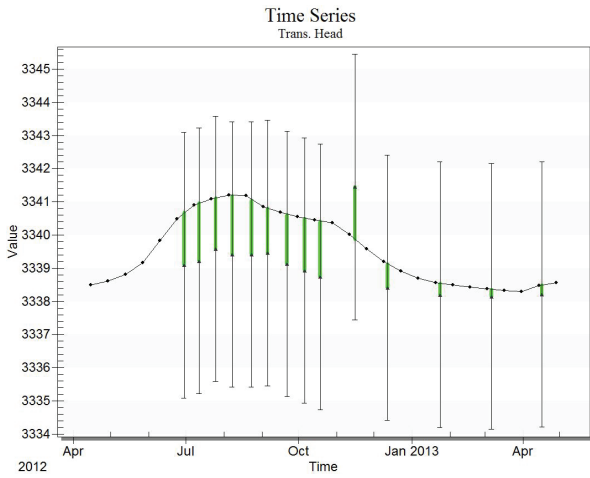
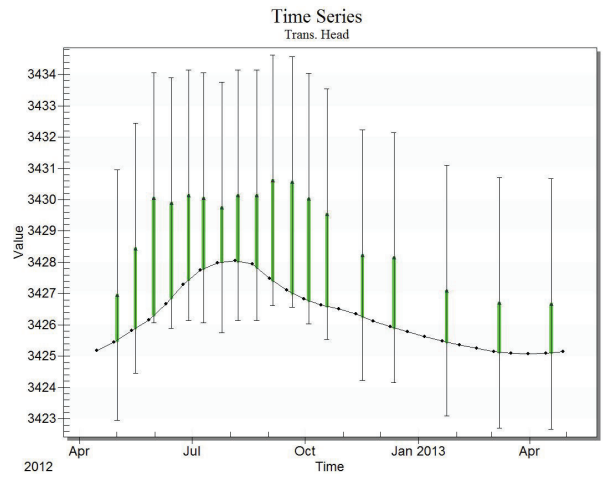


Figure E-8. Transient calibration hydrographs show observed water levels over time (middle value in each vertical hachure) vs. the simulated heads in the high K version (the dark line in each graph). The hachures encompass 4 ft of the observed value, referred to as the calibration interval.

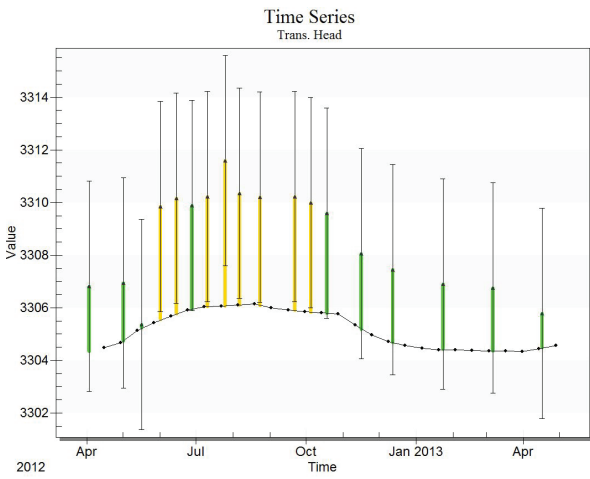
Well 128772



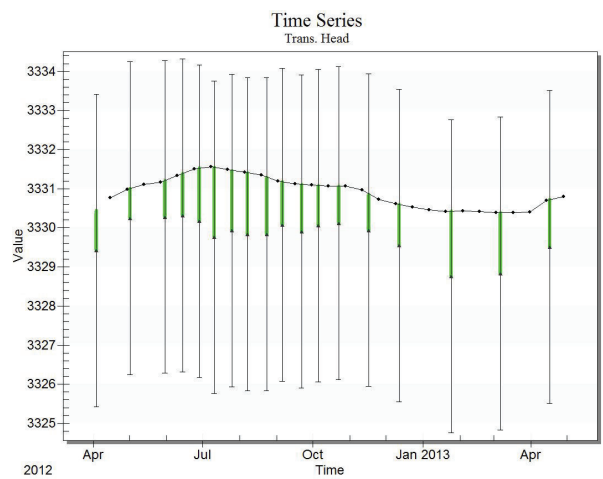
Well 158828



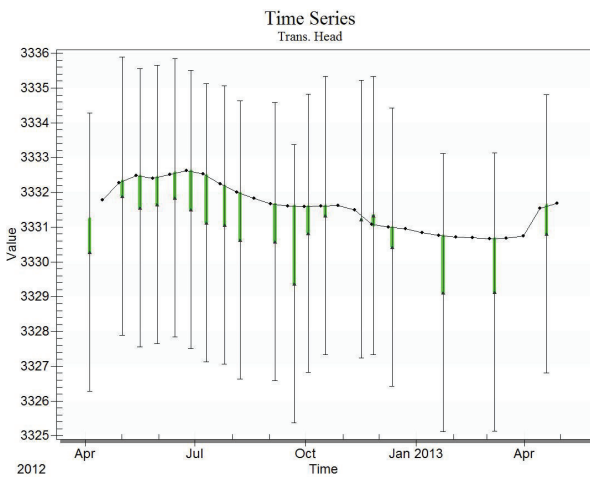
Well 161907



Well 170634



Well 232344



Well 266065

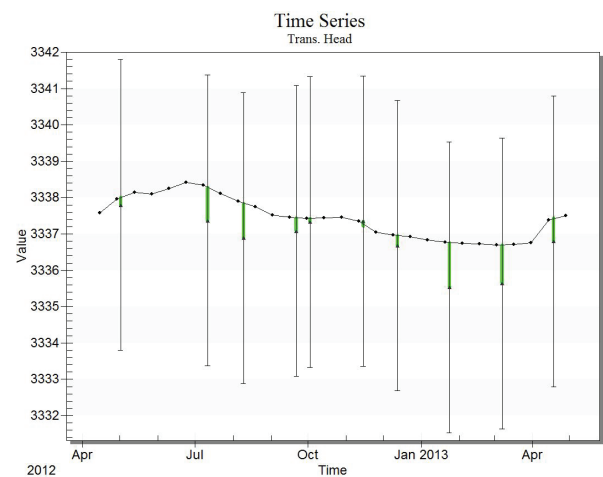
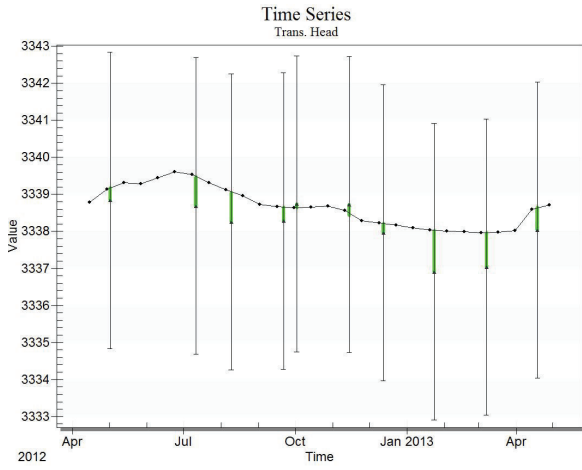
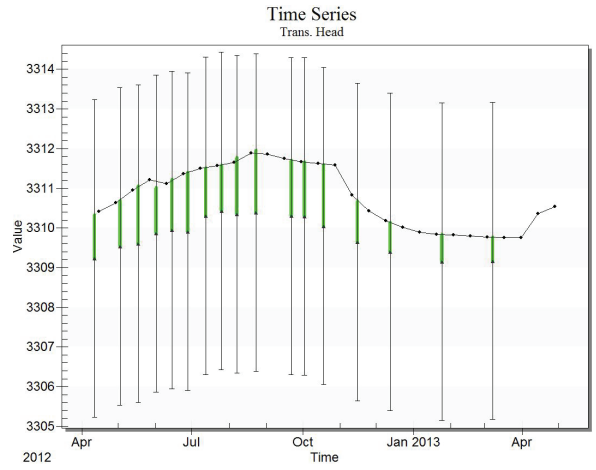


Figure E-8, Continued.

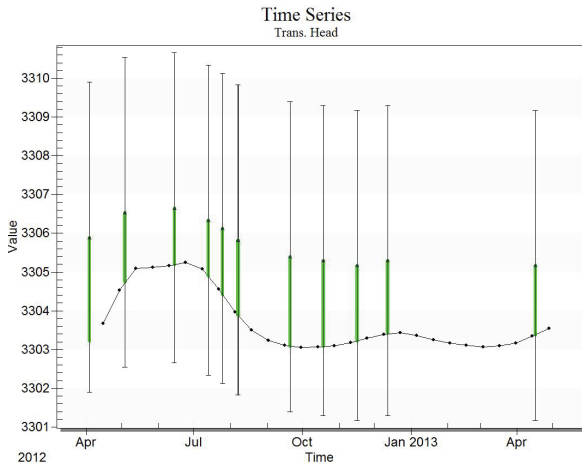
Well 266090



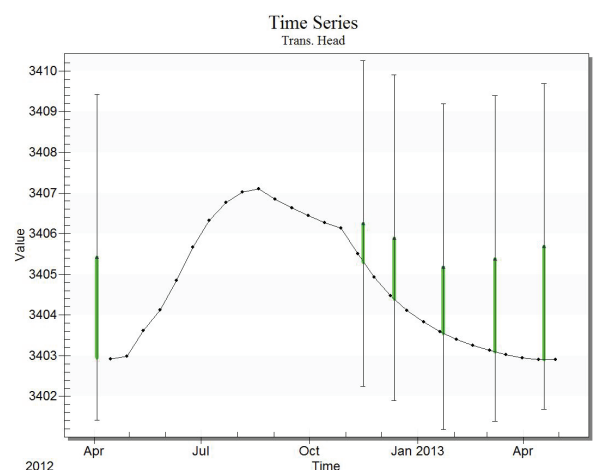
Well 266824



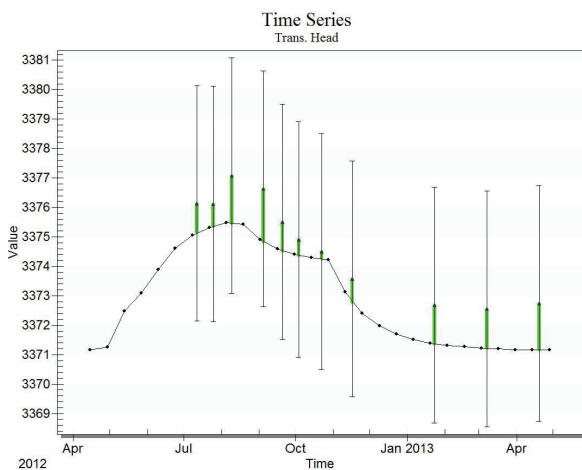
Well 266829



Well 266835



Well 266842



Well 267988

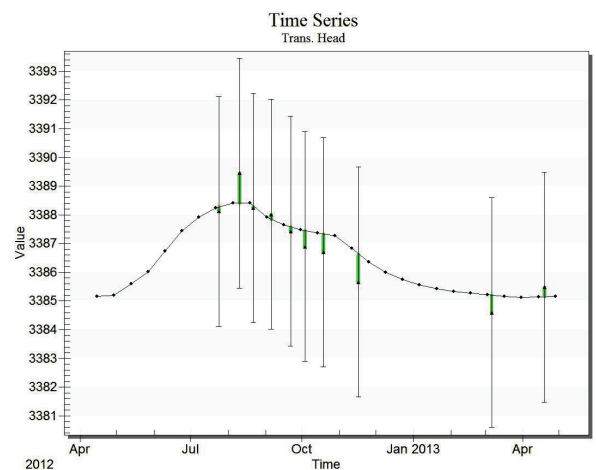


Figure E-8, Continued.

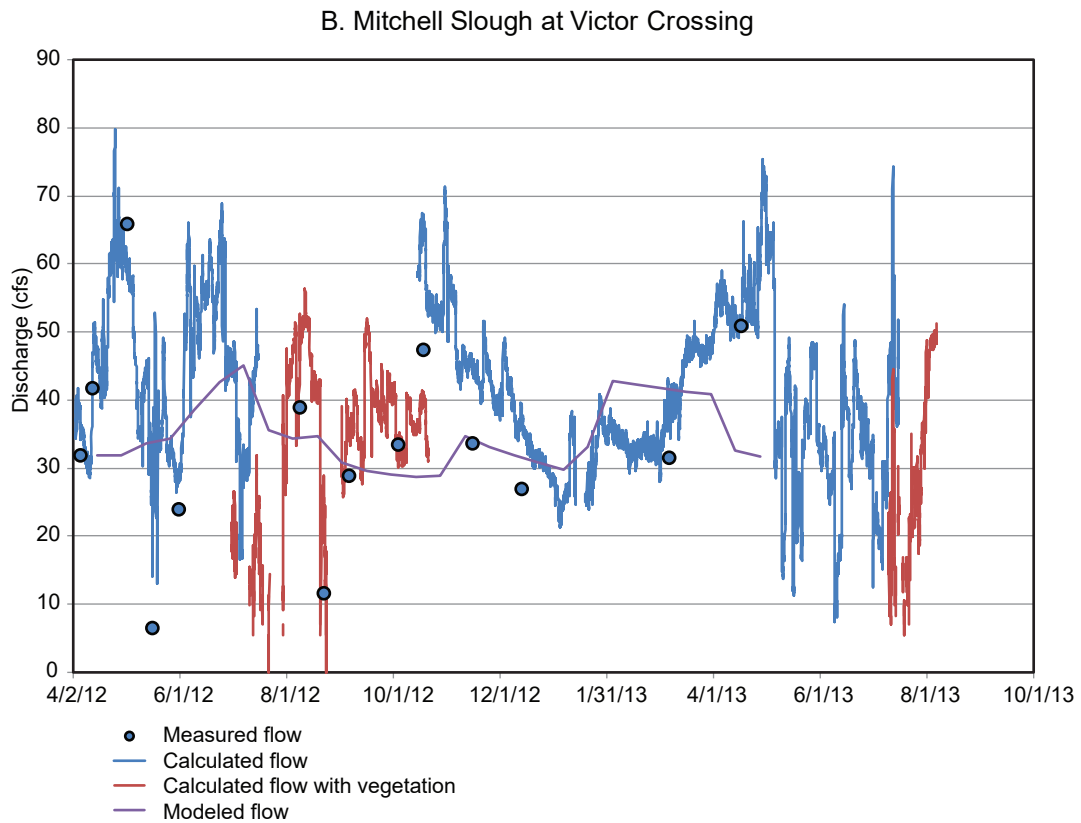
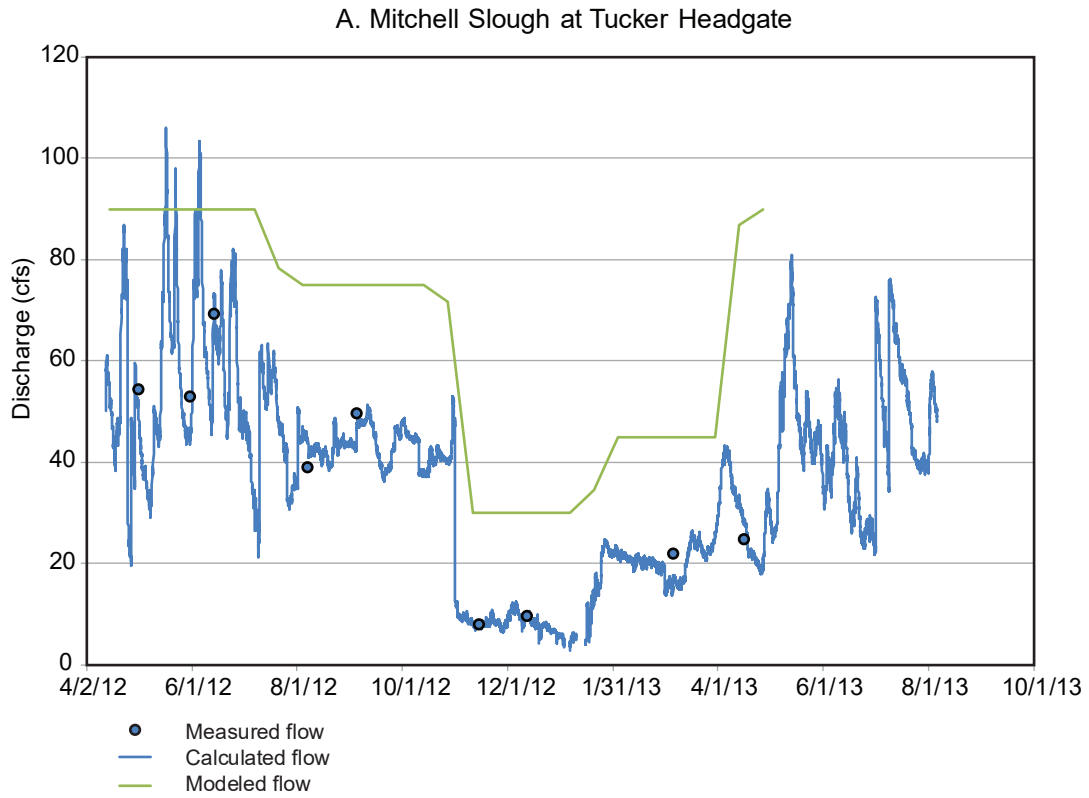


Figure E-9. Mitchell Slough measured, calculated, and modeled flows at Tucker Headgate (A) and Victor Crossing (B), low K version of the transient model.

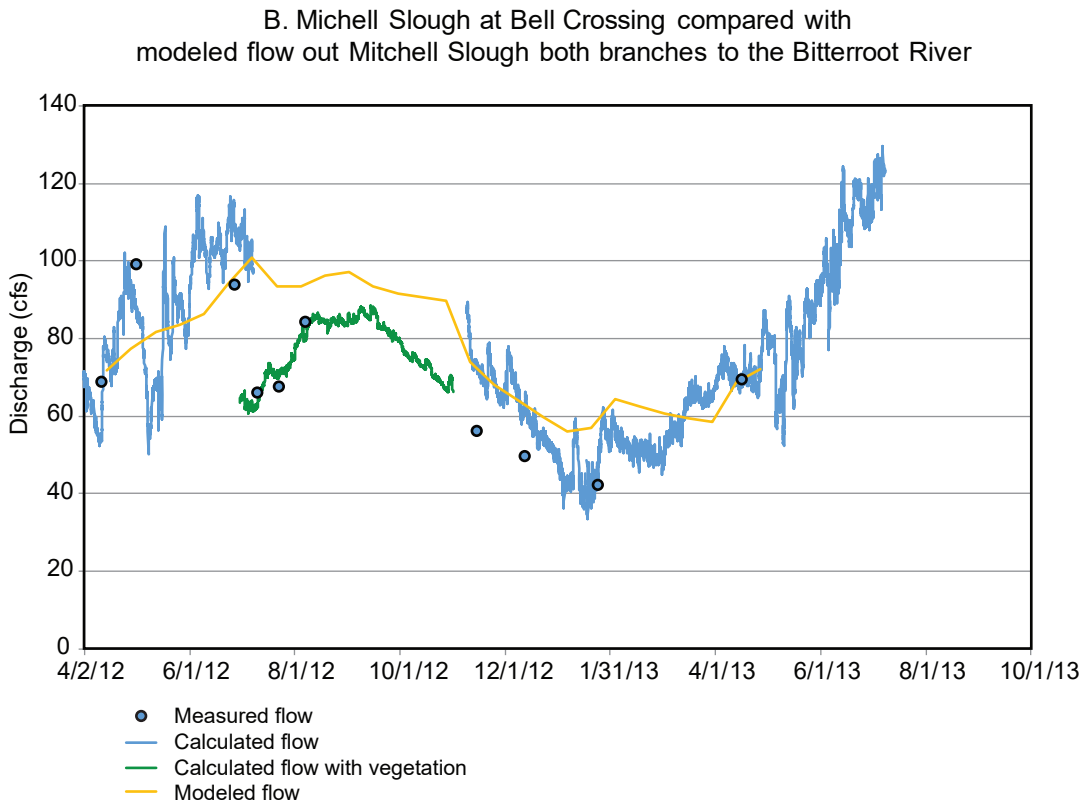
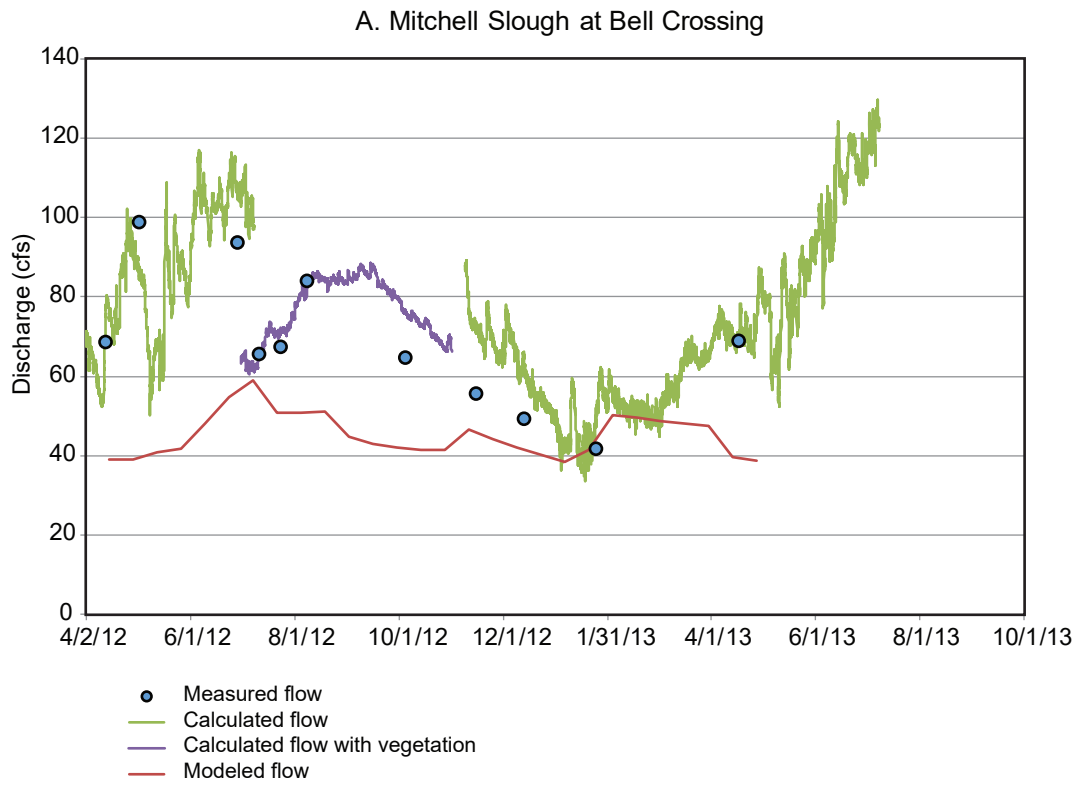
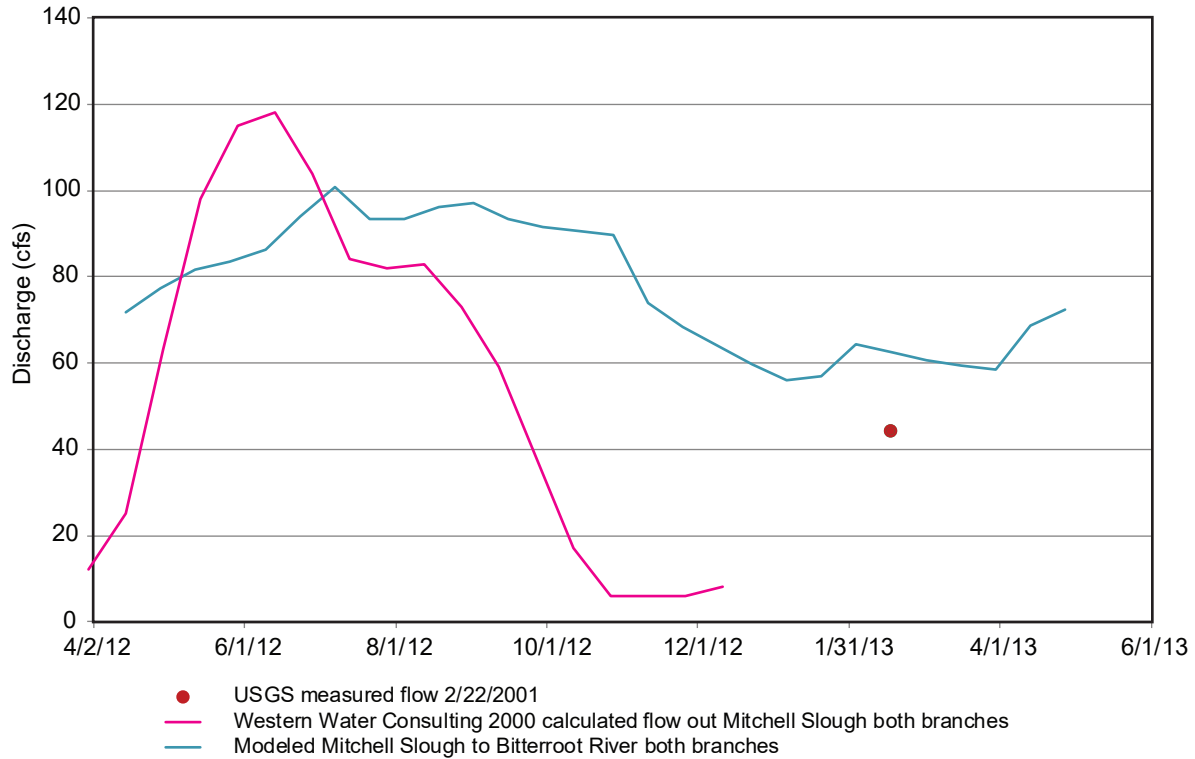


Figure E-10. Mitchell Slough measured, calculated, and modeled flows at Bell Crossing (A) and out both branches of Mitchell Slough to the Bitterroot River (B), low K version of the transient model.

A. Mitchell Slough east and west branches to Bitterroot River, measured, calculated, and modeled flow



B. Modeled drain discharges

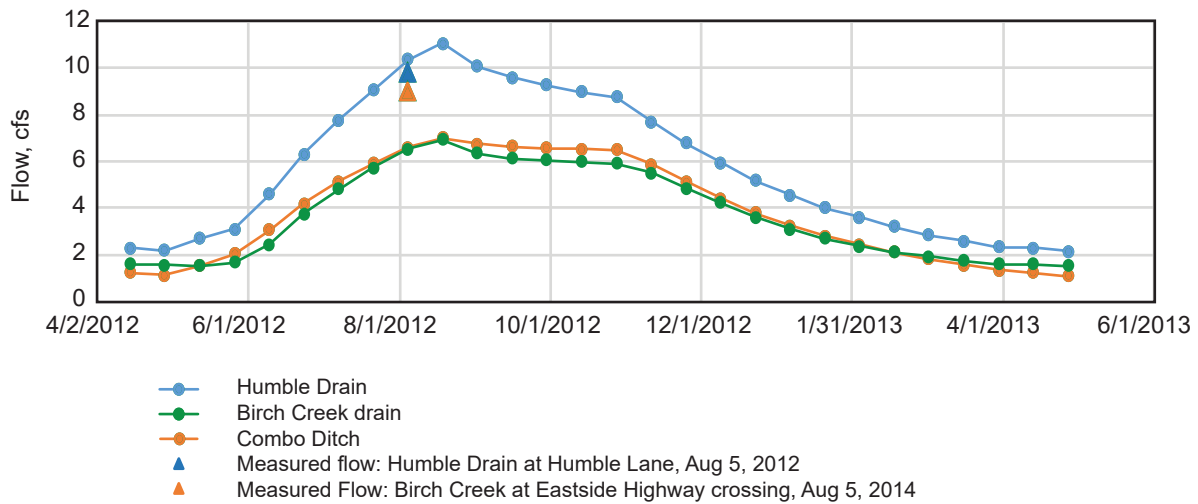


Figure E-11. Mitchell Slough flows out both channels to the Bitterroot River, measured, calculated and modeled (A), low K model; measured and modeled flows for selected ditches (B), low K version of the transient model.

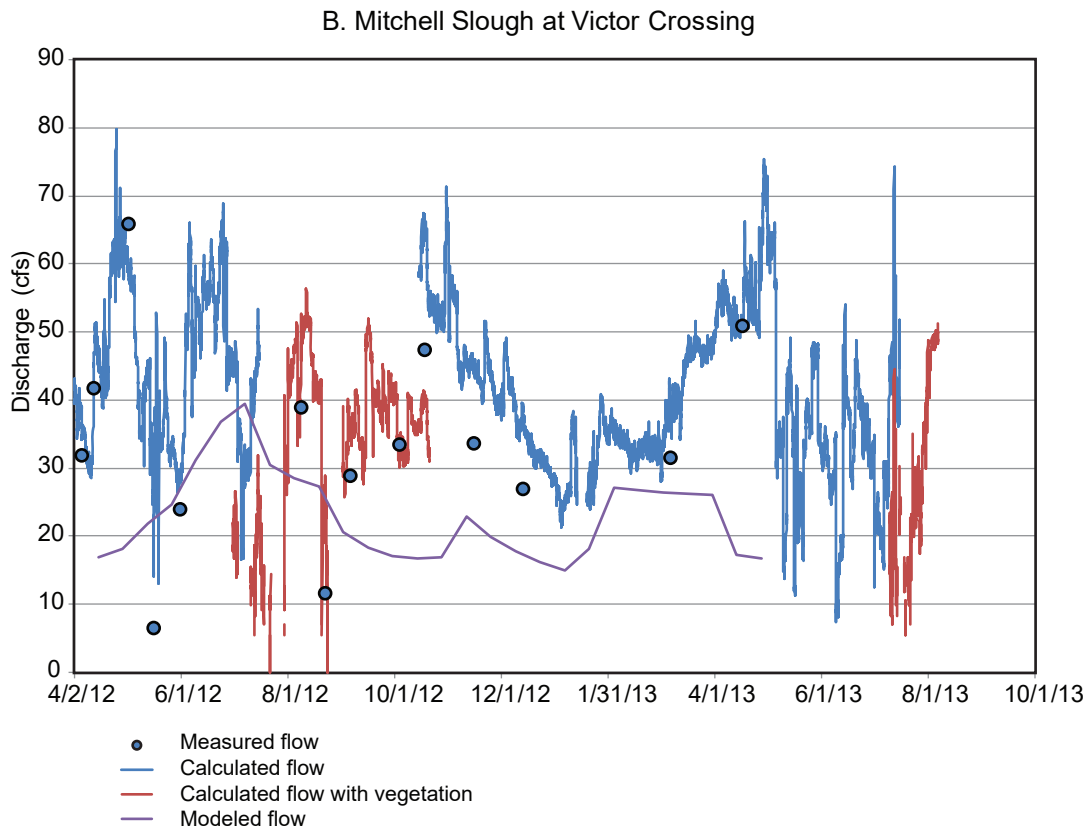
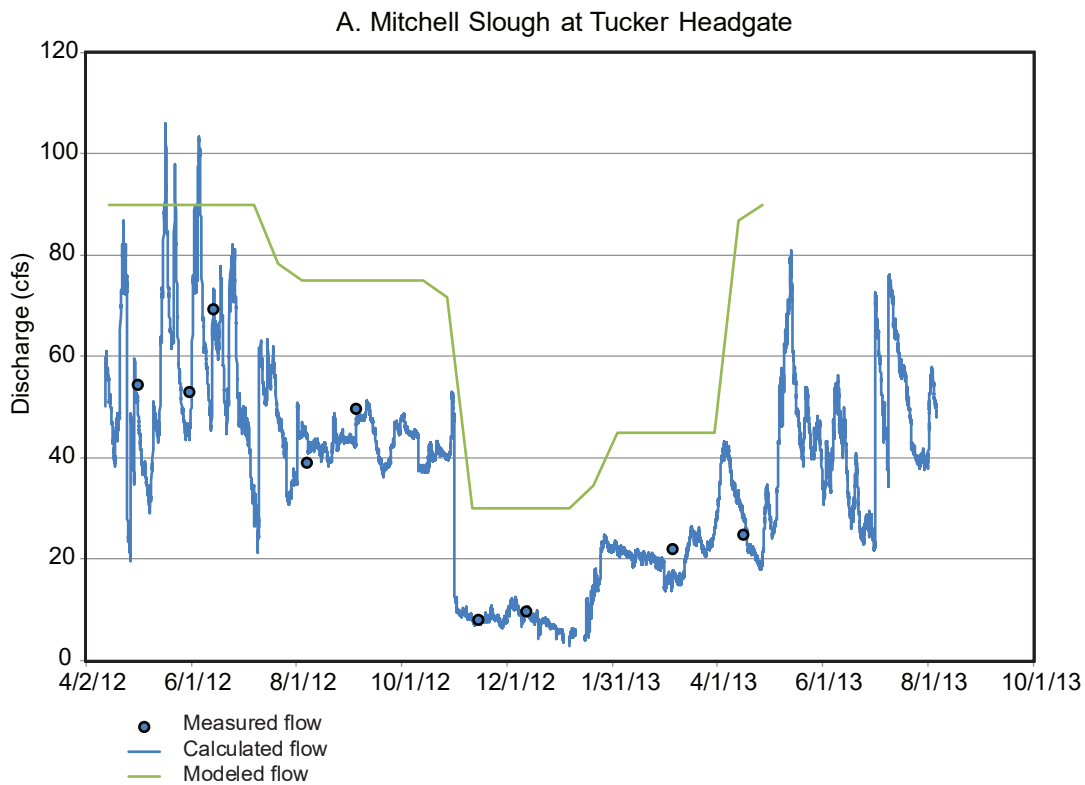


Figure E-12. Mitchell Slough measured, calculated, and modeled flows at Tucker Headgate (A) and Victor Crossing (B), high K version of the transient model.

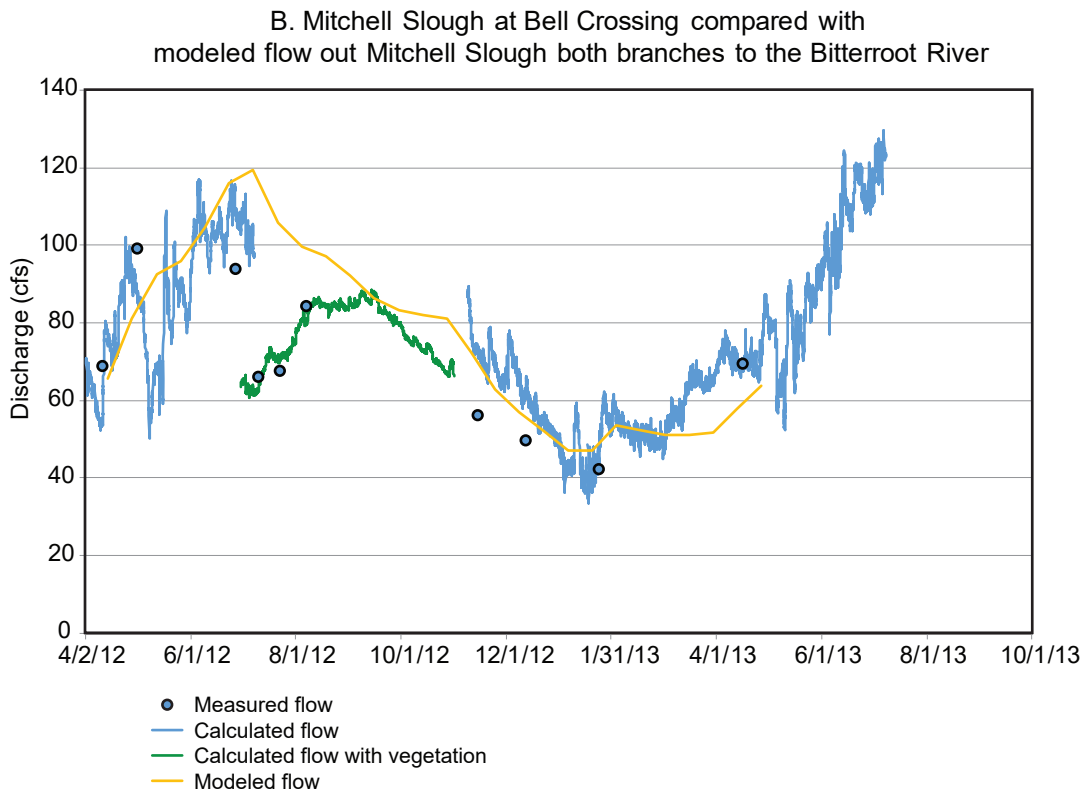
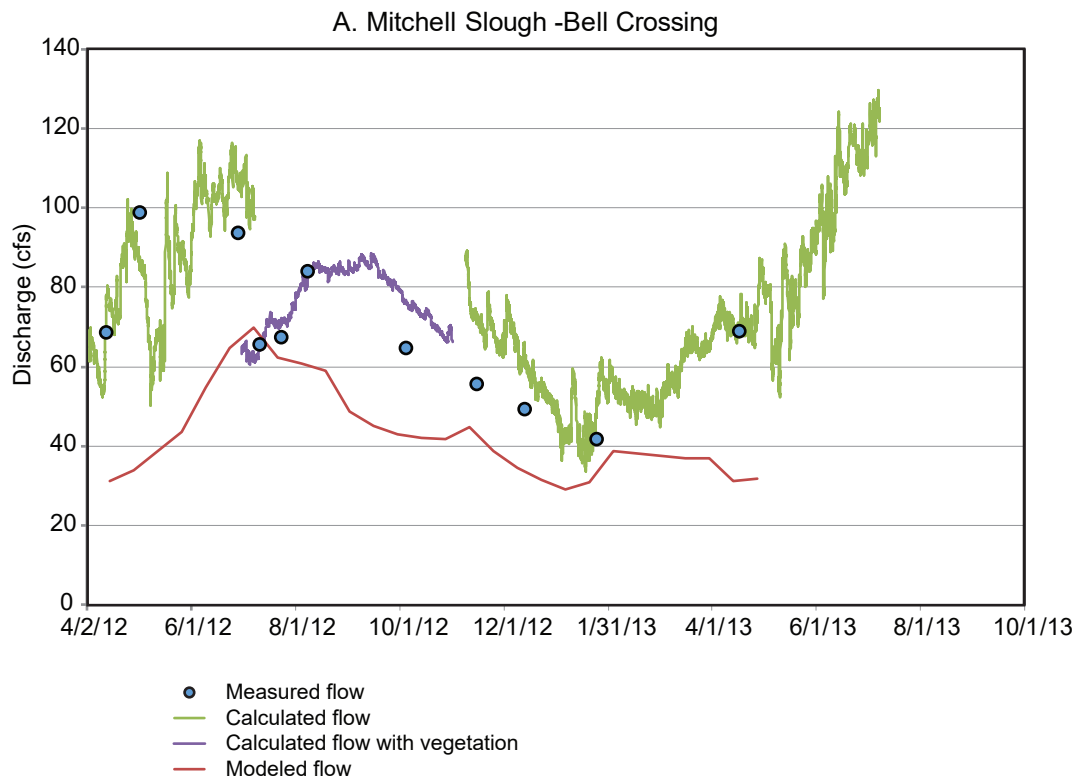


Figure E-13. Mitchell Slough measured, calculated, and modeled flows at Bell Crossing, and out both branches of Mitchell Slough to the Bitterroot River, high K version of the transient model.

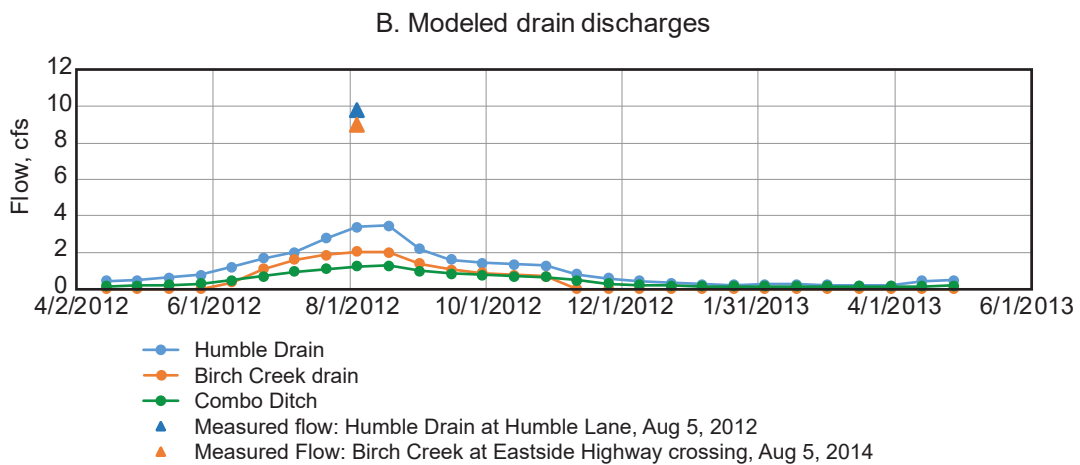
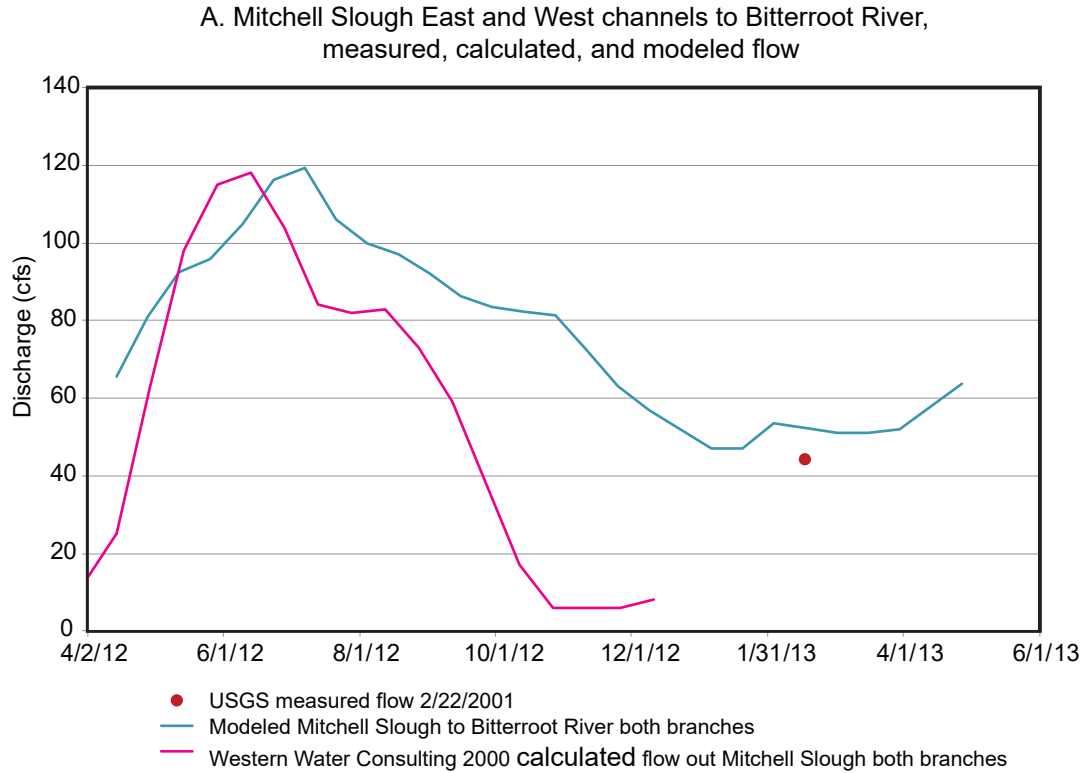


Figure E-14. Mitchell Slough flows out both channels to the Bitterroot River, measured, calculated, and modeled (A), high K model; measured and modeled flows for selected ditches (B), high K version of the transient model.

groundwater flux along the east edge of the model. Each of these parameters was varied by the same set of multipliers, including 0.05, 0.1, 0.25, 0.5, 2, 4, 10, and 20. The simulated discharge from the east branch of Mitchell Slough to the Bitterroot River was used to evaluate differences in results.

The initial sensitivity analysis conducted on the hydraulic conductivity of layer 1 showed that higher hydraulic conductivities generated using the 4 and 10 times multiplier in the MODFLOW led to better calibration statistics for heads and overall matching of seasonal water-level fluctuations in wells. A multiplier of 10 resulted in the best fit based on the mean absolute error between modeled and observed groundwater heads. Simulated discharge out of Mitchell Slough also fit reasonably well with the Bell Crossing flow data.

Based on this initial sensitivity testing, the hydraulic conductivity of layer 1 was increased from 200 ft/d (low K) to 2,000 ft/d (high K). Both versions of the model were operated during the predictive simulations, as described above. Compared to textbook ranges of hydraulic conductivities, these values range approximately from lower in the clean sand and gravel range to about the high end (U.S. Bureau of Reclamation, 1977). Groundwater levels are better calibrated in the high K model (figs. E-6, E-8). Sensitivity analysis continued, but using the higher hydraulic conductivity model.

The steady-state model is most sensitive to changes in the hydraulic conductivity values in layer 1 (table E-10). Changes in the hydraulic conductivity of layers 2 and 3 had little effect on calibration statistics. Because irrigation recharge is the dominant source of water, changes to each component of irrigation recharge affect the model calibration. Ditch leakage, which represents estimated canal losses, is the largest component of irrigation recharge. Thus, increases in leakage input to the model generate larger errors than changes in other irrigation recharge sources.

The steady-state model is relatively insensitive to the riverbed and streambed conductance values. For these parameters, riverbed conductance had the largest effect on the flow out of the Mitchell Slough east branch.

MODEL LIMITATIONS

Like all models, these steady-state and transient models of the valley floor near Stevensville are simplifications of a complex system. Model results are subject to uncertainty that relates to both simplifying assumptions in the model construction (for example, model layer thickness and parameter values, such as K) and uncertainty in the supporting data (such as measurement error related to stream flows).

The model limitations include simplifying assumptions associated with scale and parameter uncertainty. Each 300 ft x 300 ft model cell represents average conditions over the 90,000 ft² cell size and over the layer thickness, which ranges from 20 to 90 ft. Thus, simulations placing high-capacity wells in close proximity to the river are limited to modeling wells at least 300 ft from the river.

The model was constructed by applying uniform values of K across model layers. In reality, hydraulic conductivity varies within these hydrogeologic strata. The assumption of uniform K is a reasonable simplification for the purposes of this project, which sought to evaluate large-scale response of head and flux under various changes in irrigation practices. As an alternative to adding complexity to the distribution of hydraulic conductivity in layer 1, we carried forward high and low K versions of the model. We conducted a model verification exercise on the high K version of the model only, due to time constraints. Performing this analysis with the low K version would provide insight into the performance of the low K version compared to the high K version. If this set of models is adapted for other uses, the uniform K distributions could be revisited.

An additional simplification during model development included limiting representation of existing groundwater pumping. The total estimated groundwater withdrawal by wells in the study area, 390 acre-ft/yr, was less than 1 percent of the estimated groundwater budget. This existing groundwater use is not simulated in the numerical models. Groundwater pumping is restricted to simulations of proposed groundwater extraction for irrigation.

Table E-10. Sensitivity analyses results.

Steady-State Model												
Model SV_SS_12pt1.gpr												
Abbreviation	K1	K2	K layer 2	K layer 3	Ditch leakage	SFR	Riverbed	Irrigated	Specified flux	Transient K1	Low flow	Low flow
					DL	conductance	conductance	fields	recharge east	SV_TR_13pt2.gpr	High flow	Low flow
					(cfs)	SFR	RC	IRRf	FluxE	rate	occurs	rate
Flow out the east channel of Mitchell Slough												
Multiplier	0.05	74.24	71.72	71.61	57.10	55.00	78.58	64.07	68.34	67.57	end of	53.55
	0.1	73.80	71.72	71.61	57.86	60.24	76.49	64.48	68.52	75.56	SP 10	53.13
	0.25	72.93	71.72	71.63	60.17	66.13	74.76	65.68	69.06	87.08	SP 10	52.11
	0.5	71.97	71.72	71.66	64.01	69.41	73.21	67.69	69.94	97.94	SP 7	50.43
	1	71.72	71.72	71.72	71.72	71.72	71.72	71.72	71.72	113.13	SP 7	46.89
	2	74.18	71.72	71.85	87.28	73.03	70.59	79.82	75.29	131.12	SP 7	47.03
	4	84.63	71.72	72.15	119.62	72.39	69.79	95.98	82.46	156.03	SP 6	61.33
	10	128.90	71.73	73.23	216.27	71.64	68.88	146.78	105.32	210.54	SP 6	111.94
	20	194.85	71.73	75.57	393.95	70.96	62.48	234.41	145.46	256.11	SP 7	196.86
Mean absolute error based on heads at calibration targets												
Multiplier	0.05	3.68	1.34	1.34	1.51	1.92	1.33	1.37	1.37	2.90	Mean absolute error transient	
	0.1	3.02	1.34	1.34	1.50	1.62	1.34	1.37	1.37	2.66		
	0.25	2.18	1.34	1.34	1.46	1.39	1.34	1.36	1.36	2.23		
	0.5	1.58	1.34	1.34	1.40	1.34	1.34	1.36	1.36	1.88		
	1	1.34	1.34	1.34	1.34	1.34	1.34	1.34	1.34	1.76		
	2	1.49	1.34	1.34	1.37	1.29	1.34	1.33	1.31	1.97		
	4	1.71	1.34	1.34	1.96	1.31	1.34	1.43	1.31	2.18		
	10	1.95	1.34	1.38	3.55	1.31	1.33	2.17	1.69	2.40		
	20	2.07	1.34	1.45	6.12	1.32	1.33	3.46	2.43	2.54		
Root mean squared error based on heads at calibration targets												
Multiplier	0.05	5.72	1.98	1.97	2.29	2.27	1.84	2.07	2.04	4.25	Root mean squared error transient	
	0.1	4.37	1.98	1.97	2.27	2.07	1.89	2.07	2.03	3.89		
	0.25	2.96	1.98	1.97	2.20	1.97	1.93	2.05	2.02	3.33		
	0.5	2.17	1.98	1.97	2.10	1.97	1.96	2.02	2.01	3.00		
	1	1.98	1.98	1.98	1.98	1.98	1.98	1.98	1.98	2.96		
	2	2.24	1.98	1.98	1.99	1.98	1.98	1.93	1.93	3.12		
	4	2.48	1.98	2.01	2.61	1.99	1.98	2.00	1.92	3.30		
	10	2.69	1.98	2.08	5.03	2.01	1.97	2.71	2.28	3.45		
	20	2.79	1.98	2.19	9.22	2.03	1.97	4.28	3.27	3.46		

D:\Documents2\GMS_STEVI_1\SV_SS_12pt1_MODFLOW\Table of sensitivity results 12pt1.xlsx

CALCULATION DETAILS

This section presents calculations related to a variety of features in the models. Calculations were verified during model review.

1. The calculations for the East Channel and Mitchell Slough (at Tucker Headgate) are described in the main report in the section about Groundwater Modeling, Sources and Sinks.
2. Gerlinger and Webfoot Ditches: diversions are incorporated in the SFR2 package to remove water from the model expected to be diverted from the ditches for irrigation.

Gerlinger:

Most Gerlinger-irrigated lands are sprinkler or pivot irrigated and total 675 irrigated acres. A value of 633 acres was inadvertently used, resulting in 1,266 acre-ft of applied irrigation water (see below) as opposed to 1,350 acre-ft of water applied to 675 acres. Since the difference between the values is minor (about 6%), this was not corrected in the model.

Water applied is approximately 633 acres*2 ft = 1,266 acre-ft. Irrigation water is typically applied from Jun 1 to August 15 (76 days).

$1,266 \text{ acre-ft}/76 \text{ days} = 16.66 \text{ acre-ft/d} = 725,709.6 \text{ ft}^3/\text{d}$ or 8.4 cfs (June 1, 2012 to August 15, 2012). Steady-state rate = 151,003 ft³/d

Webfoot: There are the following irrigation acreages modeled for Webfoot Ditch as a source:

Flood: 209 acres * 3 ft water applied = 627 acre-ft

Sprinkler: 322 acres * 2 ft water applied = 644 acre-ft

Thus, about 1,271 acre-ft applied total flood + sprinkler irrigation water from Webfoot Ditch as modeled. Irrigation water is typically applied largely from Jun 1 to August 15 (76 days).

$1,271 \text{ acre-ft}/76 \text{ days} = 16.72 \text{ acre-ft/d} = 728,323.2 \text{ ft}^3/\text{d}$ or 8.4 cfs (June 1, 2012 to August 15, 2012). Steady-state rate = 151,547 ft³/d

3. Specified flux arcs that are assigned in GMS and function using the Wells package in

MODFLOW.

Canal arc lengths were measured in GMS with the measuring stick button.

The following are applied to arcs in Map Data coverage “East Side Flux in Canals”

Arc numbers are from figure Model Stream Features (map):

Arc 5: Union/Etna – from DF Ranch to split near Willoughby Cr – length = 23,956 ft, or 4.54 mi

$4.54 \text{ mi} * (2 \text{ cfs/mi Union} + 1 \text{ cfs/mi Etna}) = 13.62 \text{ cfs} = 1,176,768 \text{ ft}^3/\text{d}$

Applying from April 28 to October 29 = 185 days (3+31+30+31+31+30+29)

Steady-state value = 595,791 ft³/d

Arc 6: Etna – short reach from split to Willoughby Cr - length = 2,239 ft, or 0.42 mi

$0.42 \text{ mi} * (1 \text{ cfs/mi Etna}) = 0.42 \text{ cfs} = 36,288 \text{ ft}^3/\text{d}$

Flow from about May 8, 2012 to September 28, 2012 = 144 days (24+30+31+31+28)

Steady-state value = 14,307 ft³/d

Arc 7: Union – North of Willoughby Cr to model edge – length = 14,784 ft, or 2.8 miles

$2.8 \text{ miles} * (2 \text{ cfs/mile}) = 5.6 \text{ cfs} = 483,840 \text{ ft}^3/\text{d}$

Applying from April 28 to October 29 = 185 days (3+31+30+31+31+30+29)

Steady-state value = 245,066 ft³/d

Arc 4: Supply Ditch – southern arc across model space – length = 16,306 ft, or 3.09 mi

$3.09 \text{ mi} * (1.5 \text{ cfs/mi Supply}) = 4.635 \text{ cfs} = 400,464 \text{ ft}^3/\text{d}$

Flow from about May 8, 2012 to September 28,

2012 = 144 days (24+30+31+31+28)

Steady-state value = 157,883 ft³/d

Arc 3: Southern edge-of-model Arc (east side flux plus Corvallis ditch)

Length = 16,116 ft = 3.05 mi

East Side Flux value = 129,600 ft³/d (42,492 ft³/d /mile) (0.49 cfs/mi)

Corvallis Ditch 3.05 mi * 1.5 cfs/mi = 4.575 cfs = 395,280 ft³/d

Using 185 day application, steady-state value should be 200,210 ft³/d

Add summer leakage from canal to year-round-flux:

395,280	200,210	
<u>+ 129,600</u>	<u>+ 129,600</u>	
524,880	329,810	steady state

Arc 2: Middle edge-of-model Arc (east side flux plus Supply ditch)

Length = 28,373 ft = 5.374 mi

East Side Flux value = 216,000 ft³/d (40,194 ft³/d/mile) (0.47 cfs/mi)

Supply Ditch 5.374 mi * 1.5 cfs/mi = 8.061cfs = 696,470 ft³/d

Using 185 day application, steady-state value should be 352,764 ft³/d

Add summer leakage from canal to year-round-flux:

696,471	352,764	
<u>+ 216,000</u>	<u>+ 216,000</u>	
912,471	568,764	steady-state

Arc 1: Northern edge-of-model Arc (east side flux plus Supply ditch)

Length = 12,608 ft = 2.388 mi

East Side Flux value = 97,200 ft³/d (40,704 ft³/d /mile) (0.47 cfs/mi)

Supply Ditch 2.388 mi * 1.5 cfs/mi = 3.582cfs = 309,485 ft³/d

Using 185 day application, steady-state value should be 156,755 ft³/d

Add summer leakage from canal to year-round-flux:

309,485	156,755	
<u>+ 97,200</u>	<u>+ 97,200</u>	
406,685	253,955	steady-state

4. Polygons used to apply recharge to irrigated lands.

Table E-8 lists the named polygons in GMS (fig. E-4A) that are used to delineate the recharge rates applied to irrigated land, the size of each polygon, and the recharge rates assigned for steady-state and transient model versions. This list was generated from steady-state model version SV_SS_8pt10.gpr. As modeled, there are 7,576 irrigated acres, with 4,198 acres designated as sprinkler irrigation and 3,378 acres designated as flood irrigation. In actuality, one 114-acre field, IRR_Corvallis_spr_2, is irrigated with a pivot system.

5. Well irrigation scenario calculations—for the Individual Irrigation Wells Providing all East Channel Irrigation Water (Scenario 3). Table E-11 provides the details of how the pumping rates for modeled, hypothetical groundwater irrigation wells were generated.

6. Individual Irrigation Wells Replacing East Channel Sprinkler Irrigated lands calculations (Scenario 4) are presented in table E-12.

Table E-11. Individual irrigation wells providing all East Channel water (scenario 3).

Area	Fields	Irrigated acres	Demand* acre-ft	Demand/Day acre-ft	ft ³ /d	ft ² /min	GPM	Number of wells	Rate per well	Rate, ft ³ /d (for model)
IRR_N	IRR_N_FLD_1	212	424	5.578947368	243,018.9	168.7632	1,262.348	3	421	-81,006
	IRR_N_FLD_2									
	IRR_N_spr									
Webfoot N	IRR_N_spr_2	289	578	7.605263158	331,285.3	230.0592	1720.843	4	430	-82,821
	IRR_N_spr_3									
	IRR_Webfoot_FLD_1									
	IRR_Webfoot_FLD_2									
	IRR_Webfoot_FLD_3									
IRR_Webfoot_spr_1										
IRR_Webfoot_spr_2										
Union	IRR_UD_FLD_1	595	1190	15.65789474	682,057.9	473.6513	3,542.912	8	443	-85,257
	IRR_UD_FLD_2									
	IRR_UD_spr_1									
	IRR_UD_spr_2									
	IRR_UD_spr_3									
Gerlinger	IRR_Gerlinger_spr_1	481	962	12.65789474	551,377.9	382.9013	2,864.102	6	477	-91,896
	IRR_Gerlinger_spr_2									
Webfoot_S	IRR_Webfoot_FLD_4	217	434	5.710526316	248,750.5	172.7434	1,292.121	3	431	-82,917
	IRR_Webfoot_spr_3									
	IRR_Webfoot_FLD_6									
	IRR_Webfoot_spr_4									
	IRR_Webfoot_FLD_5									
Victor_MS	IRR_Victor_FLD_3	313	626	8.236842105	358,796.8	249.1645	1,863.75	4	466	-89,699
	IRR_MS_spr									
	IRR_Victor_FLD_4									
	IRR_Victor_FLD_2									
IRR_Victor_FLD_1										
Etna	IRR_ETNA_spr_2	1,060	2,120	27.89473684	121,5095	843.8158	6,311.742	13	486	-93,469
	IRR_ETNA_spr_1									
	IRR_ETNA_FLD									
South	IRR_South_FLD_1	779	1,558	20.5	892,980	620.125	4,638.535	10	464	-89,298
	IRR_BirchCr_spr_1									
	IRR_DF_spr_1									
	IRR_South_FLD_2									
	IRR_South_FLD_3									
IRR_DF_spr_2										
Totals		3,946						51		

*assuming sprinkler irrigated crops are applied 2 ft of water per irrigation season, demand mainly from June 1 - August 15th (76 days)

Table E-12. Individual wells replacing East Channel irrigated lands (scenario 4).

Area	Fields	Wells added in scenario:	Irrigated acres for each field polygon	Irrigated acres for area	Demand* acre-ft	Demand/day acre-ft	ft ³ /d	ft ³ /min	GPM	Number of wells	Rate per well	Rate (for model) ft ³ /day
IRR_N	IRR_N_spr IRR_N_spr_2 IRR_N_spr_3	4c	156	191	382	5.026315789	218946.3158	152.0460526	1137.304474	3	379	-72982
			14									
			21									
Webfoot_N	IRR_Webfoot_spr_1 IRR_Webfoot_spr_2	4b	52	123	246	3.236842105	140996.8421	97.91447368	732.4002632	2	366	-70498
			71									
Union	IRR_UD_spr_1 IRR_UD_spr_2 IRR_UD_spr_3	4d	36	63	126	1.657894737	72217.89474	50.15131579	375.1318421	1	375	-72218
			17									
			10									
Gerlinger	IRR_Gerlinger_spr_1 IRR_Gerlinger_spr_2	4c	198	481	962	12.65789474	551377.8947	382.9013158	2864.101842	6	477	-91896
			283									
Webfoot_S	IRR_Webfoot_spr_3 IRR_Webfoot_spr_4	4b	158	178	356	4.684210526	204044.2105	141.6973684	1059.896316	3	353	-68015
			20									
Victor_MS	IRR_MS_spr	4c	56	56	112	1.473684211	64193.68421	44.57894737	333.4505263	1	333	-64194
Etna	IRR_ETNA_spr_2 IRR_ETNA_spr_1	4d	89	321	642	8.447368421	367967.3684	255.5328947	1911.386053	4	478	-91992
			232									
South	IRR_BirchCr_spr_1 IRR_DF_spr_1 IRR_DF_spr_2	4d	339	545	1090	14.34210526	624742.1053	433.8486842	3245.188158	7	464	-89249
			29									
			177									

* assuming sprinkler irrigated crops are applied 2 ft of water per irrigation season, demand mainly from June 1 - August 15th (76 days)

GROUNDWATER MODEL PRODUCTS

Each model is available in the high and low K versions, as described above.

The Map Data in GMS is generally used to assign model input to map features that are nodes, arcs, or polygons. The following list shows the functions of each Map Data layer:

Boundary	Arc and polygon to define the active cells in the MODFLOW grid
Specified Heads 1	Nodes and arcs to define the specified head cells at the north and south ends of the model
HK Layer 1	Polygon to define hydraulic conductivity of layer 1
HK Layer 2	Polygon to define hydraulic conductivity of layer 2
HK Layer 3	Polygon to define hydraulic conductivity of layer 3
SFR2	Nodes and arcs define stream flow routing package stream segment placement
Rivers	Nodes and arcs used to define river placement and streambed conductance
East Side Flux n Canals	Nodes and arcs used to define specified flow along certain canals. Groundwater flow from the east is assigned to canals along the eastern edge of the model
Irr_area_polygon	Polygon used to specify bulk recharge over a large area of irrigated lands, mostly on the low terrace—inactive in this model version.
Confined Storage	Polygon used to specify confined storage—inactive in this model version
Spec Yield	Polygon used to specify specific yield—inactive in this model version
USGS_March_1958	Points define static water-level elevations from McMurtrey and others (1959), adjusted to NAVD 1988 datum by adding 3.6 ft to each value
Secondary Storage	Polygon used to specify secondary storage—inactive in this model version
Irrigation_Canal_Type	Polygons used to specify recharge to the aquifer from excess water applied to irrigated fields—Polygons are named according to the expected source and type of irrigation as described in this appendix
Riparian ET	Polygon used to specify evapotranspiration for cottonwood and willow mapped in the modern floodplain—note, if these data are “mapped to MODFLOW” using GMS, the variable ET_Surface elevations must be reset. This can be done by copying the MODFLOW – Global Options - Top Elevation array and pasting it into the MODFLOW – Optional Packages – EVT-Evapotranspiration– ETSS. Elevation array.
SS Head Nov 2012 Rev	Points define static water elevations determined for November 2012 for wells used in this project

Map and Images Provided:

FileName	Features
ShadedRelief_FocusArea_SP_M_July2014.tif	Shaded relief from USGS DEM
NAIP Color 2011.tif	NAIP imagery, 2011
Topo_100k_clip_SP_ft.sid	1:100,000 scale USGS topographic map
mosaic_24k_SP_ft_clip.sid	1:24,000 scale USGS topographic map
Geology.shp	Lines of surficial geologic features mapped by Lonn and Sears (2001)

Stevensville Steady-State Models with Borehole DataHigh K Version:

SV_SS_High_K.gpr	GMS project file
\SV_SS_High_K_MODFLOW	GMS folder that must accompany project file
\MODFLOW_SV_SS_High_K	Folder containing the MODFLOW version
SV_SS_High_K.nam	MODFLOW 2000 name file to run using mf2k
Mf2k	MODFLOW 2000, version 1.19.01 03/25/2010
Generated from file SV_SS_12pt1.gpr	

Low K Version:

SV_SS_Low_K.gpr	GMS project file
\SV_SS_Low_K_MODFLOW	GMS folder that must accompany project file
\MODFLOW_SV_SS_Low_K	Folder containing the MODFLOW version
SV_SS_Low_K.nam	MODFLOW 2000 name file to run using mf2k
Mf2k	MODFLOW 2000, version 1.19.01 03/25/2010

Generated from file SV_SS_8pt10.gpr

Calibration file:

November 2012 SWLs BWIPMONST_ModelArea_Rev.csv

Stevensville Transient 13-mo Calibrated ModelsHigh K Version:

SV_TR_High_K.gpr	GMS project file
\SV_TR_High_K_MODFLOW	GMS folder that must accompany project file
\MODFLOW_SV_TR_High_K	Folder containing the MODFLOW version
SV_TR_High_K.nam	MODFLOW 2000 name file to run using mf2k
Mf2k	MODFLOW 2000, version 1.19.01 03/25/2010

Generated from file SV_TR_13pt2.gpr

Low K Version:

SV_TR_Low_K.gpr	GMS project file
\SV_TR_Low_K	GMS folder that must accompany project file
\MODFLOW_SV_TR_Low_K	Folder containing the MODFLOW version
SV_TR_Low_K.nam	MODFLOW 2000 name file to run using mf2k
Mf2k	MODFLOW 2000, version 1.19.01 03/25/2010
Generated from file SV_TR_9pt13.gpr	
Transient Calibration file:	
SWLs BWIPMONST_Transient.csv	

Stevensville Transient 10-yr Calibrated Models

High K Version:

SV_TR_High_K_10yr.gpr	GMS project file
\SV_TR_High_K_10yr_MODFLOW	GMS folder that must accompany project file
\MODFLOW_SV_TR_High_K_10_year	Folder containing the MODFLOW version
SV_TR_High_K_10yr.nam	MODFLOW 2000 name file to run using mf2k
Mf2k	MODFLOW 2000, version 1.19.01 03/25/2010
Generated from file SV_TR_14pt1.gpr	

Low K Version:

SV_TR_Low_K_10yr.gpr	GMS project file
\SV_TR_Low_K_10yr_MODFLOW	GMS folder that must accompany project file
\MODFLOW_SV_TR_Low_K_10_year	Folder containing the MODFLOW version
SV_TR_Low_K_10yr.nam	MODFLOW 2000 name file to run using mf2k
Mf2k	MODFLOW 2000, version 1.19.01 03/25/2010
Generated from file SV_TR_11pt11.gpr	

REFERENCES

- Aquaveo, LLC, 2014, Groundwater Modeling System (GMS), v. 9.2.9.
- Harbaugh, A.W., Banta, E.R., Hill, M.C., and McDonald, M.G., 2000, MODFLOW-2000, the U.S. Geological Survey modular ground-water model—User guide to modularization concepts and ground-water flow process: U.S. Geological Survey Open-File Report 00-92, 121 p.
- Linsely, R.K., Kohler, M.A., and Paulhus, J. L.H., 1982, Hydrology for engineers: New York, McGraw Hill, 3rd ed., 508 p.
- National Agricultural Imagery Program (NAIP), 2011, Natural-color aerial photos of Montana, 2011, <http://nris.mt.gov/gis/> [Accessed May 2014].
- Prudic, D.E., Konikow, L.F., and Banta, E.R., 2004, A new stream-flow routing (SFR1) package to simulate stream-aquifer interaction with MODFLOW-2000: U.S. Geological Survey Open-File Report 2004-1042, 95 p.
- U.S. Bureau of Reclamation (USBR), 1977, Ground water manual: A water resources technical publication: Department of the Interior, U.S. Government Printing Office, 480 p.
- U.S. Geological Survey (USGS), 1999, EROS Data Center, National Elevation Dataset, ed. 1, raster digital data: Sioux Falls, SD [Accessed February 2013].